2015-07-27

Pegylation and Bioactive Modification of Pancreatic Islet Surfaces to Enhance Graft Survival in Cell Therapy for Type I Diabetes

Jaime A. Giraldo
University of Miami, jagiraldod@gmail.com

UNIVERSITY OF MIAMI

PEGYLATION AND BIOACTIVE MODIFICATION OF PANCREATIC ISLET SURFACES TO ENHANCE GRAFT SURVIVAL IN CELL THERAPY FOR TYPE I DIABETES

By

Jaime A. Giraldo

A DISSERTATION

Submitted to the Faculty
of the University of Miami
in partial fulfillment of the requirements for
the degree of Doctor of Philosophy

Coral Gables, Florida

August 2015

UNIVERSITY OF MIAMI

A dissertation submitted in partial fulfillment of
the requirements for the degree of
Doctor of Philosophy

PEGYLATION AND BIOACTIVE MODIFICATION OF PANCREATIC ISLET SURFACES TO ENHANCE GRAFT SURVIVAL IN CELL THERAPY FOR TYPE I DIABETES

Jaime A. Giraldo

Approved:

_____ Cherie L. Stabler, Ph.D. Professor of Biomedical Engineering	_____ Fotios Andreopoulos, Ph.D. Professor of Biomedical Engineering
_____ Herman S. Cheung, Ph.D. Professor of Biomedical Engineering	_____ Allison Bayer, Ph.D. Professor of Microbiology and Immunology
_____ Norma S. Kenyon, Ph.D. Professor of Surgery, Microbiology and Immunology	_____ Dean of the Graduate School

GIRALDO, JAIME A. (Ph.D., Biomedical Engineering)

Pegylation and Bioactive Modification of Pancreatic Islet Surfaces to Enhance Graft Survival in Cell Therapy for Type I Diabetes. (August 2015)

Abstract of a dissertation at the University of Miami.

Dissertation supervised by Professor Cherie L. Stabler.
No. of pages in text. (135)

Islet transplantation is a promising therapy for Type 1 Diabetes Mellitus (T1DM), an autoimmune disease characterized by the destruction of the insulin producing beta cells pivotal to regulation of blood glucose. Despite vigorous and often injurious systemic immunosuppression, host inflammatory and immune responses lead to islet dysfunction and destruction over time. PEGylation, the grafting of poly(ethylene glycol) (PEG) to the periphery of cells or cell clusters, has the potential to mitigate inflammation and immune recognition via generation of a steric barrier. While explored as a plausible immunoprotective barrier in previous studies, this dissertation seeks to fully characterize the impact of an optimized PEG grafting procedure on long-term engraftment, as well as explore its potential to boost the efficacy of systemic immunosuppression. The effect of PEGylation on the survival of islet allografts was assessed in both murine and non-human primate (NHP) models of transplantation. Further, the potential of Staudinger ligation for tethering bioactive conjugates to confer immunomodulatory function was screened. The aim of this work was to determine the potential of and mechanism by which PEG protects islet allografts from the host immune response and establish the feasibility of incorporating bioactive motifs onto surfaces to further enhance graft survival.

Acknowledgements

I would like to extend my sincere thanks to my advisor, Cherie Stabler, Ph.D., for providing me with the opportunity to pursue my doctoral studies under her mentorship. Dr. Stabler's unwavering support, patience, and guidance were invaluable and a critical component of my success throughout my graduate career. Moreover, her relentless pursuit of excellence is a virtue that has been ingrained in me throughout the course of this experience, and for that I am forever grateful. I would also like to thank Herman Cheung, Ph.D., Fotios Andreopoulos, Ph.D., Allison Bayer, Ph.D., and Norma S. Kenyon, Ph.D., for taking the time out of their busy schedules to participate as members of my dissertation committee and always making themselves available whenever their assistance and guidance was needed. A special thanks is extended to Dr. Kenyon and the Diabetes Research Institute's (DRI) Pre-Clinical Research team, without whom none of the studies on non-human primates would have been possible. In particular, I would like to thank Dora Berman-Weinberg, Ph.D., Alex Rabassa, and Melissa Willman, for always lending a helping hand when needed. Thanks to Antonello Pileggi, M.D., Ph.D., R. Damaris Molano, D.V.M, and the other members of the DRI's Pre-Clinical Cell Processing and Translational Core who played critical role in all the murine islet and transplant studies. Additionally, thanks to Oliver Umland, Ph.D., for his assistance with flow cytometry experiments and Kevin Johnson for his help with processing of histological samples. I am grateful to all the faculty and staff of the DRI, in particular Armando Mendez, Ph.D., Juan Dominguez-Bendala, Ph.D., Ricardo Pastori, Ph.D., Christopher Fraker, Ph.D., and Alice Tomei, Ph.D., for their constant guidance, encouragement, and support. Thanks to all the members of the

Stabler Lab, the faculty and staff of the University of Miami's Biomedical Engineering Department, and, last but not least, thanks to all my friends and family for their support.

Table of Contents

List of Figures

List of Tables

Chapter 1. Specific Aims

1.1 INTRODUCTORY REMARKS

Clinical islet transplantation (CIT), the intraportal infusion of allogeneic islets into the patients' liver, is currently the gold standard in cell therapy for treatment of Type I Diabetes Mellitus (T1DM). Although CIT has been successful in improving metabolic control in patients, loss of a large portion of the infused islet mass due to direct contact with blood, the ensuing inflammation, and recurring immune response to the allograft imposes the requirement of a supplementary immunosuppressive therapy. Albeit partially effective, these pharmaceutical regimens have detrimental effects on the patient and adversely affect islet graft function. A more attractive alternative would be to obviate the need for systemic immunosuppression via polymeric modification of cellular surfaces capable of mitigating inflammation during the early engraftment period and masking of cell surface antigens, resulting in camouflage of the cell graft from the recipient's immune system. Moreover, bioactive modification of these surfaces bestowing the ability to directly modulate immune cell function locally would prove invaluable.

1.2 SPECIFIC AIMS

The **long-term goal** of this project is to evaluate and develop methods of protecting donor islets from both adverse acute inflammatory reactions and recurring adaptive immunity after transplantation through polymeric and bioactive surface modification. The **objective** of this dissertation was to evaluate the effects of PEGylation, the grafting of methoxy-poly(ethylene glycol) (mPEG) onto the islet surface, on islet viability and function *in vitro*, islet graft survival after allogeneic transplantation, and to elucidate the

mechanism through which graft protection is conferred. In addition, it sought to determine the feasibility of tethering bioactive motifs onto surfaces to enable modulation of immune cell function upon cell-surface interactions for incorporation into cell surface coatings in the near future. We **hypothesized** that PEGylation would result in enhanced graft survival and reduce the necessity for potent immunosuppressive regimens, and that immune cell function could be directed through tethering of bioactive motifs onto surfaces. We tested our central hypothesis by pursuing the following aims:

AIM 1 Optimize the procedure for grafting PEG onto islet surfaces and evaluate its potency for immunocamouflage in murine allograft models. The conditions for grafting PEG onto the islet surface were optimized in order to maximize cell viability and polymer grafting. PEGylation of murine islets was verified, followed by an evaluation of its effects on islet viability and function *in vitro* through Live/Dead staining and glucose stimulated insulin release assays. Following verification of adequate islet function, the immunoprotective capability of PEGylation was determined by evaluating the long-term (>100 days) function and persistence of the grafts through *in vivo* testing in a fully mismatched allogeneic murine model of transplantation.

AIM 2 Evaluate the complementary impact of PEGylation with short-course immunotherapy in murine allograft models. Following characterization of the impact of PEGylation on islet viability and function *in vitro* and *in vivo*, the effect of PEGylation in combination with a mild short-course immunotherapy was evaluated to determine if a synergistic effect between the complementary therapies could be observed; resulting in enhanced graft survival and persistence.

AIM 3. Elucidate the impact of islet PEGylation on local host responses with and without complementary short-course immunotherapy. Following the long-term *in vivo* experiments, the effects PEGylation, both alone and in combination with a mild short-course immunotherapy, on the graft microenvironment were characterized through histological assessments. Moreover, the transplants were replicated and the effects of the different treatments on the graft microenvironment during the early engraftment period (≤15 days) were characterized to elucidate the mechanism by which immunoprotection is achieved.

AIM 4. Examine the translational potential of PEGylation by scaling up procedure and testing in nonhuman primate model. The feasibility of scaling up the PEGylation procedure and its potential for clinical translation were examined through pilot studies conducted using a non-human primate (NHP) model of allotransplantation, which includes a mild immunotherapy. *In vitro* characterization and long-term graft function and persistence were evaluated. Additionally, the effect of the treatment on the graft microenvironment was preliminarily evaluated.

AIM 5. Screen the potential of Staudinger ligation for tethering bioactive agents to direct immune responses. To determine the feasibility of using PEGylated surfaces as a platform to engineer surfaces for controlled presentation of bioactive agents or motifs, in vitro studies were conducted. The ultimate goal of these pilot studies were to evaluate the capacity of surface modification to directly modulate immune cell function.

1.3 CONTENTS OF THIS DISSERTATION

The main objective of this dissertation was to determine the immunoprotective capability of PEG grafting onto the islet surface and characterize its ability to mitigate

immunosuppression requirements in a transplantation setting. Further, these platforms were used to explore the potential to chemoselectively tether bioactive motifs onto surfaces for modulation of immune cell function. **Chapter 2** describes background information concerning Type I Diabetes, current treatment strategies and challenges encountered in CIT, and the latest developments in the areas of encapsulation and bioactive materials in this context.

Chapters 3-5 explore the evaluation of PEG grafting onto murine islet surfaces, its effects on viability and function *in-vitro*, and long-term function and persistence of transplanted grafts. Additionally, it examines the effects on the graft microenvironment after long-term engraftment and during the early stages immediately following transplantation. **Chapter 6** examines the effects of PEGylation on islet viability and function, as well as long-term graft function and persistence, in an NHP model of transplantation. **Chapter 7** continues with the development of PEG-protein conjugates and a method to chemoselectively tether them onto surfaces with the goal of directing immune cell function for future incorporation into encapsulation materials and islet surfaces. **Chapter 8** summarizes the work contained within this dissertation and discusses recommendations on future work to further the research contained herein.

Chapter 2. Background and Significance

2.1 TYPE I DIABETES AND CURRENT THERAPIES

Type I diabetes mellitus (T1DM) is an autoimmune disorder characterized by destruction of the insulin producing β cells within a patient's pancreatic islets of Langerhans.[1] It accounts for an estimated $14.9 billion in healthcare costs in the U.S. each year, with as many as three million Americans living with the condition and more than 15,000 children and 15,000 adults diagnosed annually.[2] Exogenous insulin replacement is the most common treatment, where manual delivery is dictated by periodic monitoring of blood glucose levels. However, mimicking the complex and nonlinear dynamics of natural insulin secretion from native beta cells through insulin shots or even implantable pumps is a difficult task. Given this lack of precise control, T1DM patients currently face earlier mortality and a higher risk of angiopathic lesions, often resulting in neuropathy, nephropathy, and retinopathy.[3]

Replacement of beta cells via cellular transplantation has the promise of providing a long-term cure for T1DM. At the forefront of cellular replacement therapy is clinical islet transplantation (CIT), which currently involves the intraportal infusion of allogeneic islets **(Figure 1)**.[4, 5] In summary, these trials found strong improvement in metabolic control, with 57% of patients achieving insulin independence and ~70% with measureable c-peptide levels after 5yrs.[5-11] While CIT is promising, it has become evident that the significant inflammatory and immunological host responses to the implant, as well as the undesirable location of the liver, lead to islet dysfunction and destruction.

The early loss of transplanted islets has been partially attributed to the hepatic site, where as much as 60% of the islets may be lost during engraftment.[12-14] As islet emboli

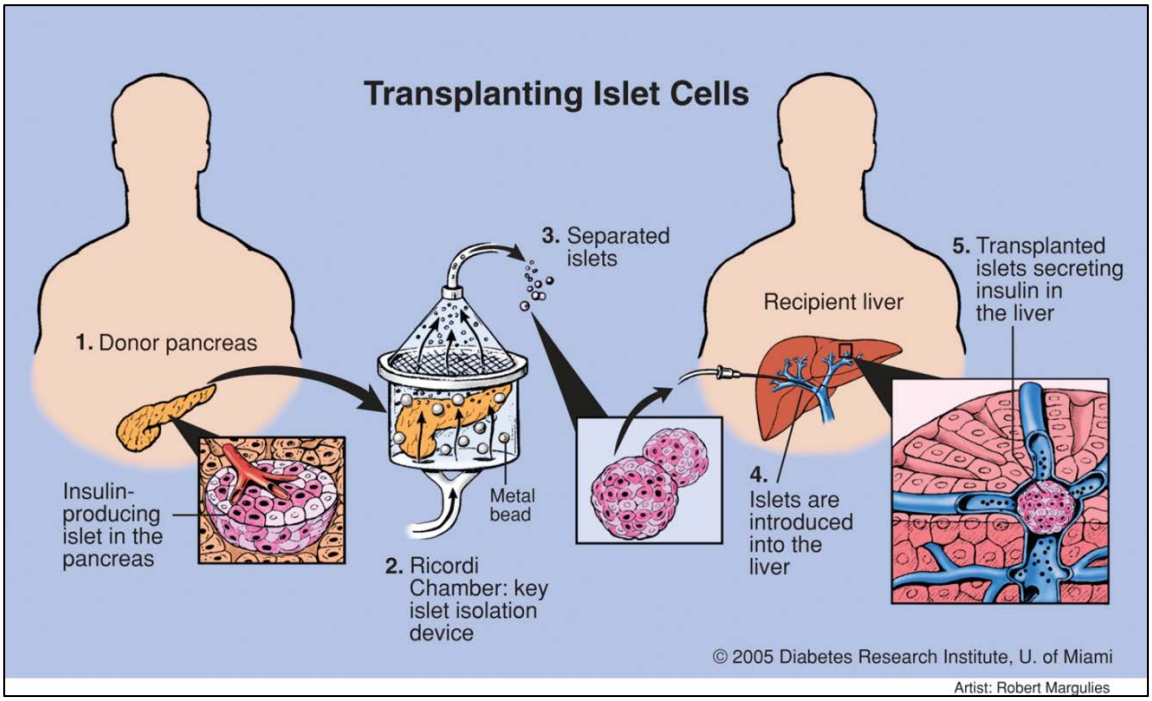

Figure 1. Diagram depicting Clinical Islet Transplantation

lodge in the hepatic microvasculature, capillary bed occlusion results in hypoxia and subsequent inflammatory cytokine release by surrounding tissue.[15] Of greater significance, islets in direct contact with blood instigate a potent inflammatory response, termed instant blood-mediated inflammatory reaction (IBMIR).[15-18] Additionally, islets experience non-native mechanical stress and exposure to toxins filtering through the liver.[19] Finally, recurrent autoimmunity persists leading to allograft rejection in spite of glucocorticoid-free immunosuppression regimens.[20-24] Consequently, alternative transplant sites are being explored, and even engineered, in order to enhance islet cell survival and reduce the functional islet mass for CIT.[25]

2.2 IMMUNOISOLATION THROUGH ENCAPSULATION

2.2.1 THE IMMUNE SYSTEM AND ISLET TRANSPLANTATION

While optimization of transplant sites through bioengineering can dramatically decrease the functional islet mass for syngeneic animal models, immunological responses to the transplant will still require potent immunosuppressive drugs. To alleviate this issue, strategies that can significantly reduce, or even eliminate, immune attack of the transplanted islets would prove highly beneficial. In order to do so, one must take into consideration the several interrelated mechanisms for wound healing and defense the body has developed, including blood coagulation, inflammation and innate immunity, and adaptive immunity, all of which play a role in islet graft rejection.

Coagulation is the mechanism through which the body stops bleeding from injured vasculature by the transformation of blood into a fibrin gel plug, or clot.[26, 27] This process is tightly regulated by a variety of factors in the blood that, when activated, produce a chain reaction known as the "coagulation cascade" which ends in clot formation (**Figure 2**). Two pathways exist in the initiation of the coagulation cascade, the intrinsic pathway and the extrinsic pathway. Usually, as a result of injury, the extrinsic pathway is responsible for clot formation. Upon vessel damage, blood escapes the endothelium and is exposed to subendothelial tissues, whose cells express the membrane protein tissue factor (TF). The interaction of TF with the blood plasma protein Factor VII results in its activation into Factor VIIa, and initiation of the coagulation cascade (**Figure 2**). This process is of interest in the context of CIT since islets express TF and, as a result, are vulnerable to thrombotic reactions when exposed to blood. This phenomenon, termed IBMIR as described above, has been well documented [16-18, 28], and also results in the

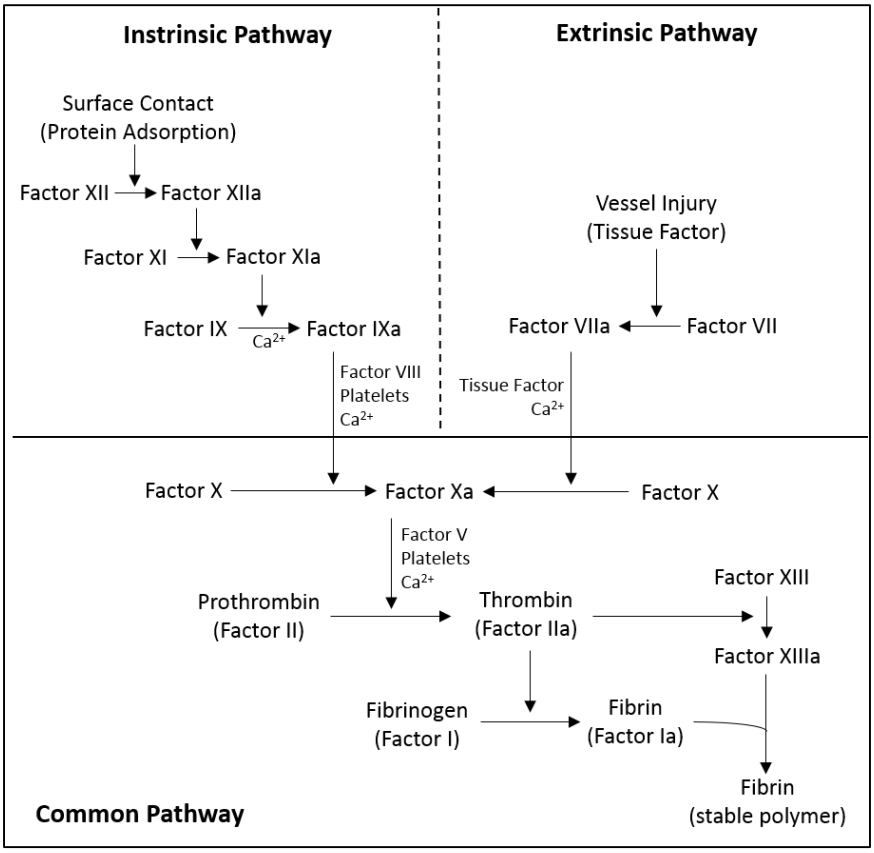

Figure 2. The coagulation cascade. Schematic depicting different factors involved in initiation of blood coagulation through both the intrinsic and extrinsic pathways, which ultimately converge into the common pathway and result in clot formation.[27]

activation of the complement cascade and infiltration of leukocytes, resulting in the loss of a large percentage of the islet mass transplanted.[28]

In addition to blood coagulation, inflammation is another mechanism of concern in islet transplantation. Inflammation refers to the local response of tissue to injury and serves to neutralize or destroy foreign infections, such as microbes or viruses, and set the stage for tissue repair and/or scar formation.[26, 27] The main effectors of inflammation are phagocytic cells such as granulocytes and macrophages, and NK cells. As a first line of defense, these cells are also part in the innate immune response, an evolutionarily primitive general nonspecific response triggered by molecular structures commonly found in

microbes. In addition to custodial duties, these cells secrete a variety of factors and cytokines that serve to regulate and coordinate the cellular response. Although these cells are limited in the ability to distinguish different antigens, they do serve as a bridge to the adaptive compartment of the immune system, since they present antigens to lymphocytes and provide context in which these cells are to respond. For CIT, inflammation and the innate immune system are of interest, as they include the first responders in an immune response, determine the type of response that will take place, and regulate tissue repair and resolution of injury.

The adaptive immune system is of utmost importance when discussing any type of transplantation. It is a more evolutionarily advanced defense mechanism capable of identifying specific antigens not associated with the "self" and is characterized by three stages: (1) antigen recognition; (2) cell activation and clonal expansion; and (3) foreign body attack. This compartment of the immune system is referred to as adaptive because it has the ability to recognize antigens never seen before and to "adapt" by generating memory effector cells that can mount a more vigorous response upon subsequent exposures of the same microorganisms. The main effectors of this compartment of the immune system include T cells, B cells, and secreted antibodies. Although not fully characterized, most evidence indicates that helper (CD4+) and cytotoxic (CD8+) T cells play a major role not only in islet but allograft rejection in general.[29-33]

The adaptive immune system relies on two pathways for the recognition of foreign antigens: (1) direct and (2) indirect antigen presentation **(Figure 3)**. In the direct presentation pathway, donor antigen-presenting cells (APCs), in this case the transplanted graft itself or passenger APCs, activate T cells through the major histocompatibility

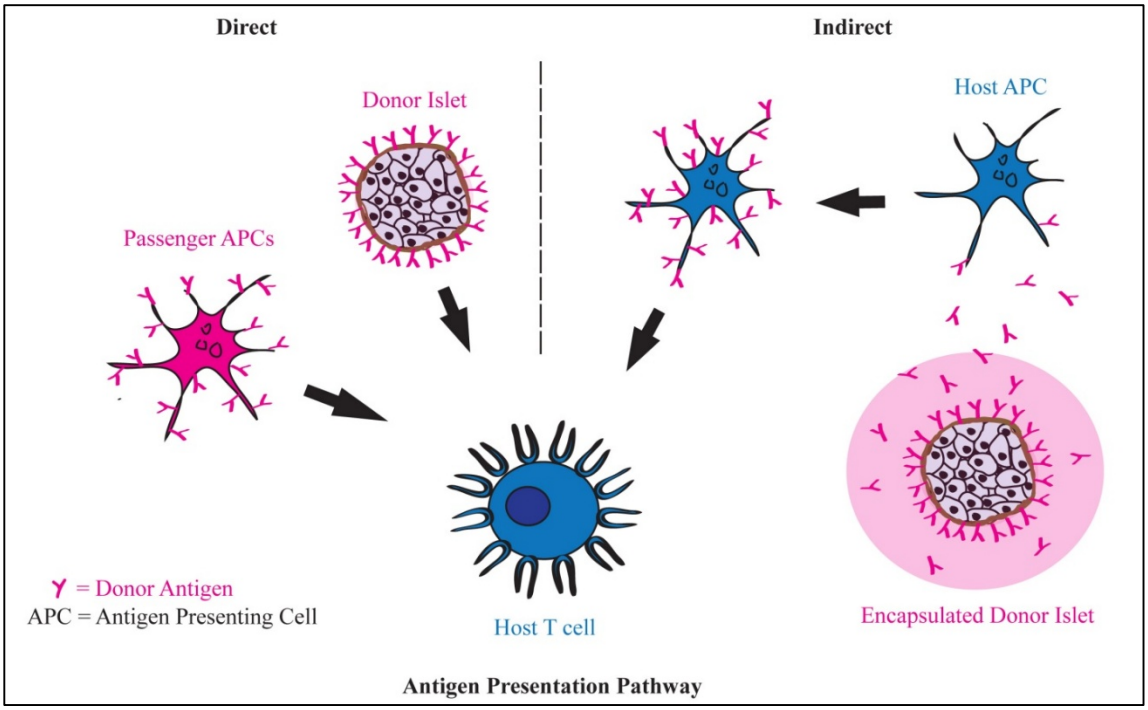

Figure 3. Antigen presentation pathways. Schematic depicting the direct and indirect antigen presentation pathways.[34]

complex via direct cell-to-cell contact. In the indirect presentation pathway, host APCs pick up donor cell antigen fragments and present them to T cells, inducing activation.[34]

When T cells encounter an antigen, they rely on the integration of two signals from antigen-presenting cells (APCs) to determine how they will respond (**Figure 4**).[35-38] The primary signal is the antigen itself which is presented to the T cell by the APC in the form of an antigen-MHC complex and is transduced through the T cell receptor. Its main role is identifying the antigen in question. The secondary signal is that of the co-stimulatory molecule. This signal, expressed by the antigen-presenting cell (APC) as a result of the microenvironment and thus the functional status of the APC, provides the context in which the T cell is to respond to the antigen being presented. The secondary signal can either be a positive signal that induces T cell activation and an inflammatory response, as is the case

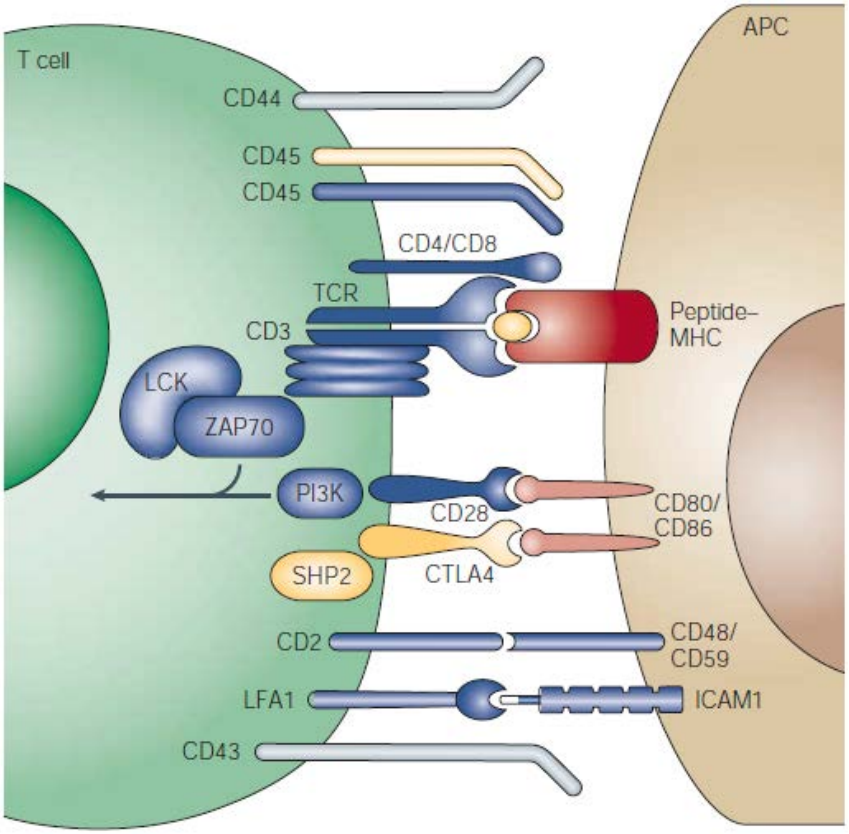

Figure 4. The immunological synapse and the two signal model of T cell activation.[40]

with interaction of the surface markers CD80 and CD86 on APCs with a T cell's CD28 receptor, or a negative signal resulting in T cell inhibition and an anti-inflammatory response, as is the case with interaction with the T cell's CTLA-4 receptor (**Figure 4**). This depiction is a simplification of an extremely complex signaling network involving different pathways linked to several cytokines, integrins, and other cell surface receptors at the immunological synapse that exceed the scope of this dissertation, all of which are ultimately integrated by the cell to respond accordingly.

Currently, CIT is carried out in combination with the potent immunosuppressive agents that act through different mechanisms to inhibit T cell activation, and thus the adaptive immune system. These include sirolimus, tacrolimus, and daclizumab (**Figure**

5).[5] Tacrolimus inhibits calcineurin, one of the proteins involved in the transduction of the T-cell receptor signal, which impairs the expression of genes involved in T-cell activation, a critical one being that coding for the IL-2 cytokine.[39-41] Sirolimus and daclizumab impede T-cell activation by obstructing the signal from the IL-2 receptor through inhibition of the mTOR protein in the receptor's signal transduction pathway and by blocking the IL-2 receptor itself, respectively.[40-42] Cyclosporine A, another calcineurin inhibitor, has also been used in an experimental setting to complement

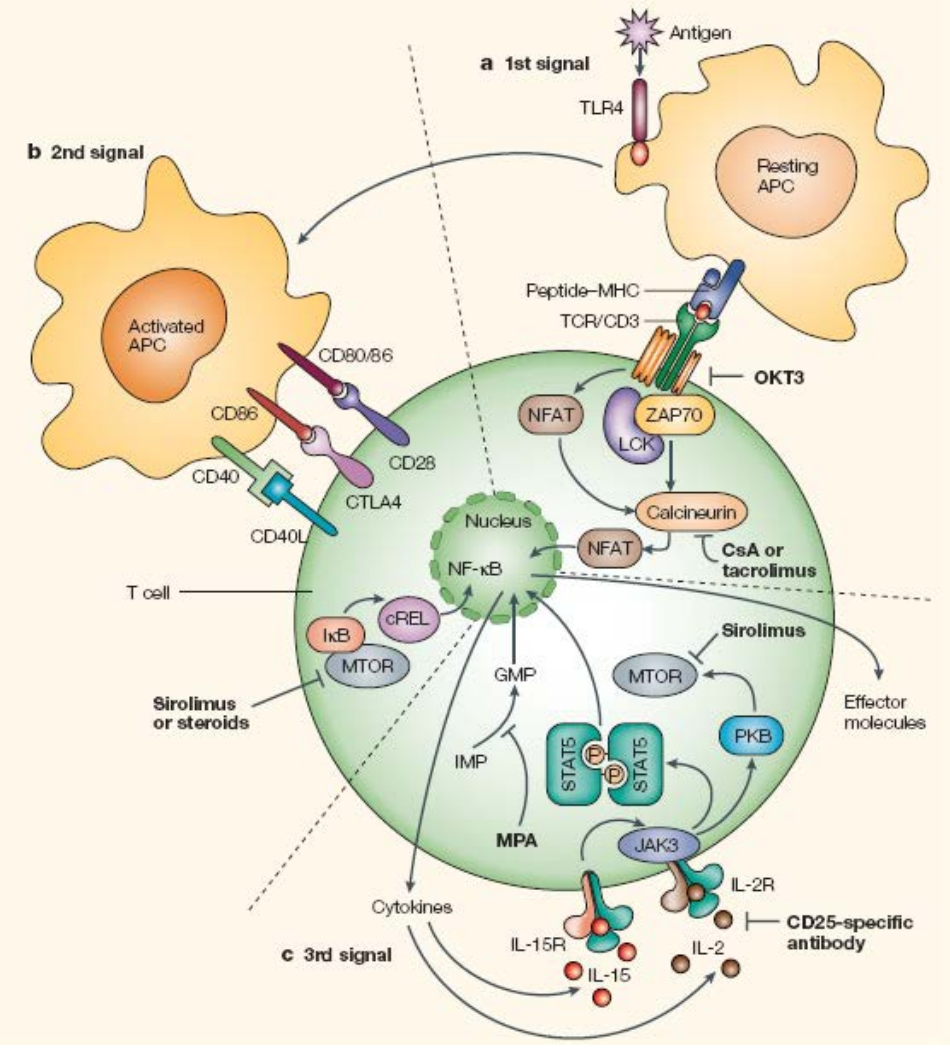

Figure 5. Common immunosuppressants used in solid organ transplantation and their mechanism of action.[45]

PEGylation in small animal transplant models.[43] Antibodies that target the T cell receptor, such as Muromonab-CD3 (OKT3), are drugs commonly used in solid organ transplantation to prevent and treat acute rejection by inducing T cell apoptosis. Finally, Thymoglobulin, a product composed of a mixture of different antibodies with specificities for different immune response antigens, adhesion molecules, cell-trafficking molecules, and a variety of other antigens involved in different pathways is also in use to deplete the patient of T cells.[44, 45] Although these drugs enhance graft survival, when used systemically they represent a risk to the patient who will have an impaired immune system. They have been shown to produce adverse effects on the patient and in addition impair islet graft function. As a result, it would prove advantageous to use mild immunotherapies or localized drug delivery and immunosuppression when possible.

Since the 1980s, researchers have tested several designs for a bioartificial pancreas capable of replacing the organ's endocrine function while preventing graft rejection due to the immune response. In principle, a stable biocompatible semipermeable barrier made from a variety of natural and/or synthetic materials should separate the tissue graft from the host's immune effectors, both cellular and humoral, while allowing for proper diffusion of nutrients such as oxygen and glucose, as well as metabolic waste and therapeutic cell products, such as insulin.[3, 46]

2.2.2 MACRO-SCALE ENCAPSULATION

Bioartificial pancreas devices are generally classified in two categories according to their implantation strategies: (1) intravascular or (2) extravascular **(Figure 6)**. Several groups investigated arteriovenous shunts anastomosed directly into the circulatory system. These early intravascular devices generally consist of a synthetic hollow fiber

semipermeable membrane that passes through a compartment seeded with pancreatic islets.[47-50] It was reasoned that close proximity to circulation would facilitate proper insulin secretion kinetics in response to blood glucose levels; however, *in vivo* studies were plagued with problems of membrane collapse, thrombosis, and limitations in transport properties.[47, 51]

Extravascular devices refer to macroencapsulated cells that are implanted outside of the vasculature, e.g., subcutaneously, intraperitoneally, or in the omentum. Although these devices, such as hollow fibers, diffusion chambers, and polymeric sheets, yielded encouraging results in rodents[52-59] and canines,[60-62] their large size and exclusive reliance on diffusive transport resulted in islet dysfunction and device failure in the long term. Mathematical modeling predicts inadequate transport profiles, indicating scalability

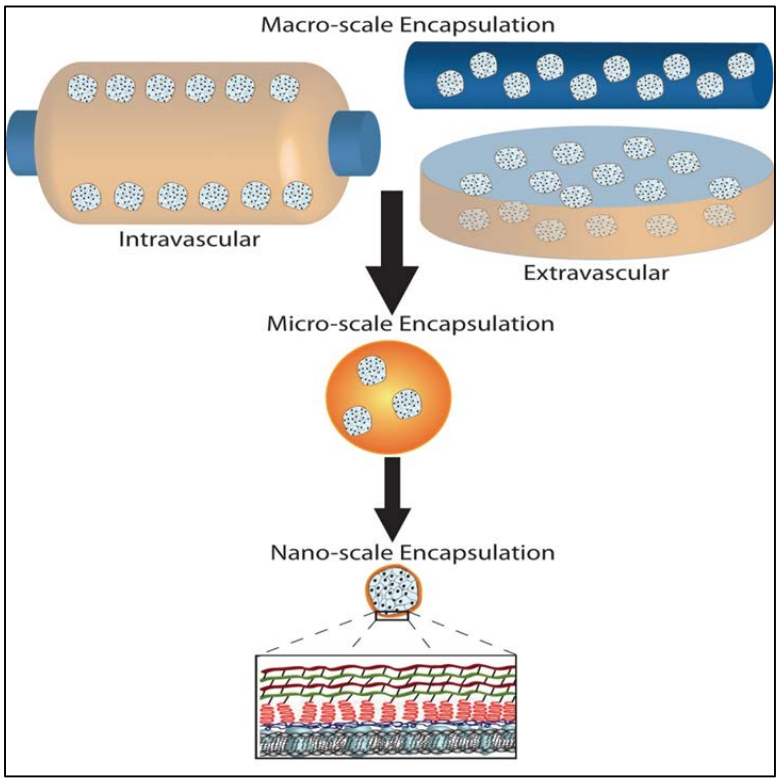

Figure 6. Summary of different encapsulation devices and strategies at different scales.[34]

of these devices to larger animal models will be problematic after islet density optimization, thereby rendering such implants bulky or requiring multiple devices.[53, 60, 63-66]

2.2.3 MICRO-SCALE ENCAPSULATION AND CONFORMAL COATING

Encapsulation of small groups or individual islets within micro-scale capsules evolved as an alternative strategy to macro-scale devices, where the increased surface-area-to-volume ratio results in enhanced transport properties. Traditional islet microencapsulation involves enclosing islets in a semipermeable alginate/poly-lysine (PLL) capsule held together by ionic interactions where porosity, and thus diffusive properties, is commonly controlled by altering the quantity and molecular weight of PLL used during processing.[67-69] Agarose has also been extensively studied as an encapsulation material, where beads are generated by cooling cell/agarose-oil emulsions to induce gelation.[70, 71]

Although the surface-to-volume ratio is improved in these capsules, drawbacks remain. Despite their micron-scale size, a large void space is generated between the islet and its surrounding environment, imposing significant increases in implant size and longer diffusion distances for nutrients and insulin.[72] Depending on the implant site and state of vascularization, this large void space could lead to graft dysfunction and apoptosis due to hypoxia[73] and a lag in glucose-stimulated insulin release into the bloodstream.[74, 75] In addition, the instability of the ionic interactions lead to decomposition of the capsule under physiologic conditions over time.[76]

While reduction of the alginate capsule size has been achieved via air-driven droplet generators[77, 78] or high voltage pulses,[79-81] these methods resulted in an

increased incidence of inadequate or incomplete coating of the islets and thus graft rejection by immune attack.[68] To avoid these issues and precisely control membrane properties, several groups developed methods to conformally coat islets in polymeric gels in the range of 10–100 μm thick. Approaches include entrainment through traversing liquid–liquid interfaces via a variety of methods such as centrifugation,[82, 83] selective withdrawal,[84] emulsions,[85] interfacial photopolymerization,[86, 87] and flow focusing methods.[88, 89] All of these methods establish the feasibility of conformal coating for islet encapsulation, but further *in vivo* studies need to be performed to evaluate the efficacy of these coatings in preventing rejection.

2.2.4 NANO-SCALE ENCAPSULATION

While research in conformal coating was progressing, researchers in the field of blood transfusion were developing alternative cell-coating strategies for a universal blood substitute. Sparked by the findings that covalent attachment of methoxy-poly(ethylene glycol) (mPEG) to exogenous proteins increased half-life and reduced immunogenicity without affecting function,[90, 91] researchers attempted to immune-camouflage red blood cells with a biocompatible steric barrier by cross linking the cell surface proteins with mPEG. Indeed, PEGylation, as this procedure has been termed, of red blood cells via a cyanuric chloride cross linker resulted in reduced antigenicity *in vitro* and *in vivo* and maintained normal cell function.[92] This inspired the PEGylation of a wide variety of tissues used for transplantation, including pancreatic islets, and gave rise to the concept of nanoscale encapsulation via surface modification.

Several groups have carried out PEGylation on the surface of islets through varying approaches, which include linking islet surface amine groups with isocyanate and *N*-

hydroxysuccinimide (NHS) functionalized PEG polymers,[43, 93-96] or inserting lipid moieties linked to a PEG chain within islet cell membranes.[97, 98] Not only did PEGylation have no adverse effects on islet viability or function,[93, 94] but it was also found to reduce islet recognition and activation of immune cells *in vitro*,[95, 96] prolong survival of the allograft in the absence of immunosuppression,[99] and reverse diabetes when combined with reduced immunosuppression in rodent models.[43]

Covalent modification of amine groups on islet surface proteins presents a problem due to periodic turnover of membrane components[93] and possible interference with cell surface protein activity.[100] To avoid these issues, Wilson and colleagues[101] have used a non-covalent approach of coating islets via electrostatic interactions with modified PLL. Exposure to PLL alone, as with other polycations, results in high levels of cytotoxicity; however, if modified to the appropriate degree with PEG, the PLL, referred to as PP-OCH_3, can interact with the islet surface without inducing apoptosis. In addition, the chemoselective reactive groups hydrazide, azide, and biotin were introduced by functionalization of the PEG macromers prior to PLL modification.[101-103] PEGylation and noncovalent coating of islet surfaces also function as foundations for the fabrication of complex coatings though layer-by-layer assembly. These layers are stabilized by ionic interactions between oppositely charged polymers[104] or by complimentary chemoselective reactive groups tethered to adjacent layers.[100, 105, 106] While still in the preliminary stages, nanoscale encapsulation has the potential to permit for the reengineering of the islet surface with polymers in a manner that is precisely controlled.

2.3 IMMUNOMODULATION AND BIOACTIVE POLYMERS

While encapsulation has the capacity to prevent immune activation via the direct antigen presentation pathway, antigen shedding from the transplanted cells and subsequent indirect pathway activation is difficult to prevent due to permeability requirements that must be satisfied to allow nutrient influx and insulin outflux **(Figure 3)**. There has been growing interest in modifying encapsulation materials to confer biological functionality, thus controlling the *in vivo* microenvironment, to enhance islet viability and function and modulate the immune response. For example, after isolation, islets exhibit a progressive decline in function as measured by insulin expression, insulin content, and glucose-stimulated secretion. This issue can be circumvented by reestablishing islet–ECM interactions using ECM protein coatings or adhesive peptide sequences.[107] Weber and associates exploited this and demonstrated enhanced glucose-stimulated insulin secretion of murine islets for up to a month *in vitro* following encapsulation in PEG hydrogels containing collagen IV, laminin, and the adhesive peptide RGD.[108] Lin and Anseth[109] described a PEG-diacrylate-derived hydrogel co-functionalized with the laminin adhesive sequence IKVAV and a glucagon-like peptide-1 analog modified with a carboxyl terminal cysteine group to allow for covalent thiol-acrylate photo crosslinking. Glucagon-like peptide-1 has been previously described to protect islets from cytokine-induced apoptosis and enhance insulin secretion. Murine islets encapsulated in these gels exhibited enhanced viability and function compared to controls, although overall viability was low due to free radical generation during the polymerization process.[109] These strategies mitigate islet cell death, thus reducing shedding of antigens and inflammatory signals that could trigger an indirect immune response.

Furthermore, proinflammatory cytokines freely diffuse through the polymers, instigating graft cellular apoptosis.[108] To combat these responses, another avenue for polymer functionalization seeks to confer additional immune-protective effects *in vivo* via immunomodulation of the host environment. Su and coworkers[110] described a four-arm PEG-derived hydrogel network generated through amine-thioester native chemical ligation co-functionalized with an IL-1 receptor antagonist peptide sequence and an adhesive peptide sequence via maleamide-thiol cross linking. The scheme allows for efficient control of gelation and functionalization due to the chemoselectivity of the reactions. Despite debatable results of cytotoxic T cell co-culture experiments and the preliminary nature of the publication, this study showed enhanced viability and function as measured by glucose-stimulated insulin secretion in MIN6 cell clusters as a result of IL-1 receptor inhibition after exposure to multiple inflammatory cytokines. Lin and colleagues[111] described the co-functionalization of PEG-diacrylate hydrogels with an RGD adhesive peptide and a tumor necrosis factor-α (TNFα) sequestering peptide sequence, resulting in inhibition of TNF receptor 1 activation. Upon encapsulation within these gels, TNFα challenged murine islets exhibited decreased caspase 3/7 activity, indicative of inhibition of apoptotic pathways, along with metabolic activity and insulin secretion comparable to that of encapsulated, unchallenged islets. One more recent approach employed TGF-β1 and IL-10 modified PEG to generate hydrogels capable of reducing dendritic cell activation.[112] Modifications to encapsulation materials such as these show promise in enhancing islet function and prolonging graft survival once implanted in the recipient.

Surface modifications of the polymeric coatings with anti-inflammatory agents can also serve to mitigate IBMIR-associated responses and generalized inflammatory

processes. For example, reactive groups on functionalized encapsulating polymers can be used for ligation of different bioactive effectors such as thrombomodulin, with the idea of generating a localized anti-inflammatory microenvironment.[102, 103] Other examples include tethering of urokinase, heparin, and poly(lactic-co-glycolic acid) (PLGA) nanoparticles loaded with leukemia inhibitory factor (LIF) for its controlled release.[98, 113, 114]

Pathways involved in the regulation of the adaptive immune compartment are also of particular interest due to the certainty of alloimmunity and its central role in graft rejection.[33, 115, 116] One such pathway involved in the regulation of the adaptive immune response is the Programmed Death-1 (PD-1) receptor/programmed death ligand 1 (PD-L1) pathway. PD-L1 is a member of the B7-CD28 superfamily of co-stimulatory molecules which has been extensively studied and identified as a key regulator of T cell inhibition.[35-38, 117-123] Engagement of PD-L1 with the PD-1 receptor on the T cell surface has been shown to result in reduced T cell proliferation and differentiation, reduced T cell survival, and decreased cytokine production.[38, 117-123] Additionally, this pathway has also been identified as a major mechanism in regulation of peripheral tolerance through induction of regulatory T cells (Tregs) and T cell exhaustion.[38, 117-124] By tethering PD-L1 onto the surface of islets destined for transplant, one could exploit its inhibitory functions and further promote allograft survival by directing immune cell function towards a more tolerogenic nature.

Chapter 3. Islet PEGylation Optimization and Evaluation of Immunocamouflage Potency in Murine Allograft Models

3.1 INTRODUCTORY REMARKS

As mentioned above, grafting of mPEG onto cell surfaces is an attractive alternative approach to full barrier polymeric encapsulation, as it has shown promise in mitigating the immunogenicity of cells without affecting their function. Conjugation of PEG to proteins or cell surfaces is typically achieved using the heterofunctional PEG: NHS-PEG-CH3, also known as NHS-mPEG. NHS ester-activated polymers spontaneously react with primary amines in physiologic to slightly alkaline conditions (pH 7.2 to 9) to yield stable amide bonds (**Figure 7**), while the methyl group (CH3) provides an inert terminal group. PEGylation of the islet cell cluster is a highly attractive approach to immunocamouflage the foreign graft, as this simple and efficient conjugation strategy can easily be performed prior to transplant without the need of altering the transplantation procedure (i.e. islets can still be infused into the liver). Given this appeal, islet surface PEGylation has been explored using varying approaches, with no adverse effects on islet function or viability observed.[93, 94] In vivo, however, PEGylation has not been shown to significantly extend allograft survival in rodent models, with the exception of a single study exhibiting modest protection using a triple PEGylation procedure.[99]

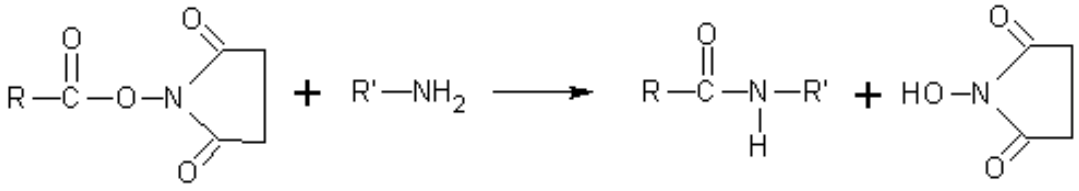

Figure 7. Reaction between NHS ester and primary amine to form a stable amide bond.

Islets are exceptionally sensitive cell organoids. As a result, their surrounding environment must be carefully controlled during any type of manipulation to minimize cell death. Therefore, before one can begin to assess the efficacy of PEGylation in protecting islets from an immune response, the procedure for carrying out the polymer grafting reaction must be optimized. Additionally, the source of the polymer is an important factor to take into consideration, as most, if not all, of the commercially available polymers are not certified for use with cell cultures and, due to the nature of the manufacturing process and the organic solvents involved, have the potential to result in islet cell death. Herein, the optimization of the PEGylation procedure, along with testing a variety of sources of NHS-mPEG polymer to ensure adequate islet viability and function, is described. Subsequently, the immunoprotective effects of PEGylation were evaluated *in vivo* in a fully mismatched MHC murine model of transplantation.

3.2 MATERIALS AND METHODS

3.2.1 COMMERCIALLY AVAILABLE POLYMERS

Various lots of NHS-mPEG polymer (MW 5000 Da, Laysan Bio, Inc.) were screened in polymer grafting optimization experiments. In selected experiments, NHS-PEG-N_3 polymer (MW 5000 Da, Laysan Bio) substituted for PEGylation screening, as the N_3 terminal group for required for chemoselective tethering of agents. The azide terminal group in these polymers should not impact the outcome of the experiments, as N_3 is stable and is nontoxic in bound form. This chemistry will be further discussed later in Chapter 7, where it is employed for tethering bioactive motifs onto surfaces.

3.2.2 NHS-mPEG POLYMER SYNTHESIS

As an alternative to commercially available polymers and to ensure proper polymer purification and organic solvent removal, NHS-PEG-CH_3 was also fabricated in-house. This was done by dissolving NH2-PEG-CH_3 (2 g, JenKem Technology USA, MW 5000 Da) in 4 mL of anhydrous N,N'-dimethylformamide (DMF) at 37 ˚C under Argon. A solution consisting of glutaric anhydride (50 mg) dissolved in 0.4 mL DMF was then injected drop-wise into the PEG solution, followed by drop-wise injection of a solution consisting of 112 µL triethylamine in 0.4 mL DMF. After stirring for 25 min, the product (COOH-PEG-CH_3) was precipitated with 60 mL cold diethyl ether, collected by centrifugation, and dissolved in 60 mL absolute ethanol at 37 ˚C. The solution was then filtered through a 5 mm silica gel plug inside a Pasteur pipet and the polymer was precipitated and collected by cooling in an ice-water bath and centrifugation. This product was rinsed by vortex-shaking with 60 mL cold diethyl ether, collected by centrifugation, and dried under reduced pressure.

The above product (925 mg) and N-hydroxysuccinimide (65 mg) were dissolved in 1.5 mL DMF at 37 °C under Argon. A solution of 176 µL diisopropylcarbodiimide (AnaSpec) was dissolved in 0.4 mL DMF and injected to the PEG solution. After stirring for 2 h under Argon, the product was precipitated with 40 mL cold diethyl ether and collected by centrifugation. This was subsequently dissolved in 32 mL absolute ethanol at 37 °C, precipitated by cooling in an ice-water bath, and collected by centrifugation. The product was rinsed with 40 mL cold diethyl ether, collected by centrifugation, and dried under reduced pressure. The final yield was 900 mg of NHS-mPEG powder. Chemical modifications throughout this process were monitored by ATR-FTIR.

3.2.3 ANIMALS

All animal studies were reviewed and approved by the University of Miami Institutional Animal Care and Use Committee. All procedures were conducted according to the guidelines of the Committee on Care and Use of Laboratory Animals, Institute of Laboratory Animal Resources (National Research Council, Washington DC). Animals were housed within microisolated cages in Virus Antibody Free rooms with free access to autoclaved food and water at the Department of Veterinary Resources of the University of Miami. The Preclinical Cell Processing and Translational Models Core at the Diabetes Research Institute performed the rodent islet isolations, diabetes induction, and animal monitoring. Male DBA/2J (H-2^d) mice between 10-12 wks of age were used as islet donors and male C57BL/6J (H-2^b) mice between 7-9 wks of age were used as transplant recipients (Jackson Laboratory; Bar Harbor, Maine).

3.2.4 ISLET ISOLATION AND CULTURE

Mouse islets were obtained from donor mice via mechanically-enhanced enzymatic digestion followed by density gradient purification, as previously described.[125] Islet purity was assessed by dithizone (Sigma) staining, and the islets were counted and scored for size using an algorithm for the calculation of the 150 μm diameter islet equivalent (IEQ) number. The DRI Preclinical and Translational Models Core performed all mouse islet isolations. Mouse islets were cultured in complete CMRL 1066-based medium (Mediatech), which is CMRL 1066 supplemented with 10% fetal bovine serum (FBS; Mediatech), 20mM Hepes Buffer, 1% penicillin-streptomycin (Sigma), and 1% L-glutamine (Sigma).

3.2.5 PEGYLATION PROCEDURE OPTIMIZATION AND IN-VITRO ISLET CHARACTERIZATION

3.2.5.1 OPTIMIZATION OF PEG GRAFTING REACTION CONDITIONS

The primary objective of these series of experiments were to identify a set of culture conditions that would promote optimal grafting of the PEG to the islet surface, without impacting islet function or viability. In accordance to what has been published in the literature with regards to cell PEGylation, solutions of 4mM PEG polymer were tested. Since NHS reacts with free primary amines, the solvent used during this reaction must be free of proteins or amine groups, to avoid cross-reaction of the PEG with free amines in the culture solution and ensure maximal polymer grafting to amines on the islet surface. As islets are exceptionally fragile and sensitive to their surrounding environment, the primary concern was variation in the pH of the solution over time. To investigate this, the polymer was dissolved in DPBS and the pH was measured immediately after dissolution (t = 0) and every 15 minutes thereafter for a total time of 2 hours. During this time, the solution was incubated at 37°C as this is the temperature used for PEGylation of islets.

3.2.5.2 POLYMER SOURCE TESTING

As mentioned above, cytotoxicity due to improper purification of the polymer and remnants of organic solvents from the manufacturing process are a concern when using commercially available polymers that are not cell culture tested and certified. As a result, trial experiments to assess cytotoxicity were performed on different polymers lots purchased. Following 48 hr culture, PEGylation was carried out by incubation of islets in 4mM solutions of different lots of purchased NHS-PEG-N_3 polymer in DPBS (pH 7.8) supplemented with Ca/Mg and 11 mM D-Glucose for 45 min at 37°C at a cell density of

600 IEQ/mL. After incubation, islets were washed thrice in full media, cultured overnight, and viability was assessed the following day by Live/Dead staining.

3.2.5.3 OPTIMIZED PEGYLATION PROCEDURE

Isolated islets were cultured for 48 h prior to PEGylation. On the day of the procedure, islets were counted, washed thrice in DPBS, and incubated for 45 minutes at 37°C in a 4 mM NHS-mPEG solution in DPBS (pH 7.8) supplemented with Ca/Mg and 11 mM D-Glucose at a cell density of 1500 IEQ/mL. Following PEGylation, the islets were washed thrice in full media and placed in the incubator for overnight culture prior to assessment or transplantation. For imaging of islet coating, NHS-PEG-FITC (5,000 MW, NANOCS) was used in lieu of NHS-mPEG.

3.2.5.4 CONFIRMATION OF PEG GRAFTING ONTO THE ISLET SURFACE

The grafting of PEG to the islet surface was confirmed through the visualization of NHS-PEG-FITC. Islets were imaged 24 h after conjugation on a Leica SP5 inverted confocal microscope. Single plane images and merged multi-slice images (4-8 μm thickness; 8-15 slices per image; 1024x1024; 20x objective) were collected. Islets were counterstained with Hoescht 33342 dye for cell nucleus visualization.

3.2.5.5 LIVE/DEAD STAINING

Live/Dead staining was performed using the LIVE/DEAD Viability/Cytotoxicity Kit (Molecular Probes, L-3224). Islets were washed with PBS, resuspended in the Live/Dead solution containing 2 μL Calcein-AM/8 μL Ethidium Homodimer/2 mL PBS, and incubated for one hour prior to imaging on the confocal microscope.

3.2.5.6 GLUCOSE-STIMULATED INSULIN RELEASE (GSIR) ASSAY

A static incubation column method for glucose-stimulated insulin release was performed to determine insulin responsiveness of control and PEGylated islets. Sephadex G-10 beads (GE Healthcare, Cat. No. 17-0010-02) were swollen and sterilized by heating to a slow boil in PBS (pH 7.4) for 1 hour. Krebs 1x buffer (115mM NaCl, 4.7mM KCl, 2.5mM CaCl2, 1.2mM KH2PO4, 1.2mM MgSO4, 26mM NaHCO3, 25mM Hepes, 0.2% BSA, pH7.4) was prepared as high (3mg/mL) and low (0.4mg/mL) glucose solutions. The beads were then cooled by subsequent addition of cold PBS. While stirring, a P-1000 micropipettor was used to add bead suspension to commercially available Poly-Prep chromatography columns (BioRad, Cat. No. 731-1550). The beads were added an allowed to settle until they reached the 400 μL mark on the column. The volume of beads added was noted to ensure the same volume was added to each column. 150 IEQ's, control or treated, were then added to each column followed by addition of beads until they reached the 1mL mark, essentially embedding the islets within the beads. The PBS was allowed to flow through the column followed by addition of 4mLs of low glucose solution. This solution was also allowed to flow through and the columns were allowed to equilibrate for 1 hour in the incubator at 37^0C and a 5% CO2 atmosphere. After equilibration, a series of incubations in low, high, and low glucose buffers were carried out, each consisting of adding 4 mLs of buffer, allowing the solution to flow through the columns, incubating as described above, and collecting 1mL of the solution for analysis by adding 1mL of buffer using a P-1000 micropipettor following the incubation. Samples were stored at -80*C immediately after collection. Insulin content in the samples was measured using a commercially available Mouse Insulin ELISA Kit (Mercodia, Cat. No. 10-1247-10).

3.2.6 ALLOGENEIC MURINE ISLET TRANSPLANTS

As described above, male DBA/2J (H-2^d) mice between 10-12 wks of age were used as islet donors and male C57BL/6J (H-2^b) mice between 7-9 wks of age were used as transplant recipients (Jackson Laboratory; Bar Harbor, Maine). Mice were rendered diabetic by intravenous administration of 200 mg/kg streptozotocin (STZ; Sigma, St. Louis, MO) freshly dissolved in citrate buffer streptozotocin as previously described[105] and were only used as recipients after 3 consecutive readings of non-fasting blood glucose levels > 350 mg/dL using portable glucose meters (OneTouchUltra2; Lifescan, Milpitas, CA). Islets (700 – 800 IEQ) were transplanted in the kidney subcapsular space of anesthetized mice 24 hr after coating, for a total of 3 days post-isolation, as previously described.[126] Briefly, one by one, mice were anesthetized with 2% isofluorane, their left dorsal flank was shaved and sterilized with chlorhexidine and a small transverse incision was then made through the skin and muscle just above the kidney into the abdominal cavity. The kidney was then gently extruded through the incision, a small hole was poked into the renal capsule, and islets were gently deposited in the subcapsular space using a Hamilton syringe and PE-50 tubing making an effort to minimize damage to the kidney parenchyma. The small hole in the capsule was then cauterized and the kidney carefully reinserted into the abdominal cavity followed by suturing of the muscle and stapling the skin shut. Saline was used periodically to ensure proper hydration of the organ throughout the procedure and standard pain management and antibiotic therapy was given following the all surgeries.

For these experiments control animals received untreated islets with saline (n = 20) and PEG animals received PEGylated islets and saline (n = 11). Saline solution was administered because these animals served as controls for additional experiments described

in Chapter 4, where other experimental groups received a short-course immunotherapy. Normoglycemia of the recipients was defined as non-fasting glycemic levels < 200 mg/dL for 2 consecutive readings. Mice that remained hyperglycemic for over 10 d following transplant were classified as Primary Non-function, euthanized, and censored from long-term graft analysis. Graft rejection was defined as functional grafts that exhibited diabetes recurrence, i.e. glycemic levels > 300 mg/dL for over 3 d, at which point the animal was euthanized and the graft explanted for analysis. All long-term (> 100 d) functional grafts were electively explanted in a survival nephrectomy to confirm subsequent diabetic status of recipients. For these studies, kidneys were fixed in 10% formalin solution, embedded in paraffin, and cut into 5 μm sections for staining.

3.2.7 STATISTICAL ANALYSIS

For in vitro studies, comparisons between groups were made using the same islet preparation, with a minimum of three independent replicate measurements were made for each assay. Results are expressed as the mean ± SD. A minimum of three independent experiments (e.g. three islet isolations) were performed for each assessment, with graphs summarizing results from a representative experiment. Statistical analyses for islet viability and insulin secretion experiments used multi-factor analysis of variance, with student t-tests for comparison between individual groups. For time to reversal analysis (% normoglycemia), Mantel-Cox (logrank) test was performed to evaluate differences between groups.

3.3 RESULTS

3.3.1 PEGYLATION PROCEDURE OPTIMIZATION

3.3.1.1 OPTIMAL pH FOR PEGYLATION REACTION

Monitoring of solution pH over the 2 hour period following polymer dissolution revealed a gradual decrease of approximately 0.4 units per hour, as shown in **Figure 8**. This change towards a more acidic environment would be detrimental to islet health; therefore, to compensate for this change, it was determined that the pH of the PBS solution to be used for the procedure should be adjusted to 7.8 beforehand, taking into account that the PEGylation reaction with islets is carried out for 45 minutes. This modification should result in a solution pH would be at or close to physiological pH 7.4 near the end of the incubation period.

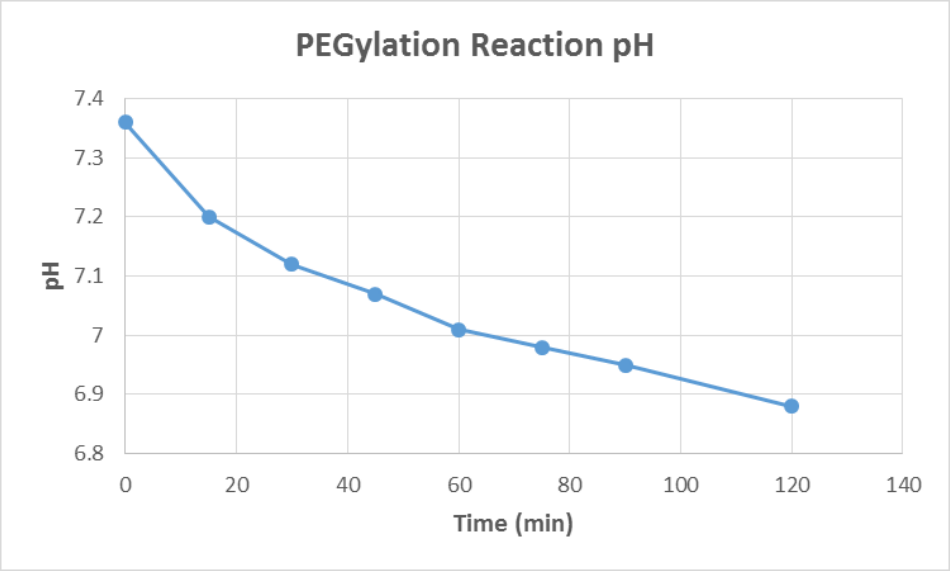

Figure 8. Change in pH over time in 4mM NHS-mPEG solution incubated at 37°C.

3.3.1.2 COMMERCIALLY AVAILABLE POLYMERS RESULT IN VARIABLE LEVELS OF CYTOTOXICITY

Once the appropriate reaction conditions were determined, various lots of the same polymer were purchased from a single vendor and tested on islets to screen for cytotoxicity to evaluate whether commercially available polymers were appropriate for use with cell cultures. Live/Dead imaging showed a high degree of variability in cell viability among the different lots tested, with some batches of the polymer completely decimating the islets, while others resulted in modest levels of cell death (**Figure 9**). Due to the unpredictability of the cytotoxic properties of these commercially available polymers, it was determined that the most predictable results would be achieved by synthesizing our own polymers in-house to ensure proper purification and complete removal of organic solvents.

3.3.2 IN-VITRO ASSESSMENTS OF ISLET VIABILITY AND FUNCTION FOLLOWING PEGYLATION

After the conditions for the PEGylation reaction were optimized and the source of polymer to be used defined, *in vitro* assessments of the effects of PEGylation on islet health were carried out. In this study, PEGylation of the islet cluster was achieved via grafting high molecular weight NHS-PEG-CH3, whereby the N-Hydroxysuccinimide (NHS) group spontaneously reacts with primary amines to yield a stable amide bond. A high MW PEG was used to encourage binding to the peri-islet extracellular matrix (ECM), which has a high density of free amines. In an effort to maximize PEG grafting to the peripheral ECM, islets were cultured for 48 hrs after enzymatic isolation to permit rebuilding of the ECM prior to PEGylation. The incubation conditions during the 45 min PEG grafting procedure, such as pH and temperature, was tailored to optimize the NHS reaction, but mitigate impact

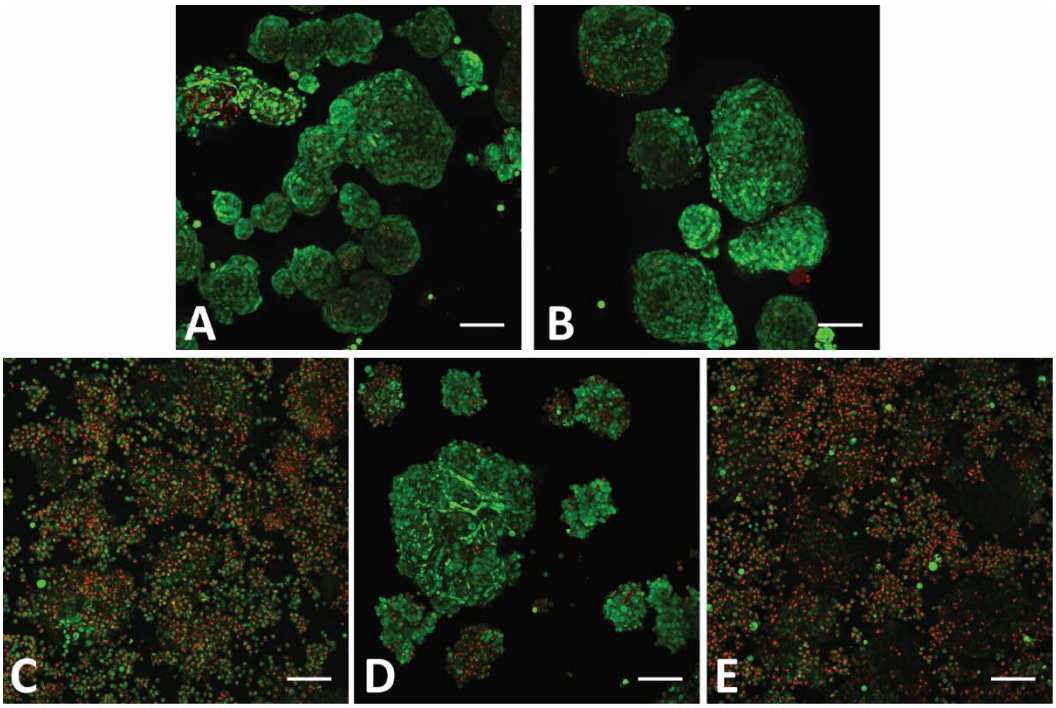

Figure 9. Live/Dead confocal imaging of islets 24 hrs after PEgylation with different lots of NHS-PEG-N3 polymer purchased from commercial vendor. A: Unmanipulated control; B: manipulated control; C:-D: different lots of purchased polymer. Scale bar = 100um.

on islet viability and function. To visually assess the grafting of PEG to the surface of the islet, a fluorescein labeled PEG (NHS-PEG-FITC) was used. Confocal microscope images revealed a high degree of polymer grafting relegated to the periphery of the pancreatic islet. While the majority of the islet surface exhibited some fluorescence, indicating the distributed presence of PEG chains, the uniformity and intensity of the PEG grafting were highly variable across and within islet preparations **(Figure 10)**. As shown, some islet preparations displayed more uniform coatings, while others demonstrated more defined clustering of PEG within specific areas. The peripheral conjugation, variation, and clustering of the coating validated our theory that the majority of the PEG would bind to the ECM; these observed patterns are due to deviations in the stripping of the native ECM

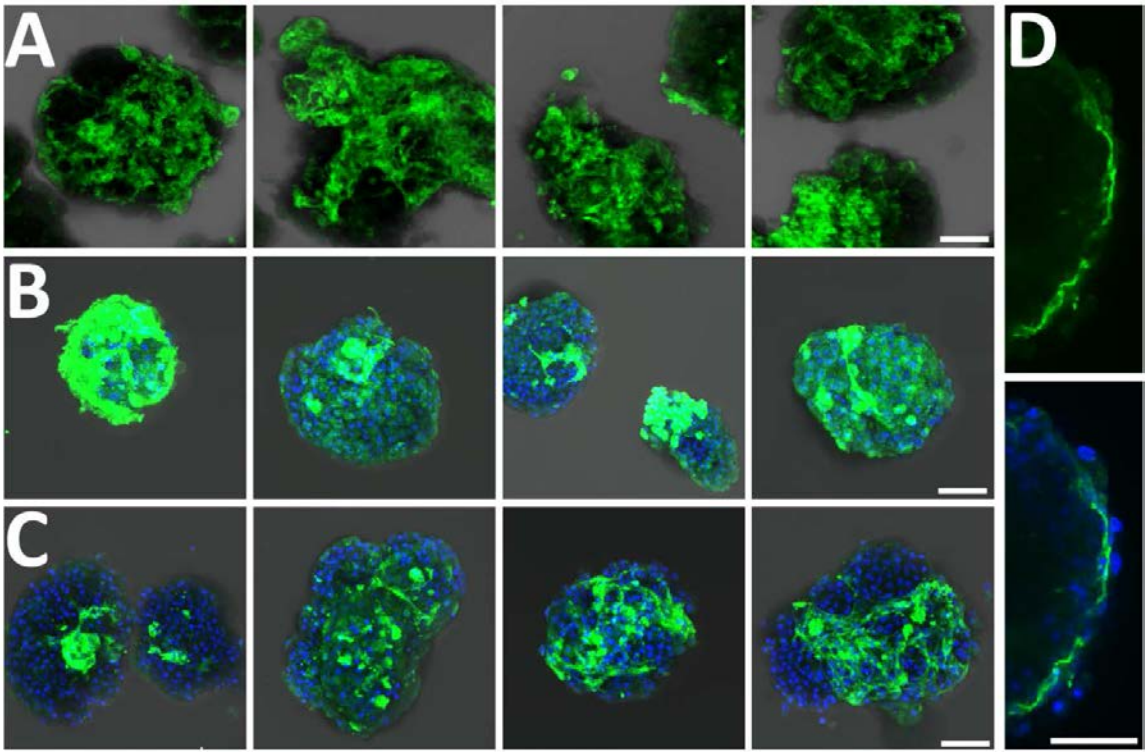

Figure 10. Visualization of PEG grafting on pancreatic rodent islets. Multislice projection confocal images of representative islets from three separate islet isolations (A, B, and C), demonstrating variation of grafting of NHS-PEG-FITC. Hoechst nuclei counterstain (blue) was used for B and C. D) Single slice confocal image of PEGylated islet, illustrating conjugation of PEG to the islet periphery (top: PEG only, green; bottom: merged image of PEG, green, and Hoechst nuclei counterstain, blue). Scale = 50 μm**.**

during enzymatic digestion of the pancreas, as well as disparities in the rebuilding of this ECM matrix during culture.

Following PEGylation, the viability and function of the grafted islet were assessed by live/dead imaging and glucose simulated insulin release, respectively. As shown in **Figure 11**, highly viable islets were observed following PEGylation, with no discernible elevation in dead cells. Following stimulation with low or high glucose, control and PEGylated islets responded in a dynamic manner. The average amount of insulin released from control islets after low and high glucose incubations were 1.77 ± 0.63 and 66.1 ± 3.07

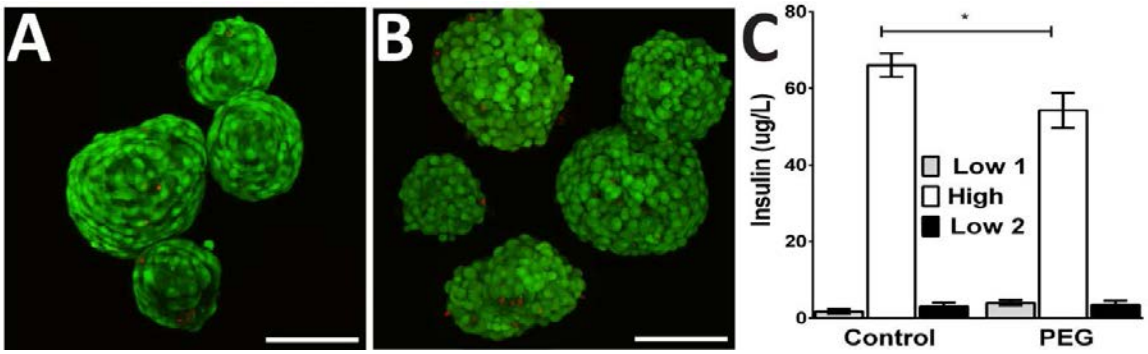

Figure 11. Assessment of rodent islet viability and function 24 h following PEGylation. Representative live/dead multislice projection confocal microscopy images of A) control and B) PEGylated islets (green = viable; red = dead). C) Glucose stimulated insulin secretion (GSIR) dynamics of rodent islets indicate appropriate responsiveness following PEGylation. *$P < 0.05$. Scale bar = 100 μm.

ng/mL, respectively. Corresponding incubations of PEGylated islets resulted in comparable, but statistically different, insulin levels of 4.01 ± 0.66 (P = 0.0159) and 54.27 ± 4.6 ng/mL (P = 0.0286), demonstrating islets retain secretory function and responsiveness after the procedure **(Figure 11)**. Taken together, these data demonstrate that PEGylation islets are highly viable and insulin responsive.

3.3.3 IMMUNOPROTECTION OF PEGYLATED ISLETS IN A FULL MHC MISMATCHED MURINE MODEL OF TRANSPLANTATION

To investigate the potential of islet PEGylation to improve graft outcomes, DBA/2J (H-2^d) islets were implanted within full MHC mismatched murine C57BL/6J (H-2^b) recipients. Following transplantation, 20 of the 20 control mice (100%) and 10 of the 11 (91%) mice receiving PEGylated islets reverted to normoglycemia. As shown in **Figure 12**, 90% of the control islet transplants rejected within 60 d. For recipients of PEGylated islets, a significant increase in the number of grafts exhibiting long-term function was observed, with 6 of the 10 grafts (60%) showing euglycemia for the duration of the study

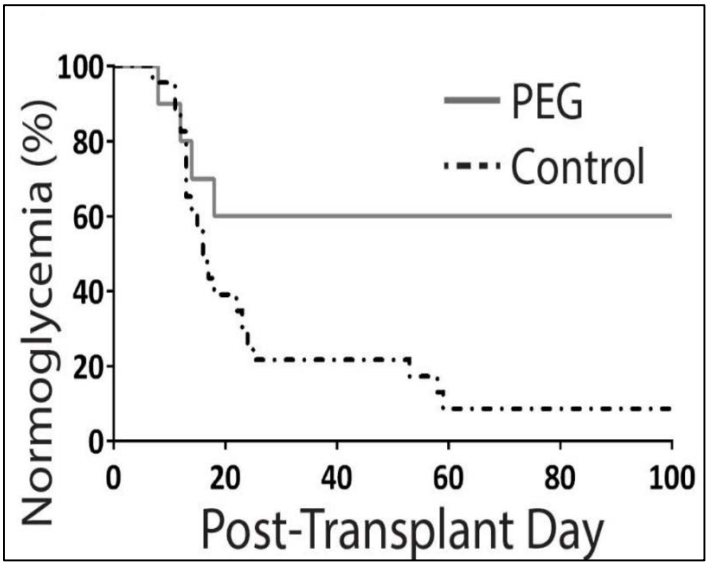

Figure 12. Enhanced engraftment of PEGylated islets. A significant percentage of PEGylated grafts (n = 11) exhibited long-term function, as demonstrated by % normoglycemia, compared to controls (n = 20) (*P* = 0.01).

(> 100 d) (P = 0.01). These 4 rejected grafts destabilized within the first 20 d. Survival nephrectomy of the long-term functional grafts resulted in hyperglycemia, validating the efficacy of the transplanted islets.

3.4 DISCUSSION AND CONCLUSIONS

The PEGylation of surfaces has long been known to reduce protein adsorption and cell attachment.[92, 127] This property makes PEG a promising candidate in efforts to mitigate inflammation during the early transplant period by masking of cell surface antigens thus reducing exposure of inflammatory markers, such as tissue factor, and adsorption of plasma proteins onto the islet surface, which initiates the coagulation cascade that results in IBMIR and instigates immune cell attachment. Further, PEG has been used to immunocamouflage cellular transplants by masking cell surface antigens to prevent T cell recognition and activation.[92, 127] Although grafting of PEG to the islet surface alone

did not confer complete protection of the graft from the host's immune response, this simple conjugation strategy provides a barrier that leads to a significant impact in graft outcomes. In comparison with immunosuppressive agents used as a monotherapy (e.g. α-LFA-1, cyclosporine, rapamycin, CTLA4-Ig, and CD40L mAb) (55-57), islet PEGyation provides similar protection, without the negative impact of systemic immunosuppression.[5, 128-131]

As mentioned above, islet PEGylation alone was not sufficient to completely protect all islet grafts from rejection. One possible reason for variability in outcomes is the irregular nature and variability of polymer grafting onto the islet surface, due to deviations in the stripping of the native ECM during isolation, as well as variations in the rebuilding of this ECM matrix during culture. Presently, coating uniformity is impossible to foresee or control, which leads to unpredictability in outcomes. Approaches seeking to generate uniform surfaces of free amines via protein absorption or coating, or methods to support islet capsule regeneration in culture prior to PEGylation could resolve this challenge. Alternatively, formation of ultrathin coatings via layer-by-layer approaches, stabilized via hydrogen bonding, streptavidin-avidin binding or chemoselective crosslinks, may result in more predictable and uniform coatings capable of complete encapsulation of islet clusters.[100, 104-106, 132] While new approaches are being developed, the simplicity of the PEGylation procedure, the lack of complex instrumentation required, the capacity to maintain the intrahepatic site, and the predicted ease in regulatory approval due to the pervasive use of PEG in pharmaceuticals makes this an attractive approach for mitigating host responses to islet transplants which can easily be incorporated into current transplantation protocols. As such, studies exploring the potential of islet PEGylation, in

combination with conventional clinical islet immunosuppressive regimens, to improve long-term graft outcomes in larger animal models would be of great interest.

In conclusion, PEGylation of the islet surface was confirmed and shown to have no adverse effect on islet viability or function after optimization of the PEGylation procedure and careful consideration of the polymer source. *In vivo* experiments were subsequently pursued to assess the effects of PEGylation on long-term islet graft survival. Transplant studies clearly demonstrated the capacity of islet PEGylation to confer modest protection from immune attack in a full MHC mismatched mouse model, with transplant survival enhanced from 10% to 60%. Overall, this simple approach provides a useful tool in the toolbox of immunomodulatory agents for dampening inflammatory and immunological responses to islet allografts.

Chapter 4. Synergistic Effect of Cell Surface PEGylation and Short-Course Immunotherapy on Allogeneic Murine Islet Graft Survival.

4.1 INTRODUCTORY REMARKS

While islet PEGylation as a singular approach results in a modest degree of immunoprotection, as shown in Chapter 3, modifications could be made to enhance the efficacy of this approach. A few selected studies have demonstrated a synergistic impact when PEGylation is combined with low-dose or local immunosuppression.[114, 133, 134] In this manner, PEGylation of the islet surface could serve as a complementary therapy with short course or low dose systemic immunotherapy to improve graft outcomes. Lymphocyte Function-associated Antigen-1 (LFA-1) is a surface integrin found on a variety of immune cell phenotypes involved in cell trafficking to sites of injury and/or infection, stabilization of the immune synapse during antigen presentation and cell activation, and cell co-stimulation (**Figure 5**). LFA-1 blockade is a monotherapy that has demonstrated modest success in preventing murine allograft rejection, but has demonstrated synergistic effects when paired with other immunosuppressive treatments.[126, 135, 136] Herein, the effects of PEGylation in combination with a short-course LFA-1 blockade on graft survival in a fully mismatched MHC murine model of transplantation were explored.

4.2 MATERIALS AND METHODS

4.2.1 ANIMALS, ISLET ISOLATION, AND ISLET CULTURE

Animals used for these experiments are of the same background as already described in Chapter 3. Please refer to Section 3.2.3 for further details on strains used and

animal care information. Similarly, islet isolation and culture procedures have been described in Section 3.2.4

4.2.2 ISLET PEGYLATION

Islets were PEGylated according to the optimized procedure described in Section 3.2.5.3.

4.2.3 ALLOGENEIC MURINE ISLET TRANSPLANTS

Transplants for these experiments were performed in parallel to those described in Chapter 3 and carried out as described in Section 3.2.6. Control mice and animals receiving PEGylated islets described previously were used as controls for comparison with these experiments. To test the efficacy of a complementary therapy comprised of PEGylated islet transplants and mild short-course immunosuppression, two additional experimental groups were evaluated. The first is an LFA-1 blockade alone control group, where animals received untreated islets and short-course αLFA-1 antibody (KBA clone, 100 μg/day, i.p. on days 0 – 6) (n = 10).[126] The second is the combination therapy group, where animals received PEGylated islets in conjunction with short-course αLFA-1 antibody (n = 13). It is because of these groups that the animals from the control and PEG groups discussed in Chapter 3 received saline.

Again, as described in Chapter 3, normoglycemia of the recipients was defined as non-fasting glycemic levels < 200 mg/dL for 2 consecutive readings. Mice that remained hyperglycemic for over 10 d following transplant were classified as Primary Non-function, euthanized, and censored from long-term graft analysis. Graft rejection was defined as functional grafts that exhibited diabetes recurrence, i.e. glycemic levels > 300 mg/dL for over 3 d, at which point the animal was euthanized and the graft explanted for analysis. All

long-term (> 100 d) functional grafts were electively explanted in a survival nephrectomy to confirm subsequent diabetic status of recipients. For these studies, kidneys were fixed in 10% formalin solution, embedded in paraffin, and cut into 5 μm sections for staining.

4.3 RESULTS

4.3.1 SYNERGISTIC EFFECT OF ISLET PEGYLATION AND SHORT-COURSE IMMUNOTHERAPY

To evaluate if combining short-course immunotherapy with islet PEGylation would have a synergistic effect, additional groups were added to the study. For immunotherapy, αLFA-1 antibody (100 μg/d) was given only on days 0-6.[126] Groups received either

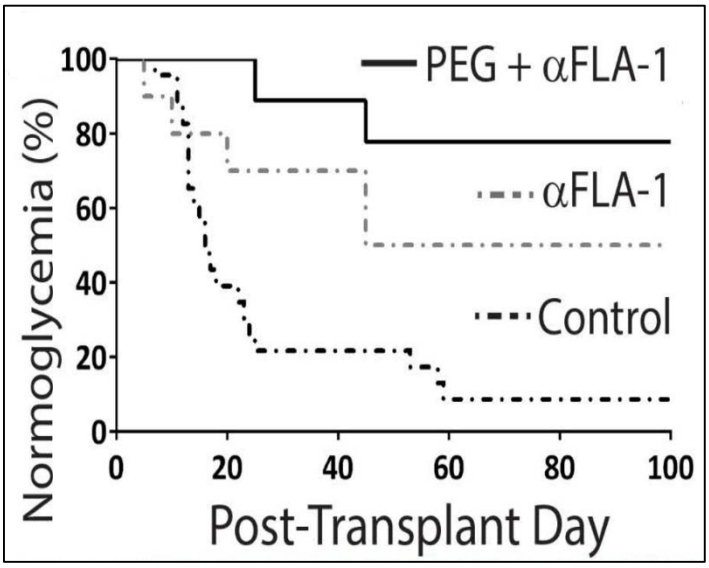

Figure 13. Supplementation with short-course αLFA-1 enhanced survival of PEGylated islets. PEGylated murine islets demonstrate significant improvement in long-term survival in mismatched murine allograft transplants when combined with short-course αLFA-1. Combination of PEGylation with LFA-1 blockade (n = 13) resulted in a higher percentage grafts functioning long term (78%; $P = 0.003$) when compared to controls (n = 20), while LFA-1 blockade only (n = 10) resulted in survival rates of 50%, equivalent to PEGylated islets alone ($P = 0.80$).

unmodified islets with αLFA-1 monotherapy or PEGylated islets with αLFA-1 monotherapy. Following transplantation, all 10 of the 10 mice (100%) receiving unmodified islets with αLFA-1 and 9 of the 13 (69%) mice receiving PEGylated islets with αLFA-1 reverted to normoglycemia. As shown in **Figure 13**, mice receiving unmodified islets and αLFA-1 resulted in 50% of the allografts functioning over 100 d. When PEGylated islets were paired with systemic αLFA-1, graft survival was enhanced to 78% of the transplants. The two rejected grafts in this group destabilized at 25 and 45 d. Graft removal of long-term functioning grafts caused hyperglycemia, confirming euglycemia was due to the transplant.

4.4 DISCUSSION AND CONCLUSIONS

Chapter 3 presented data that clearly showed islet PEGylation alone results in some degree of immune protection as measured by an augmentation of graft survival rates from 10% to 60% when compared to the control group. However, in order for this approach to advance through the stages of pre-clinical testing towards a viable clinical therapy, this improvement is not sufficient and must be enhanced further. Others have shown enhanced graft survival using a combination of islet PEGylation and mild immunotherapy administered for the duration of the entire study[133, 134] or by multiple rounds of PEGylation.[99] In contrast, this study sought to evaluate the efficacy of PEGylation in protecting islets when combined with LFA-1 blockade, a mild immunotherapy, administered only for the first week after transplant, thus obviating persistent immunosuppression and the risks associated with it.

When given short course LFA-1 blockade alone graft survival rates were comparable to that of islet PEGylation alone, further supporting PEGylation as a promising strategy for

immunocamouflage of transplanted islets. Furthermore, it was shown that that the combination of PEGylation and LFA-1 blockade resulted in a synergistic effect that elevated graft survival rates to 78%. This indicates that the incorporation of PEGylation to islet transplant procedures carried out with current immunosuppressive regimens could significantly improve overall transplant outcomes and reduce islet mass requirements, which could greatly contribute to solving the current issue of donor islet shortage.

Chapter 5. Effects of PEGylation, Alone or in Combination with LFA-1 Blockade, on the Graft Microenvironment.

5.1 INTRODUCTORY REMARKS

As discussed in earlier chapters, several components of the immune system are involved in rejection of transplanted islets. Direct contact with blood results in IBMIR, a reaction due to exposure to the cell surface protein Tissue Factor.[17, 18] Consequently, a chain reaction occurs beginning with the initiation of the blood coagulation cascade, ensuing inflammation, and recruitment of cells from the innate immune system, followed by those from the adaptive immune system, which mount the attack on the foreign body ultimately result in graft rejection. After observing that PEGylation alone confers a significant degree of immune protection to transplanted islets resulting in enhanced engraftment, and that this effect can be augmented by incorporating complementary LFA-1 blockade, we sought to determine the mechanism by which this protection is conferred. Therefore, the following studies were performed to elucidate which of these components of the immune system were affected by the different treatments that ultimately resulted in enhanced graft function.

5.2 MATERIALS AND METHODS

5.2.1 EVALUATION OF THE GRAFT MICROENVIRONMENT IN ANIMALS EXHIBITING LONG-TERM GRAFT FUNCTION

As stated earlier, kidneys from mice exhibiting glycemic control in the long-term were explanted and fixed in 10% formalin, embedded in paraffin, and cut into 5 μm sections for staining. Slides were subjected to H&E, Masson's Tri-Chrome, and immunofluorescence staining for the T cell marker CD3, the Treg marker FoxP3, and

Insulin. For immunofluorescence staining, slides were prepped using antigen retrieval following deparaffinization using EDTA Decloaker 5x (Biocare Medical), and blocking for 2 and 1 hr with Power Block Universal Blocking Reagent (BioGenex) and Protein Block (BioGenex), respectively. Primary antibodies, CD3 (Cell Marque; 1:50) and FoxP3 (eBiosciences; 1:100), were incubated overnight at 4°C, followed by rinsing and addition of appropriate secondary antibodies which were incubated for 1 hr at room temperature. Next, sections were washed and incubated with Insulin (Dako; 1:100) primary antibody, followed by washes and appropriate secondary antibody incubation. Nuclei were counterstained using DAPI and samples were subsequently sealed. For all immunofluorescence studies, all stains were compared to isotype controls (primary antibody omitted) to ensure specificity of detection and images were collected using a Leica SP5 Inverted Confocal Microscope.

5.2.2 EVALUATION OF THE GRAFT MICROENVIRONMENT SHORTLY AFTER TRANSPLANT

5.2.2.1 MURINE ISLET TRANSPLANTS, KIDNEY COLLECTION, AND KIDNEY PROCESSING

For short-term mechanistic studies, transplants were repeated as described in section 3.2.6 in accordance with the groups described in Chapters 3 and 4 (control, PEGylated islets, LFA-1 blockade, and the combination of PEGylated islets and LFA-1 blockade). Each group consisted of 12 mice which were euthanized at random on days 4, 8, and 15 post-transplantation for kidney extraction (n = 4 for each time points for all groups). Graft bearing kidneys were flash frozen in OCT and sections (10 μm; 2/slide) were mounted onto both glass and RNAse-free PEN membrane slides (Leica) for staining

and laser-capture microdissection (LCM), respectively. Sections were collected in 5 cycles of 4 glass slides and 2 membrane slides, thus obtaining samples from different regions of the graft for Real Time RT-PCR analysis ensuring data is representative of the entire graft (total depth of 600 μm sampled). Prior to processing each kidney extensive cleaning of the cryostat stage with 100% ethanol was done and a new blade was installed to prevent cross-sample contamination. Sections were kept on dry ice during cutting and stored at -80°C until processed.

5.2.2.2 IMMUNOHISTOCHEMISTRY

Histological analysis of OCT fixed sections was carried out by H&E and fluorescent staining. For immunofluorescence staining, slides were fixed in 4% PFA for 5 minutes, rehydrated, and blocked as described above. Primary and secondary antibodies were incubated at 4 ºC overnight and at room temperature for 1 hr, respectively. Primary antibodies and dilutions used include anti-CD68 (AbD Serotec; 1:200), anti-CD206 (Santa Cruz Biotech; 1:100), and anti-Insulin (Dako; 1:100). Nuclei were counterstained using DAPI and samples were subsequently sealed. Again, all stains were compared to isotype controls (primary antibody omitted) to ensure specificity of detection and images were collected using a Leica SP5 Inverted Confocal Microscope.

5.2.2.3 LASER CAPTURE MICRODISSECTION AND REAL TIME RT-PCR

LCM was performed using the Histogene® LCM Frozen Section Staining Kit (Applied Biosystems) following the manufacturer's instructions. Stained PEN membrane slides were kept in a vacuum chamber filled with drierite to absorb ambient moisture in order to prevent RNA degradation and LCM was carried out immediately after staining using a Leica AS LMD microscope. The LCM station was thoroughly cleaned with 100%

ethanol and RNAse Away before each dissection. The identified graft was cut from each section and collected in a single tube. RNA extraction buffer (PicoPure RNA Isolation Kit, Applied Biosystems) was added, incubated at 42 ºC for 30 min, and stored at -80 ºC. Subsequently, RNA was isolated per manufacturer's instructions, treated using Turbo DNA-free Kit (Invitrogen), and stored at -80 ºC.

For Real Time RT-PCR analysis, a selection of the genes were evaluated using the original samples. Subsequently, it was determined additional markers should be analyzed. In order to generate enough cDNA for Real Time RT-PCR analysis of the desired markers, RNA preamplification of all samples was required. This was performed using the Arcturus™ RiboAmp® PLUS Kit (Applied Biosystems) following the manufacturer's instructions. A rigorous treatment with the Turbo DNA-free was performed post-preamplification to eliminate all DNA present in the samples. All cDNA samples were synthesized using the High Capacity cDNA Reverse Transcription Kit with RNase Inhibitor (Applied Biosystems) following the manufacturer's instructions using 5 ng/μL and 25 ng/μL of RNA for original and pre-amplified samples, respectively. RT-PCR reactions were carried out using TaqMan reagents and the 2x TaqMan Fast Universal PCR Master Mix (Applied Biosystems) using 1.5 μL and 3 μL cDNA for initial and pre-amplified samples, respectively. Elimination of genomic DNA contamination or cDNA remnants from the preamplification procedure was confirmed by performing PCR reactions with cDNA samples generated without the Reverse Transcriptase (No-RT samples) and the 18s primer prior to full sample analysis. Real Time RT-PCR analysis was then performed for the primers listed in Table 1. Reactions were carried out for 40 cycles in a StepOnePlus Real-Time PCR System (Applied Biosystems), outlier replicates removed using the

ExpressionSuite Software (Applied Biosystems/Life Technologies), and relative gene expression analysis was done using the 2(-dCt) comparative method as previously published[137] comparing experimental groups to the control group from the corresponding time point. In cases were the target genes in control samples were undetected, a Ct of 40 was substituted to permit comparative analysis.

Target	**Assay ID**	**Target**	**Assay ID**
B-actin	Mm00607939_s1	Cd3d	Mm00442746_m1
GAPDH	Mm99999915_g1	Prf1	Mm00812512_m1
Pdx1	Mm00435565_m1	GzmB	Mm00442834_m1
Ptprc (CD45)	Mm01293577_m1	FoxP3	Mm00475162_m1
IFNγ	Mm01168134_m1	Emr1(F4/80)	Mm00802529_m1
TNFα	Mm00443260_g1	Mrc1 (MMR)	Mm00485148_m1
TGFβ-1	Mm01178820_m1	Nos2	Mm00440502_m1
IL-10	Mm00439614_m1	Sphk1	Mm01252544_m1
Il-4	Mm00445259_m1	Cd19	Mm00515420_m1
Il-17a	Mm00439618_m1	Klrb1c (Nk1.1)	Mm00824341_m1

Table 1. Listing of primers used for RT-PCR analysis of grafts explanted via laser capture microdissection.

5.2.3 STATISTICAL ANALYSIS

Real Time RT-PCR data was analyzed by determination of the amount of target gene expression relative to the B-Actin endogenous gene control for each sample and performing a Kruskal-Wallis non-parametric one way ANOVA followed by a Dunn's post-

test to compare the different treatment groups. For all studies, differences were considered significant when $P < 0.05$.

5.3 RESULTS

5.3.1 IMMUNOLOGICAL EVALUATION OF LONG-TERM FUNCTIONING GRAFTS

Representative tri-chrome stained sections of PEGylated islets from functional grafts (193 d post-transplant) exhibit robust islets, whereas control islets (20 d post-transplant), on the other hand, clearly show destruction of the islet graft by immune infiltrates. Histological assessment of functional grafts from mice receiving LFA-1 blockade and combination of PEGylated islets and LFA-1 blockade also found healthy engrafted islets for both groups as well (193 d post-transplant) **(Figure 14)**. Immunofluorescent staining of insulin further demonstrates the functional status of the grafts, with waning levels of insulin observed in the control group contrasted by strong insulin staining in the experimental groups (**Figure 15**).

Additional immunohistochemical evaluation of T cells was performed for long-term functioning grafts within treated groups. Most grafts showed minimal presence of T cells (**Figure 16**) with sporadic cells related to the periphery of the islet graft. For some PEG and αLFA-1/PEG combination grafts, however, areas of $CD3^{+}FoxP3^{+}$ cells were observed (**Figure 16 C-D**). Further, for selected grafts in all treated groups, pockets of mononuclear cell accumulation were observed (**Figure 16 E-F**). The infiltrate appears to be confined to an area where it appears islets were located at one point in time. Interestingly, islets adjacent to the mononuclear cells remain intact with no notable intra-islet infiltration or loss of insulin expression. Immunostaining found a high accumulation

of $CD3^+$ cells, with a strong proportion of these cells also staining positive for FoxP3, indicating the elevated presence of T regulatory cells within these areas.

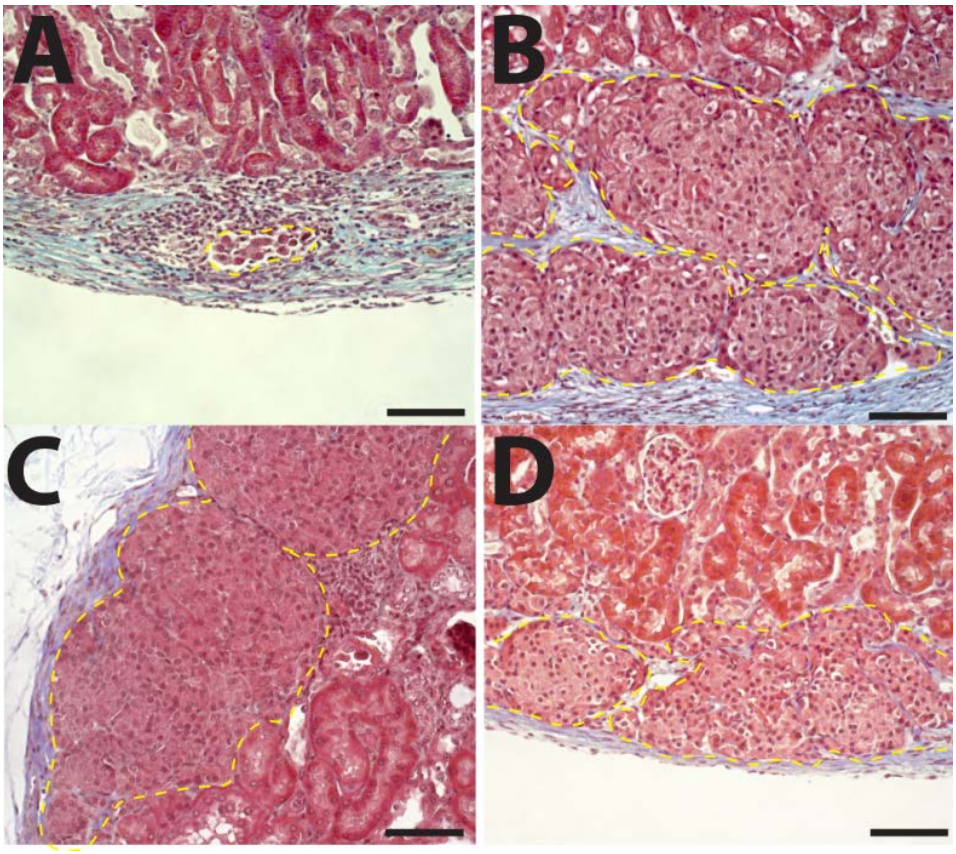

Figure 14. Islet PEGylation results in engraftment similar to that of LFA-1 blockade, which is further enhanced by combination of the two. Representative images of (A) control islets explanted 20 d post-transplant after destabilization of graft, (B) PEGylated islets, (C) islet grafts from mice receiving LFA-1 blockade, and (D) grafts from mice receiving PEGylated islets and LFA-1 blockade. Kidneys from experimental groups were electively explanted 193 d post-transplant. Explants were stained via trichrome. Yellow dashed line outline transplanted islets. Scale bar = 100 μm.

5.3.2 SHORT-TERM EFFECTS OF PEGYLATION AND LFA-1 BLOCKADE ON THE IMMUNE RESPONSE

To explore how PEGylation and/or LFA-1 blockade may modulate early host responses to encourage long-term graft acceptance, additional transplants were conducted, with grafts explanted at 4, 8, and 15 d post-transplantation. These grafts were then assessed via microdissection and subsequent gene analysis on the isolated tissue. Genes assessed sought to elucidate the nature of the immune response as a result of different treatments,

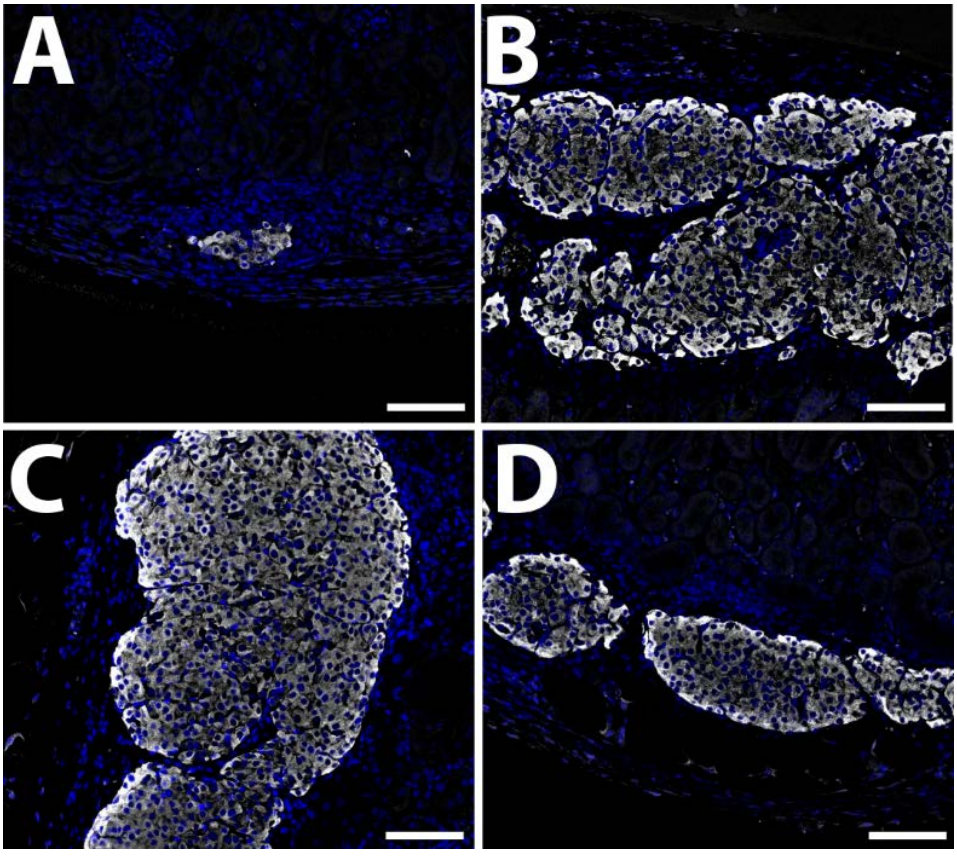

Figure 15. Experimental groups display robust insulin staining indicative of their functional status. Representative images of (A) control islets explanted 20 d post-transplant after destabilization of graft, (B) PEGylated islets, (C) islet grafts from mice receiving LFA-1 blockade, and (D) grafts from mice receiving PEGylated islets and LFA-1 blockade. Kidneys from experimental groups were electively explanted 193 d post-transplant. Explants were stained for Insulin by immunofluorescence (white). Scale bar = 100 μm.

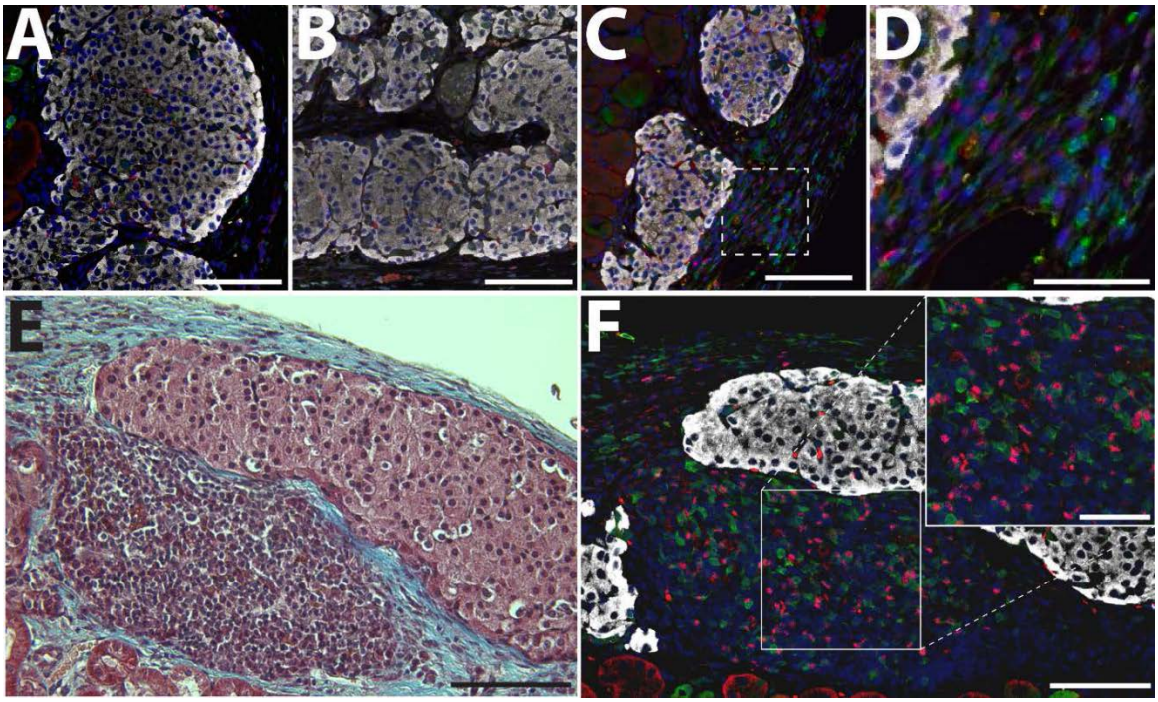

Figure 16. Immunofluorescence staining of grafts functioning long term. Representative images of successful grafts functioning long-term for αLFA-1 only (A), PEGylated only (B), and αLFA-1 and PEGylated islets (C). D) Higher magnification of graft in C (box highlights area). E-F) Representative tri-chrome and immunofluorescence stained explant demonstrating mononuclear accumulation. Grafts were immunostained for CD3 (green), FoxP3 (red), and Insulin (white); counterstained with DAPI nuclei stain (blue). A-C, E: scale bar = 100 μm. D & F: scale bar = 50 μm.

including: Ptprc (CD45) as a general marker of immune cell infiltrate; and CD3, CD19, Emr1 (F4/80), and Klrb1c (Nk1.1) as markers of T-cells, B-cells, macrophages, and NK cells, respectively. Additional genes were analyzed in order to discern between subpopulations of these immune cell phenotypes to determine whether the response was of an inflammatory or anti-inflammatory nature, these include: Prf1 (Peforin) and GzmB (Granzyme B) as markers of effector T-cells; FoxP3 as a marker of Tregs[138]; Sphk1 (Sphingosine Kinase-1) as an indicator of alternatively activated (M2) macrophages; and Nos2 as a marker of classically activated (M1) macrophages.[139-142] Finally, genes

encoding for several cytokines involved in immune cell activation and differentiation were also analyzed, including: IFNγ and TNFα as markers of an inflammatory response; and TGF-β, IL-10, and IL-4 as markers of an anti-inflammatory response.[138, 139, 141, 143] The results revealed some interesting trends and significant differences in gene expression between groups for a few of the markers studied. Markers that demonstrated significant differences are summarized in **Figure 17**, specifically CD45, Emr1 (F4/80), INFγ, and TGFβ. Of interest, while not statistically significant, on day 4, CD45 expression was downregulated for treatment groups, while Emr1 and TGF-β were elevated. By day 15, CD45 expression increased in the treatment groups, particularly in the αLFA-1 group, which exhibited a statistically significant 2.1-fold higher expression ($P = 0.02$), suggesting a delayed immunological response to the implant. Interestingly, this coincided with lower expression of IFNγ in the same group, with a 2.6-fold ($P = 0.005$) reduction in expression on day 15. Moreover, the TGF-β expression in the grafts was consistently highest in the αLFA-1 group, albeit statistically significant only on day 8 ($P = 0.005$). In the case of Emr1 (F4/80), expression was highest in the PEG group for both days 4 and 8, although this difference was statistically significant only for the latter time point, i.e. a 3.6-fold increase in expression ($P = 0.002$). By day 15 however, the αLFA-1/PEG group surpassed all others with a 4.9-fold increase in expression of Emr1 ($P = 0.003$), closely followed by the PEG group. All other markers either did not exhibit statistically significant differences in expression (CD3, GzmB, TNFα, IL-10, IL-17, and Klrb1c) or were not detected (IL-4, Prf1, FoxP3, Nos2, Sphk1, and CD19)

Taken together, gene expression results suggest a mechanism in which the migration of immune cells to the graft site was delayed. As expected, this trend is

pronounced for grafts treated with LFA-1 blockade. Further, the blockade inhibited production of inflammatory cytokines, as observed in the case of INFγ, and promotes production of anti-inflammatory cytokines, such as TGFβ, at the site. The increased levels of Emr1 expression for PEGylated islet transplants indicate macrophages play a role in their engraftment. Supplementation with αLFA-1 appears to delay this migration, as indicated by the suppression and then rise in expression of Emr1 from day 4 to 15. This is likely due to the impact of LFA-1 blockade on immune cell trafficking to the transplant site. Of note, markers used to characterize macrophage phenotype (i.e. Nos2 for M1 and

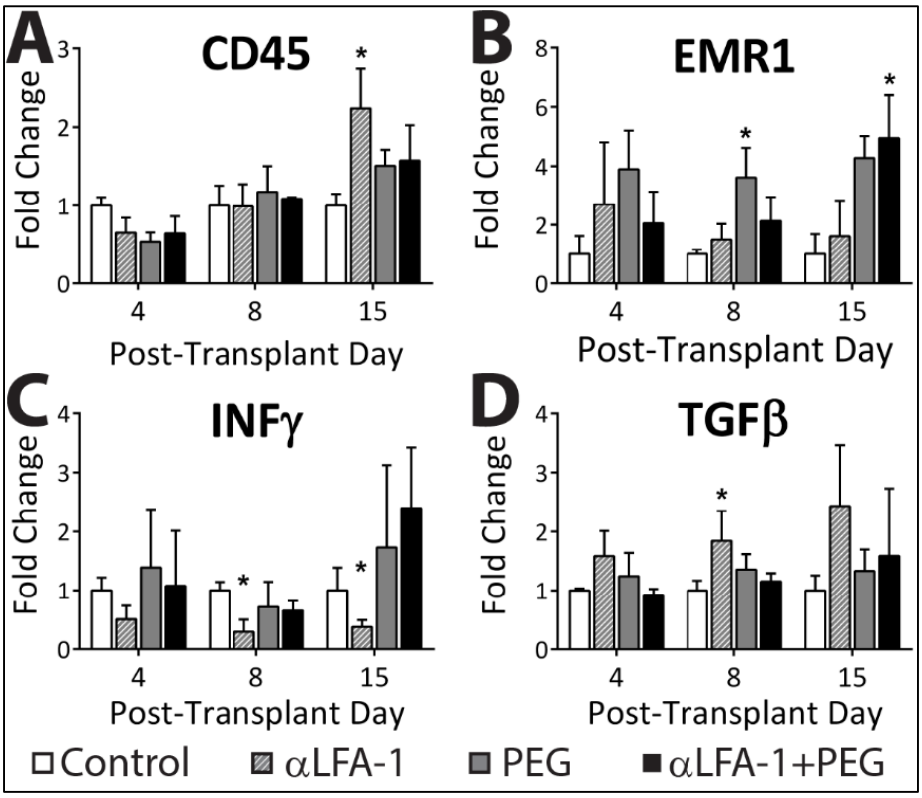

Figure 17. Real Time RT-PCR results summarizing significant changes in gene expression at graft site for transplant groups. Gene expression analysis for CD45 (A), Emr1 (B), INF-γ (C), and TGF-β (D) for control, αLFA-1, PEGylated islets, and αLFA-1 + PEGylated islets groups. Gene expression evaluated as amount of target gene relative to β-Actin and expressed as fold control. * $P < 0.05$.

Sphk1 for M2) were undetectable, thus the true characteristics of these cells could not be classified by gene analysis.

In addition to gene expression analysis, qualitative evaluation via immunofluorescent staining for the macrophage marker CD68 and the M2 macrophage marker CD206 was conducted at early graft time points **(Figure 18)**. In control samples, a high degree of CD68+CD206- cells was observed at early (d 4-8) time points. By 15 d, insulin positive cells were not observed for most grafts. Selected grafts still exhibiting sparse insulin positive islets had clear macrophage infiltration **(Figure 18C)**. The αLFA-1 only and PEG only group consistently exhibited low levels of CD68+CD206- cells across all time points. Further the macrophages appeared to remain on the islet periphery. The minimal observation of macrophages in the PEG group appears to contradict gene expression data, which found elevated Emr1 (F4/80) expression for PEGylated grafts. For the αLFA-1/PEG group, a notable increase in CD68+ was observed, but these cells were also CD206+, hence exhibiting more of an M2 phenotype. These results suggest that the mechanism by which grafting of PEG on the islet surface enhances graft survival during early time points is mediated by macrophages, particularly the higher incidence of alternatively activated macrophages (M2) in the αLFA-1/PEG group, which ultimately demonstrated the highest rate of graft survival.

5.4 DISCUSSION AND CONCLUSIONS

Examination of the transplant site in after long-term engraftment in animals receiving experimental treatments revealed low amounts of immune infiltrates which were restricted to the periphery of the islet graft. Immunofluorescent staining of these samples showed strong insulin expression indicative of healthy functional islets. Of particular

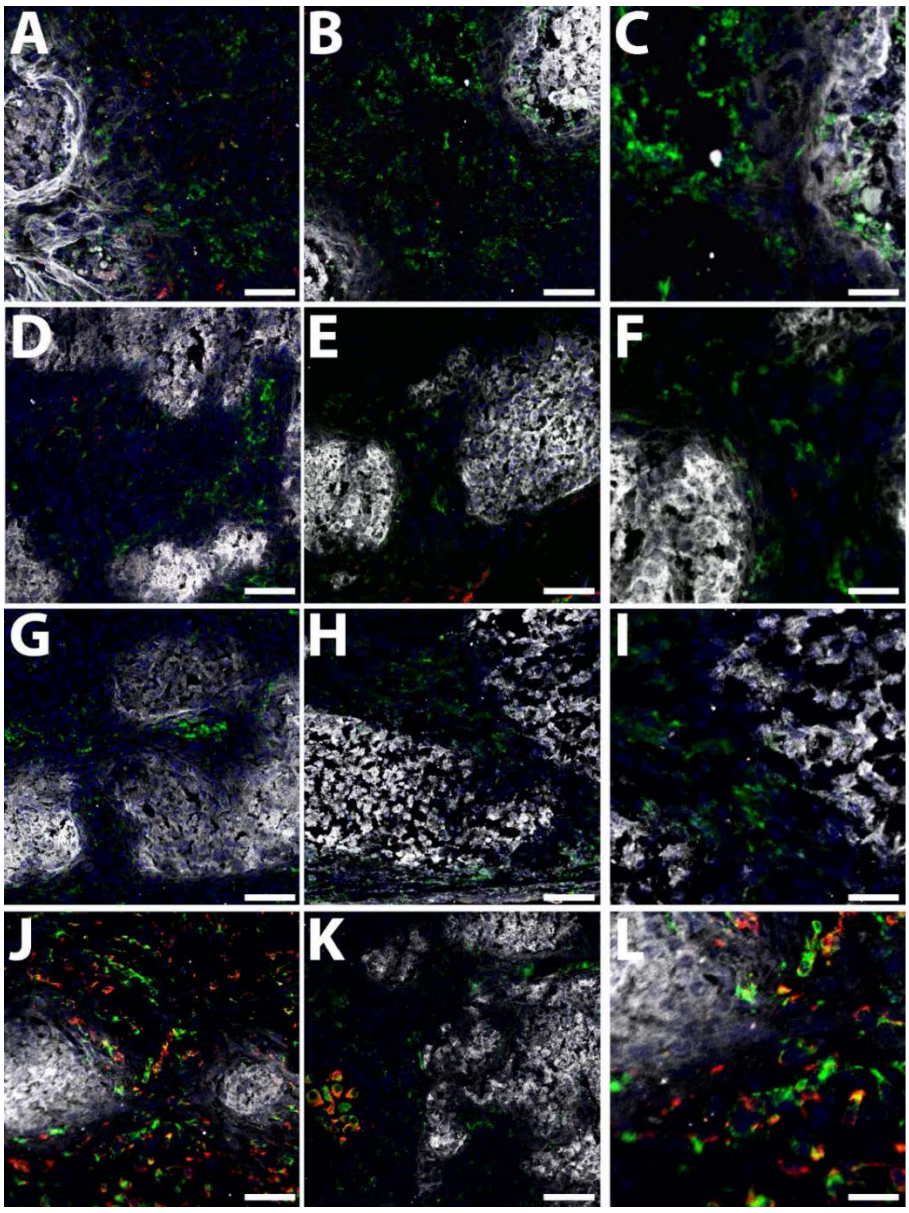

Figure 18. Immunohistochemistry of macrophage infiltration at early engraftment. Grafts were electively terminated 4, 8, and 15 day post-transplantation and immunostained for general macrophage marker CD68 (green), macrophage M2 marker CD206 (red), and insulin (white); counterstained with DAPI nuclei stain (blue). Representative images of grafts from control (A-C); αLFA-1 only (D-F), PEGylated only (G-I), and the combination of αLFA-1 and PEGylated islets (J-L) groups at elective explants on early (4 or 8 d, left column) and late (15 d, middle column) post-transplantation days with higher magnification images of areas of interest (left column). Scale bar = 100 μm for left and middle columns; 20 μm for right column.

interest were the pockets of mononuclear cells adjacent to healthy islets exhibiting robust insulin expression observed in some of the samples. These pockets clearly included T cells, some of which were Tregs, which indicate immune attack taking place. Why these cells attacked one islet and not the other adjacent to it is a good question. One possible explanation is that this is due to the variability in the grafting of polymer observed during *in vitro* testing discussed in Chapter 3. Because some islets are able to react with the polymer due to their more complete ECM capsule, they are better protected when compared to their ECM stripped counterparts which lack the free amines on the surface for the grafting reaction to take place. As a result, these cells are more susceptible to IBMIR and recognition by host immune cells.

It is important to note that the length of time the grafted polymer endures on the islet surface after transplantation remains to be determined. Concerns regarding cell membrane turnover raise questions about the polymer's persistence; however, as described above, our procedure seeks to target the ECM peri-islet capsule in an effort to minimize this contribution thus circumventing this issue. Still, the persistence of the polymer brush is an important factor that should be extensively characterized in future studies. Methods to visualize this layer include immunostaining using commercially available PEG-specific antibodies or using biotinylated PEG for detection via IHC. Moreover, the quantification of the amount of PEG grafted onto the islet surface, and thus of the polymer grafting density if taking account the islet surface area, is another variable to be characterized. This measurement could be correlated with graft success and serve as a potential measure for quality control purposes, predicting PEGylated islet batch performance. One possible method to achieve this would be to measure the amount of PEG present in a sample of

treated islets by using radioactively labeled polymer, which would yield more accurate results than those generated from using fluorescently labelled polymers and performing image analysis.

Evaluation of the transplant site during the early engraftment period showed early host responses to treatment groups implicates a delayed immunological response and modification of macrophage infiltration and subsequent activation. As supported in previous publications, delayed migration of immune cells was observed with the use of α-LFA-1.[128, 131] In comparison, host responses to PEGylated islets indicate a similar dampening in immune activation. Analysis of the role of macrophages for PEGylated islets was somewhat conflicting, with gene analysis demonstrating elevated Emr1 expression and histological analysis suggesting dampened macrophage presence. This disparity may be attributed to variations in the PEG coating of islets within the graft. For the combination group, inhibition of adaptive and innate host is clearer, with suppression of immunological activation and modulation of innate responses. Of interest, macrophage migration in this combination group was characteristically different than that observed for the other treatment groups, with a significant increase in Emr1 expression and observed macrophage infiltration into the graft. The observed tendency of these macrophages to co-express CD206, and hence lean towards an M2 phenotype, indicate the presence of these cells is beneficial, particularly when reflecting on the high graft survival of this treatment group. These results are fitting since macrophages are known to play a critical role in regulation of inflammation and initiation of an immune response. Analysis of the graft microenvironment revealed a role for immune cell suppression on graft function, as well as macrophage infiltration and phenotype. The role of T regs in long-term tolerance of

these grafts is still unclear. Some long-term explants that lack immune infiltrates exhibit sporadic T reg staining in the islet periphery, while high T reg staining was observed when mononuclear infiltrates were present, which is expected as they are actively regulating an ongoing immune response. Further studies to characterize the presence of these cells in short-term assessments, and possibly at time points after 15 days post-transplant, could shed some light on their role in long-term engraftment.

Chapter 6. PEGylation Enhances Islet Graft Survival in a Non-human Primate Transplant Model.

6.1 INTRODUCTORY REMARKS

The ultimate goal of any biomedical research project is to advance through the sequential stages from concept and benchtop validation, pre-clinical small and large animal studies, clinical scale-up and manufacturing, and clinical trials; culminating in the commercialization of novel products, medications, and/or procedures used to prevent or treat human disease. As such, after demonstrating the efficacy of PEGylation in protecting an islet allograft in a small rodent model, as described in Chapters 3 and 4, the focus turned towards establishing the feasibility to scale up this procedure to permit coating islets on a larger scale. These studies allow us to explore, identify, and address the challenges inherent in scaling up the PEGylation process by making the necessary adjustments to enhance efficiency in the process and establish feasibility at larger scales. Further, examining the safety and efficacy of this surface modification procedure within a larger animal models that closely replicate the complex immunological responses to allogeneic tissues in humans would not only contribute to scientific knowledge, but move this a step closer towards clinical trials. Consequently, the effects of PEGylation on the survival of an islet allograft was evaluated in a Cynomolgus Monkey (CM) marginal mass model. The capacity to conduct work using this model was due to a highly collaborative partnership with Dr. Norma Kenyon. Dr. Kenyon is a world-renowned leader in translational studies of islets in nonhuman primate models, thus leveraging of her expertise, as well as her team, provided us the means to implement this PEGylation procedure within her animal models.

In moving to this larger animal model, the initial challenge was in scaling up the procedure. In achieving this aim, the capacity to PEGylate islets at large scales, and its

subsequent impact on islet viability and function, was examined and validated. Further, the impact of PEGylation on inflammatory processes was tested using in vitro coagulation assays. Given that it is not expected that PEGylation would afford complete immunoprotection, the use of a supplemental immunosuppressive regimen was required for in vivo translation into this monkey model. Selection of an appropriate immunosuppressive cocktail that would provide the correct balance is exceptionally challenging. The regimen should be suppressive enough to provide adequate supportive protection during the aggressive immunological insults of early engraftment, but not be too suppressive that rejection of control islets are significantly delayed. Fortunately, Dr. Kenyon has considerable expertise in translation of immunosuppressive agents in nonhuman primate models. She recently published a study using mesenchymal stem cells (MSCs) as a supplement to a modest immunosuppressive regimen.[144] Although the mechanism of action is still under investigation, MSCs are widely known to have immunomodulatory properties, which serve to dampen allorejection. In this study, islets were co-transplanted with either MSCs or donor bone marrow cells (DBMCs), both under administration of modest immunotherapy, with the goal of determining if MSCs would promote islet engraftment through their immunomodulatory properties. Kenyon is currently working on exploring this concept further, with comparative groups of animals receiving modest immunosuppression with or without MSC. These control groups serve as excellent historical controls for evaluating the impact of PEGylation, as this regimen results in predictable, but delayed, rejection within the first 30-60 days. Further, this IS regimen provides the foundation for future paired treated versus control studies.

Herein, we explored the use of PEGylation as a complementary agent for this immunosuppressive regimen. In this manner, we were able to leverage historical controls for our pilot study. Further, with additional funding allocation from NIH, we were able to embark on additional paired transplants, which permit for a more controlled comparison of the impact of PEGylation on improving engraftment and delaying immunological rejection.

6.2 MATERIALS AND METHODS

6.2.1 NHS-mPEG POLYMER SYNTHESIS

The polymers used for these studies were the same as those synthesized in house and used for the mouse studies described above. Please refer to section 3.2.2 for further details.

6.2.2 ANIMALS

Donor and recipient cynomolgus monkeys were obtained from Charles River BRF (Houston, TX) or The Mannheimer Foundation, Inc. (Homestead, FL) and were screened negative for tuberculosis, herpes B virus, simian retrovirus, simian immunodeficiency virus, and simian T-cell lymphotropic virus-1. Animals >4 and >2 years of age were used as donors and recipients, respectively. Pair-housed monkeys were supplied with water ad libitum and fed twice daily. The University of Miami complies with the Animal Welfare Act of 1966 (PL89-544) as amended by the Welfare Act of 1970 (PL91-279), adheres to the principals stated in the Guide for the Care and Use of Laboratory Animals (National Institutes of Health publication 85–23 revised) and is accredited by the Association for Assessment and Accreditation of Laboratory Animal Care. Donor-recipient pairs were

ABO compatible.[145] The care and maintenance of all diabetic animals used in this study was performed by Dr. Norma Kenyon's group.

In the selection of donor and recipient animals, all animals were tissue typed and demonstrated to be fully or partially mismatched for major histocompatibility complex (MHC) class II alleles, as previously described.[144] For classification, the 6 haplotypes found for this cynomologus strain (H1-H6) were colored to assist in visual matching, as outlined previously.[146] In this study, 3 historical control animals were leveraged. Matching for these animals included mismatch of MHC. An example of this is shown in **Figure 19**, whereby the donor pancreas matched for haplotype H1 and H4, while the recipient matched for H1, H2, and H5. For the first pilot study, a single transplant of PEGylated allogeneic islets was conducted. In this study, the compatibility of the donor to the recipient is outlined in **Figure 20**. As noted, the donor pancreas matched for haplotype H1 and H4, while the recipient matched for H1, H2, and H3. For the paired transplants, islets from 3 donor pancreata were pooled and subsequently split into two groups. One group was PEGylated and one was simply cultured for the same time period. To provide a means for comparison, efforts were made to match the recipients by weight, exogenous insulin requirement, and MHC. As shown in **Figure 21**, the donors were of similar MHC, with expression of H1, H2, and H6, while recipients were completely mismatched with expression of H3 and H4.

6.2.3 NHP ISLET ISOLATION AND CULTURE

All of the islet isolations were performed by Dr. Kenyons' group. The donor pancreas was recovered as previously described[147] and nonhuman primate (NHP) islet isolation performed using modifications[148] of the automated method for human islet

Recipient			Donor	
DW050	9C4-14		DW008	6C44
126	126		126	118
301	301		301	313
163	163		163	145
255	255		255	249
142	137		142	Null
204	207		204	201
274	243		274	243
321	338		321	338
110	108		129	129
200	203		206	200
265	263		234	263
249	245		244	247
231	240		221	240
209	203		214	209
201	204		206	190
309	297		297	Null

Figure 19. Example of MHC class II alleles associated with haplotypes for donor and recipient cynomolgus macraques used for historical control. Key: H1: black; H2=red; H3=blue; H4=green; H5=yellow; and H6=grey.

Recipient			Donor	
AB	10C59		A	7C4-61
120	120		126	126
293	293		301	301
143	143		163	163
294	294		255	255
142	135		142	142
204	201		204	204
274	265		274	276
321	340		321	321
129	110		129	129
206	200		206	206
234	265		234	234
244	249		244	244
f-221	231		f-221	f-221
214	209		214	214
206	201		206	206
297	309		297	297

Figure 20. Example of MHC class II alleles associated with haplotypes for donor and recipient cynomolgus macraques used for first PEGylated islet transplant. Key: H1: black; H2=red; H3=blue; H4=green; H5=yellow; and H6=grey.

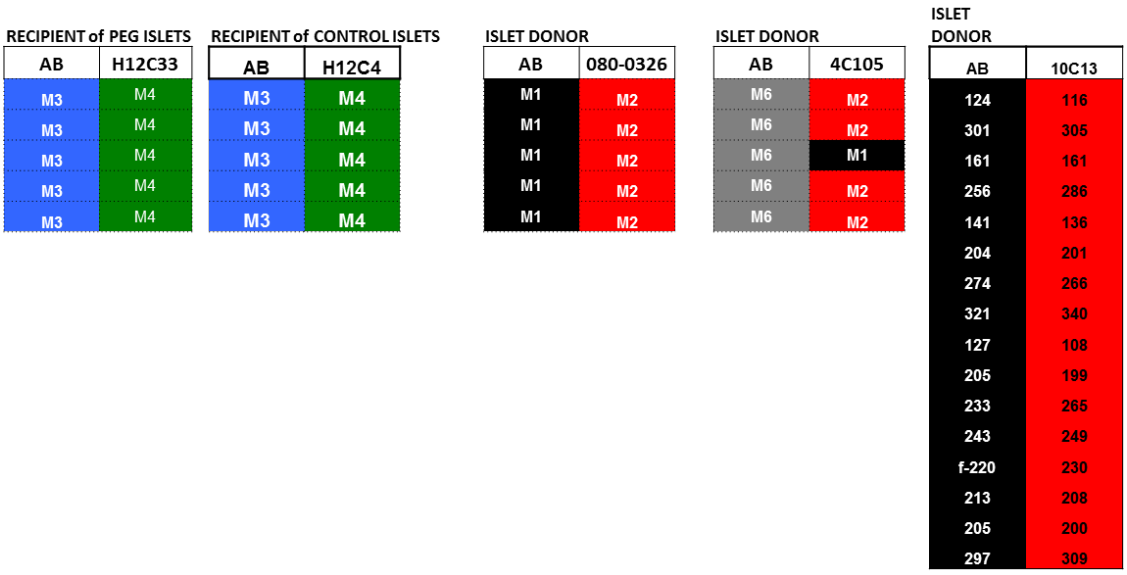

RECIPIENT of PEG ISLETS	
AB	H12C33
M3	M4
M3	M4
M3	M4
M3	M4
M3	M4

RECIPIENT of CONTROL ISLETS	
AB	H12C4
M3	M4
M3	M4
M3	M4
M3	M4
M3	M4

ISLET DONOR	
AB	080-0326
M1	M2
M1	M2
M1	M2
M1	M2
M1	M2

ISLET DONOR	
AB	4C105
M6	M2
M6	M2
M6	M1
M6	M2
M6	M2

ISLET DONOR	
AB	10C13
124	116
301	305
161	161
256	286
141	136
204	201
274	266
321	340
127	108
205	199
233	265
243	249
f-220	230
213	208
205	200
297	309

Figure 21. Example of MHC class II alleles associated with haplotypes for donor and recipient cynomolgus macraques used for the paired PEG vs control islet transplant. Key: H1: black; H2=red; H3=blue; H4=green; H5=yellow; and H6=grey.

isolation.[149] Discontinuous Euroficoll gradients (densities: 1.132; 1.108; 1.096; 1.037) were used for purification of islets from the pancreatic digest.[149, 150] The tissue was bottom-loaded with stock Ficoll and centrifuged in a COBE 2991 blood cell processor (Lakewood, CO). Islet purity was estimated to >90% based on the percentage of dithizone (DTZ) positive particles present in the preparation,[151, 152] and viability was estimated based on fluorescein diacetate/propidium iodide staining.[153]

6.2.4 PEGYLATION PROCEDURE

The PEGylation procedure used in these studies was similar to that described for PEGylation of mouse islets; however, the procedure needed to be slightly modified and scaled up to accommodate the transplant model. Because longer culture times have a more dramatic impact on NHP islet stability, islets were PEGylated 24 hr after isolation, instead of the 48 hours used for murine islets, and cultured for an additional 24 hr prior to

assessments or transplantation for a total of 48hr culture post-isolation. This modification also allowed for comparison to historical controls. Islets were PEGylated at a density of 1100 IEQ/mL of polymer solution.

6.2.5 IN-VITRO ISLET CHARACTERIZATION

6.2.5.1 CONFIRMATION OF PEGYLATION AND VIABILITY ASSESSMENTS

Grafting of PEG onto the NHP islet surface and islet viability was assessed by surface modification with NHS-PEG-FITC and LiveDead staining, respectively, and imaging on the confocal miscroscope as described for murine islets in Chapter 3 (sections 3.2.5.1 and 3.2.5.2).

6.2.5.2 GLUCOSE-STIMULATED INSULIN RELEASE - PERIFUSION

Islet cell function was evaluated *in-vitro* via assessment of glucose-stimulated insulin release (GSIR) using a column-perifusion assay.[154, 155] The perifusion assay provide a more dynamic assessment of glucose stimulated insulin secretion than static GSIR. The stimulation index (SI) was calculated as the ratio of insulin released under high (11 mM) over insulin released under low (3 mM) glucose concentrations. C-10 base solution (125mM NaCl, 5.9mM KCl, 2.56mM CaCl2, 1.2mM MgCl2, 25mM Hepes, 0.1% BSA, pH 7.4) was prepared in advance and used to prepare 1 mM, 3 mM, and 11 mM glucose solutions; 3mM KCl solution; and Glutamate solution. Perifusion columns were assembled and filled up to 1/3 using Bio-Gel beads (BioRad, Cat No. 150-4124). At this point, the perifusion machine (Biorep Technologies, Cat. No. PERI4-02) was prepared by connecting the necessary pieces of silicone tubing inside the incubator chamber over the rotor wheel of the device. Columns were then loaded with 100IEQ's each and the remainder of the column was filled with Bio-Gel beads. The column was then connected

to the device and media was perfused through the column at a rate of 100 μL/min. The sequence and duration of buffers used in the profusion are 5 min of 3 mM glucose, 10 min of 11 mM glucose, 15 min 3 mM glucose, 5 min KCl solution, and 5 min 3 mM glucose. Eluate from each column was individually collected into 96-well plate wells for 1 min through the entire 40 min procedure. Insulin content was quantified using a commercially available Human Insulin ELISA Kit (Mercodia, Cat. No. 10-1113-10). For more details on the perifusion instrument please refer to the publication cited.[155]

6.2.5.3 PLASMA RECALCIFICATION ASSAY

Platelet-poor plasma (PPP) was generated by collecting blood from an allogeneic donor animals into citrated tubes and spinning down at 3000 RPM (~1950 x g) for 15 min. Aliquots of 50 islets were made by hand-picking islets and placing them in 1.7 mL eppendorf tubes. Islets were spun down at 2 x g for 1 min and the media was removed using a P-1000 micropipettor. Each aliquot was then quickly, but gently, resuspended in 100 μL of PPP and transferred into a well of a 96-well clear-bottom assay plate. PPP alone aliquots were also made in the 96-well plate to serve as baseline controls. Once all the wells were ready, 100 μL of 25 mM $CaCl_2$ solution in ddiH_2O was added to the wells as quickly as possible using a multichannel micropipettor. The plate was then placed in a plate reader set to hold a temperature of 37 °C and read the absorbance at 405 nm every 60 sec (instrument limit) for a total time of 60 min. Wide bore pipettor tips were used to avoid injury to the islets during manipulation. Kolmogorov-Smirnov non-parametric t-test was used to determine statistical significance.

6.2.6 NON-HUMAN PRIMATE ISLET TRANSPLANTS AND GRAFT CHARACTERIZATION

6.2.6.1 DIABETES INDUCTION, METABOLIC MONITORING, AND INSULIN ADMINISTRATION

Recipient animals were NPO (nothing by mouth) the night prior to diabetes induction; streptozotocin (STZ, 1,250 mg/m^2 i.v.) was infused over an 8-minute period.[156] Diabetes in this model was defined as fasting C-Peptide (CP) levels <0.2 ng/mL, and a negative CP response (stimulated CP <0.3 ng/mL) to a glucagon challenge undertaken 4 weeks after diabetes induction. After diabetes induction, as well as post-islet cell transplant, blood glucose levels were monitored 2–3 times daily via heel stick using a OneTouch Ultra Glucometer (LifeScan, Milpitas, CA). Subcutaneous insulin was administered (Humulin N or Humulin N Lantus) as needed and based on an individualized sliding scale, aiming for fasting and postprandial plasma glucose levels of 150-250 mg/dL postSTZ and prior to transplantation. A double-antibody radioimmunoassay method (Diagnostics Products, Los Angeles, CA) was used to assess plasma insulin and c-peptide levels. Fasting CP values were normalized in relation to fasting blood glucose values using the following ratio: (CP/fasting blood glucose [FBG])x100 (ng/mg).

6.2.6.2 INTRAHEPATIC ISLET TRANSPLANTATION

The recipients were subjected to general anesthesia and underwent a minilaparotomy in order to access a mesenteric tributary of the portal vein. A small supraumbilical central midline incision was made, and the islets were infused via gravity through a 24-gauge intravenous catheter over a period of 5 min.[148] Initial studies included three (3) untreated islet (historical controls) and one (1) PEGylated islet

transplants, performed separately. Control animals received 6,000 to 7,549 uncoated islet equivalents (IEQ)/kg while the animal transplanted with PEGylated islets received 4,157 IEQ/kg. After seeing encouraging results in these pilot studies, paired experiments were conducted, with one animal receiving unmodified control islets (~8,305 IEQ/kg) and the other receiving PEGylated islets (~8,705 IEQ/kg).

6.2.6.3 POSTOPERATIVE MONITORING AND INSULIN ADMINISTRATION

Clinical signs, fluid balance, blood glucose, body weight, and nutritional intake were monitored regularly, and weekly blood tests were done to monitor overall health. Blood samples for determination of rapamycin and FK506 trough levels were obtained weekly. After islet transplantation, insulin was administered as needed to maintain FBG in the 100–150 mg/dl range and postprandial glucose in the 100–200 mg/dL range. C-peptide levels were monitored weekly.[148] For the paired transplants, blood samples were collected in Vacutainer tubes containing 3.2% sodium citrate immediately before islet infusion, and 15 minutes, 1, 3, 8,and 24 hr posttransplant. Plasma was collected and stored at -80 °C until it was analyzed to measure prothrombin time (PT), partial thromboplastin time (PTT), Thrombin-antithrombin complex (TAT), D-dimer, and fibrinogen 1 and 2 using enzyme-linked immunosorbent assay kits (Dade Behring) per manufacturer's instructions. These measurements provided an indication of activation of inflammatory processes during the early stages of engraftment.

6.2.6.4 IMMUNOSUPPRESSIVE REGIMEN AND DRUG LEVELS

Steroid-free immune suppression (SFIS) was initiated on postoperative day (POD) -1 and consisted of Thymoglubulin (10 mg/kg) on POD -1, 0, 2, and 4; daily Tacrolimus (i.e. FK506; Astellas Pharma, Deerfield, IL) at 0.02 mg/kg intramuscularly adjusted to

maintain trough levels of 8-10 ng/mL from POD -1 to POD 30; and Rapamycin (LC Laboratories, Woburn, MA) at 0.05 mg/kg intramuscularly daily adjusted to maintain trough levels of 8-12 ng/mL from POD 28 and thereafter.

6.2.6.5 LIVER BIOPSY COLLECTION AND HISTOLOGICAL EVALUATION

Under general anesthesia, the surgical site was prepared aseptically before a dermal incision was placed in the upper midline of the abdomen. Dissection was carried through the subcutaneous tissue and the linea alba (midline of rectus abdominus muscle). The inferior portion of the right lobe of the liver was exposed, and the central portion of right lobe was sutured with two sutures of 4-0 Vicryl. A "V" shaped wedge of liver was sharply excised between the sutures, and sutures were tied approximating the two cut edges for hemostasis. Linea alba Rectus Abdominus muscle was closed with running 4-0 Vicryl suture, and the skin was approximated with a 5-0 subcuticular suture.

Biopsies were fixed in 10% neutral buffered formalin, embedded in paraffin, sectioned (5 μm) and stained with hematoxylin and eosin (H&E). For immunofluorescence microscopy, sections were subjected to antigen retrieval under high pH Tris-EDTA buffer, blocked using PBS + 1% BSA for 30 minutes, and stained for CD3 (Cell Marque, 1:100), FoxP3 (BD Pharmigen, 1:200), and Insulin (Dako, 1:100). Signal amplification for FoxP3 was achieved by using biotinylated primary and secondary antibodies along with a Streptavidin-AlexaFluor 546 conjugate (Life Technologies, 1:3000). Nuclei were labelled with a DAPI counterstain. Primary antibodies were incubated overnight at 4 °C, followed by incubation with the biotinylated secondary antibody at room temperature for 1 h. Finally, a third incubation with a cocktail consisting of the streptaviding-AlexaFluor 546 conjugate, an anti-rabbit AlexaFluor488, and DAPI was carried out at room temperature

for 1 hr. Sections were washed extensively with PBS between incubations. As a negative control, the primary antibody was omitted. Slides were mounted using ProLong Gold mounting medium and imaging was performed using a Zeiss LSM 510 confocal microscope.

6.3 RESULTS

6.3.1 IN-VITRO ISLET CHARACTERIZATION

6.3.1.1 CONFIRMATION OF PEGYLATION AND VIABILITY ASSESSMENT

To scale up of the procedure to NHP models, adjustments in the rodent protocol was made. The major modification was to accommodate a shorter incubation time prior to PEGylation. As PEG grafting to the outer ECM coating is the most desirable target, islets are typically cultured as long as feasible, prior to PEGylation. For rodent islets, islets can be cultured for 48 hr and transplanted after 24 hr, resulting in a total of 72 hr culture time. For NHP islets, however, longer culture times are not desirable, due to historical observations that culture results in greater islet loss and fragmentation. To accommodate this, NHP islets were PEGylated 24 hr earlier, i.e. 24 hr post-isolation. Further, the procedure was scaled up into several dishes to maintain the same IEQ/mm culture density and PEG concentration. As was the case with the murine islets, PEGylation of NHP islets was confirmed by imaging of the FITC-PEG on the islet surface as shown in **Figure 22**. Again, although there was a high degree of PEG grafted onto the surface, variability in the surface density of the polymer between islets within a preparation and between islet preparations was observed, similar to what was seen with the murine islets. Additionally, viability staining found that the PEGylation of NHP islets did not adversely affect islet cell

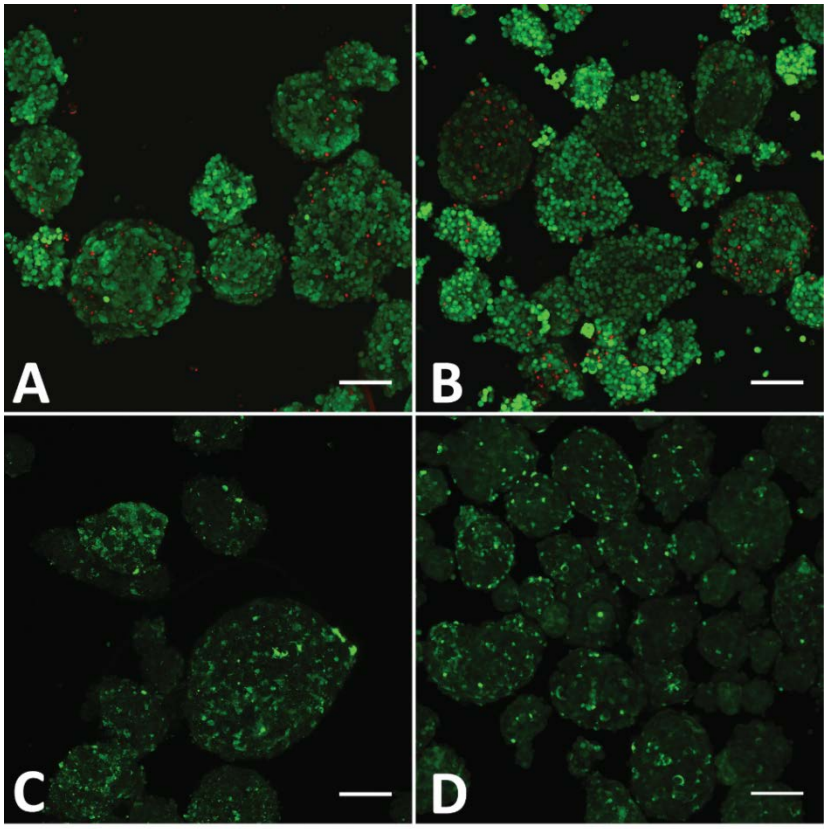

Figure 22. Visualization of PEGylation of NHP islets and impact on islet viability. Live/Dead staining of (A) control and (B) PEGylated islets shows no difference in islet viability after PEGylation. C-D: Confocal microscope images of FITC-labeled PEG, permitting visualization of coating. Imaging of fluorescent grafted polymer confirms grafting of PEG into the islet surfaces, albeit at different densities throughout the islet surface. Scale bars = 100um.

viability when compared with untreated control cells, as seen in confocal microscopy images shown in **Figure 22.**

6.3.1.2 PEGYLATED NHP ISLET FUNCTION

As an alternative to the static column incubation method for measuring glucose responsiveness and insulin secretion, perifusion, a method that permits observation of the kinetics of insulin release over time according to different stimuli, was employed to analyze PEGylated NHP islets. These experiments produced similar results to those observed for

murine islets (**Figure 23**). In this case, insulin released by control islets was computed to be 5.22 ± 0.77 and 48.91 ± 9.59 uIU/mL (mean ± S.D.) for low and high glucose samples respectively, whereas the corresponding values for PEGylated islets were 9.91 ± 1.80 and 63.36 ± 13.69 uIU/mL. These values were calculated by first averaging the insulin measured from 5 samples collected during the initial low glucose period (minutes 3-8) or 3 samples taken during the high glucose period (minutes 10-12) for replicate columns.

Consistent with the results from mouse islets, PEGylated NHP cells secrete insulin at a level comparable to that of control islets under stimulation (n.s.; $P = 0.1201$), with PEGylated islets having a slightly elevated basal release of insulin ($P < 0.0001$). Consequently, a slight, but non-significant reduction in the stimulation index from 9.33 ± 0.46 for control islets to 6.50 ± 1.55 for those grafted with polymer is observed ($P = 0.1333$).

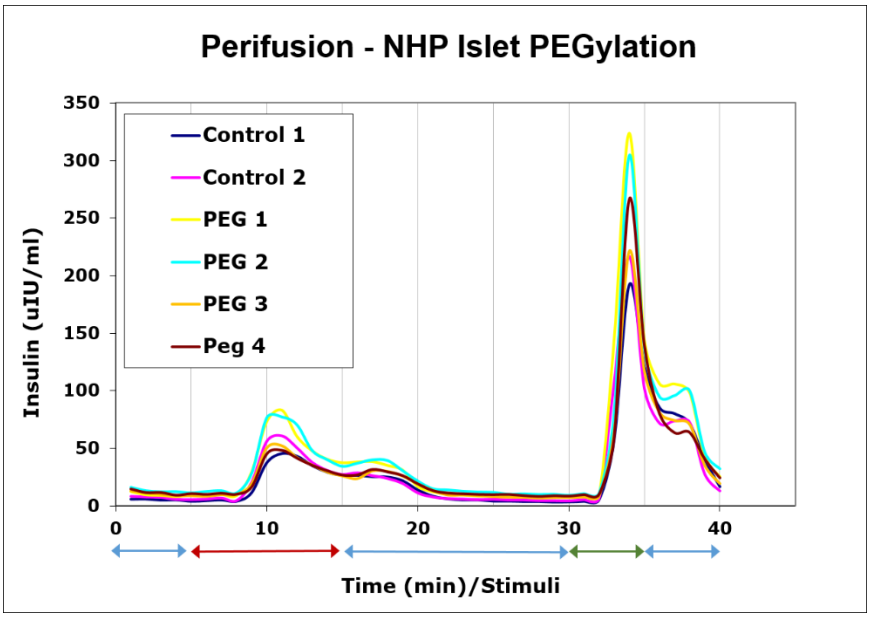

Figure 23. NHP islets retain their secretory function after PEGylation. Perifusion assay showing comparable response to glucose challenge by control and PEGylated islets. Arrows below the horizontal axis indicate buffer pumped through the system. Blue: 3mM glucose, red: 11mM glucose, green: KCl solution.

Of note, this experiment was repeated when the paired (control and PEGylated) study was performed, whereby the stimulation index for the islets were found to be statistically identical.

6.3.1.3 PLASMA RECALCIFICATION ASSAY

As bigger animal models permit for the collection of larger biological samples, the opportunity to perform additional assays that were challenging to conduct with the limited amount of samples acquired from smaller animals such as rodents was presented. One such assay was the plasma recalcification assay. This assay measures the coagulation rate of platelet-poor plasma upon exposure to different surfaces and gives an indication of the inflammatory properties of said surface, with faster coagulation corresponding to higher inflammatory potential. For purposes of this study, the assay was used to evaluate

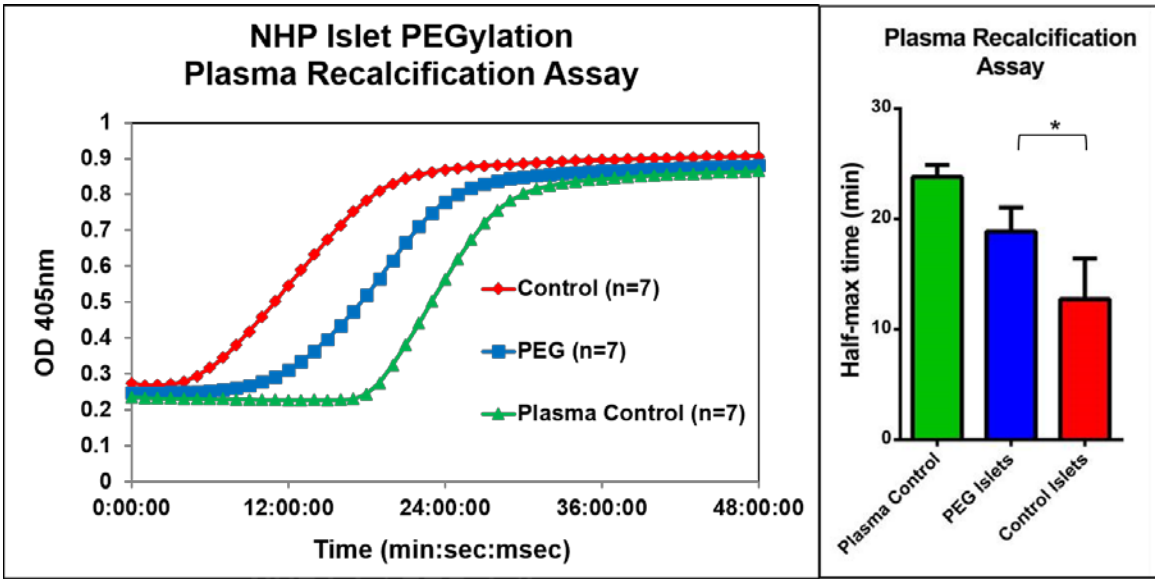

Figure 24. PEGylation of NHP islet surfaces delays platelet-poor plasma coagulation in vitro. The half-max time of the rate of coagulation of platelet-poor plasma was delayed by PEGylation from 12.74 3.68 min observed with control islets to 18.87 min (P = 0.04) indicating a reduction in the inflammatory properties of the modified islets' surface.

differences in inflammatory potential between untreated control islets and PEGylated islets. As shown in **Figure 24**, PEGylated islets were found to be significantly less inflammatory that control islets, as measured by a delay in coagulation time, with a shift in the coagulation time from 12.74 ± 3.68 min for control islets to 18.87 ± 2.18 for PEGylated islets (mean ± S.D.; P=0.04).

6.3.2 PEGYLATION ENHANCES GRAFT FUNCTION AND PERSISTENCE IN A NON-HUMAN PRIMATE MODEL OF TRASNPLANTATION WITH REDUCED IMMUNOSUPRESSION

6.3.2.1 INITIAL PILOT STUDY

In preliminary studies, 3 untreated islet (historical controls) and 1 PEGylated islet transplants were performed by intraportal infusion in cynomolgus monkeys. Control animals received an islet dosage of 6,000 to 7,549 IEQ/kg, while the PEGylated islet recipient received only 4,157 IEQ/kg or 30.7% lower than the lowest control dose. As expected by the immunosuppressive regimen, control animals began to reject their grafts from POD 23-67 (n = 3), with complete loss of function on POD 28-74, as defined by c-peptide values < 0.2 ng/mL. None of the control animals experienced insulin independence (see example in **Figure 25**). Remarkably, the animal transplanted with only 4,157 PEGylated IEQ/kg experienced excellent graft function and achieved insulin independence for a period of 83 days from POD 47-130, with c-peptide levels of 2.52 ng/ml on POD 4 (1.83 ± 0.18 for the 3 controls), a peak of 4.18 on POD 21 (peak c-peptide of controls were 2.57, 2.65 and 3.04 on POD 7-14) and maintenance of 2-3 ng/ml c-peptide through POD 272 (all controls c-peptide negative by POD 28-74) (**Figure 26**). Gradual destabilization of fasting and post-prandial blood glucose led to reinstitution of exogenous insulin therapy

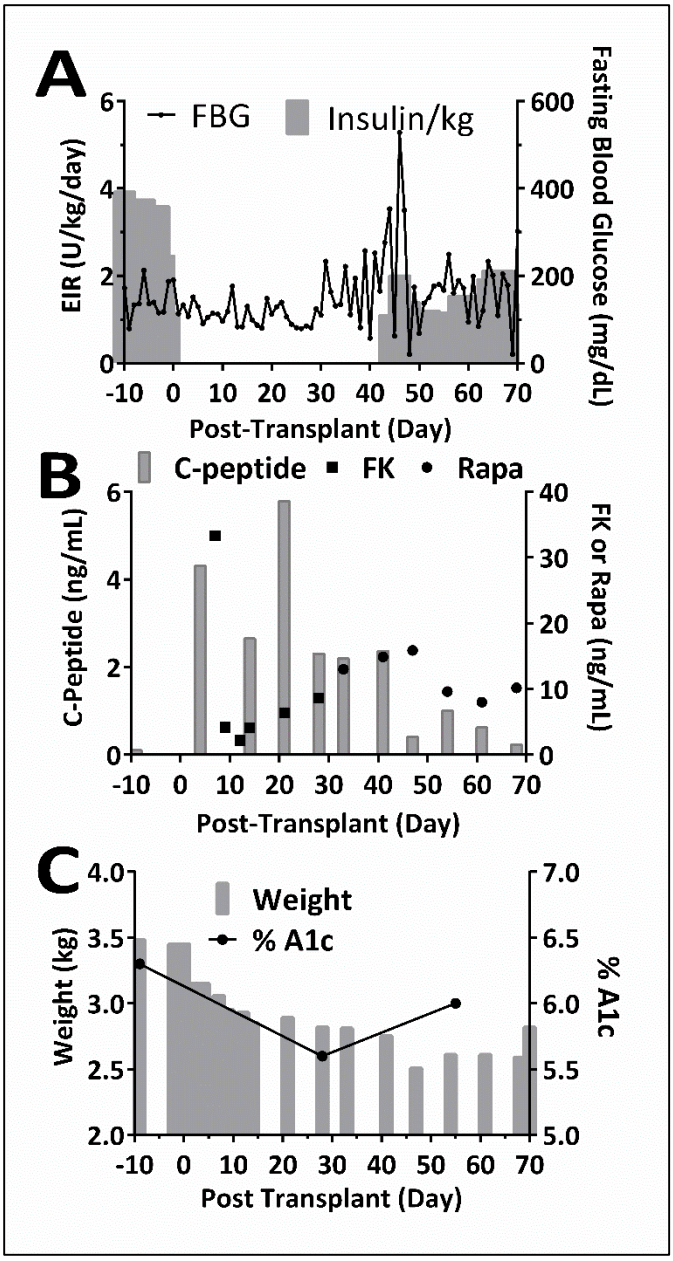

Figure 25. Transplantation of control (untreated islets) complemented by mild immunotherapy resulted in islet rejection in a Cynomolgus monkey model of transplantation. A) Fasting blood glucose and exogenous insulin requirements; B) C-peptide (grey bars) and systemic immunosuppression levels; and C) weight (grey bars) and % A1C of the recipient over the duration of the transplant. The animal was insulin independent for 43 days and rejected the graft by POD 68.

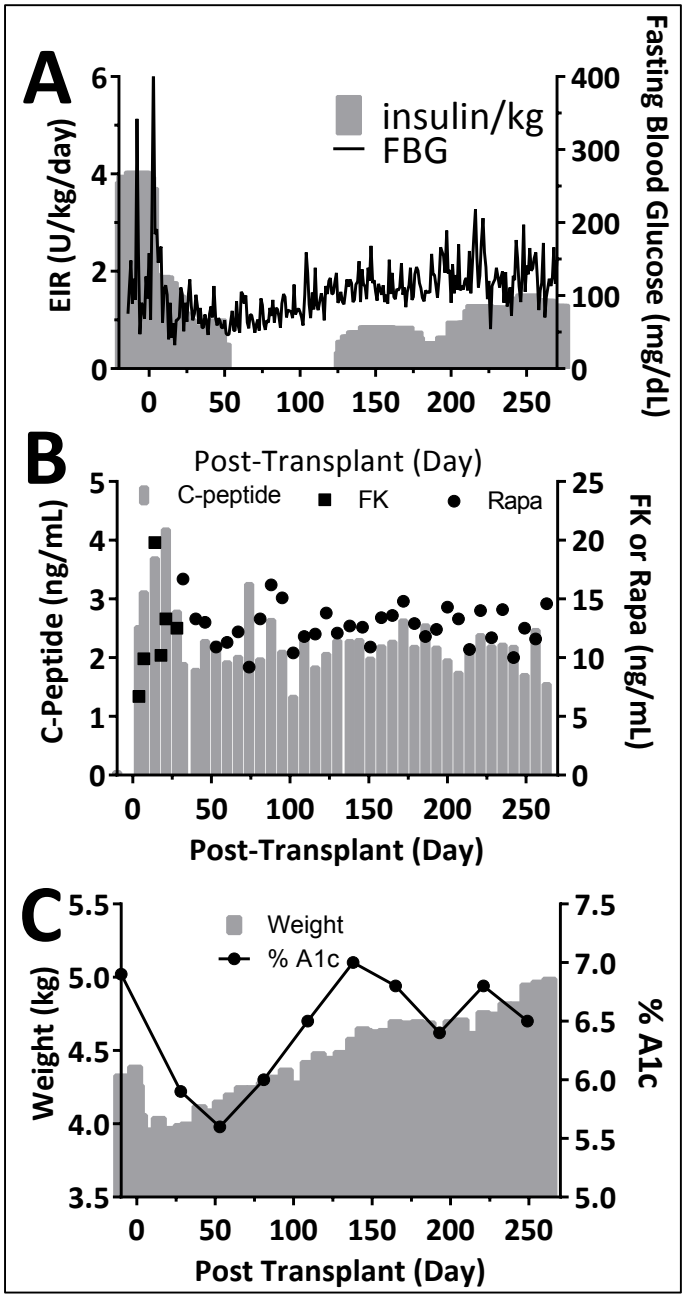

Figure 26. Transplantation of PEGylated islets complemented by mild immunotherapy resulted in insulin independence in a Cynomolgus monkey model of transplantation: 10C59 transplant. A) Fasting blood glucose and exogenous insulin requirements; B) C-peptide (grey bars) and systemic immunosuppression levels; and C) weight (grey bars) and % A1C of the recipient over the duration of the transplant. The animal was insulin independent for 83 days and maintained C-peptide levels between 2-3ng/mL through POD 272.

on POD 130. The experiment was electively terminated on POD 272. The animal gained one kg of body weight (25% weight gain) over the course of the experiment, demonstrating the safety of this approach.

Histological evaluation of explanted tissue provides some insight into the host responses to the islets. For this study, a liver biopsy was obtained on POD 207, followed by the terminal collection on POD 272, which provides a temporal assessment of this response. On POD 207 when the graft exhibited strong function, several robust islets free of notable immune infiltrates were observed, along with a few with minimal amounts of infiltrates in the periphery (**Figure 27, A-C**). Following euthanization of the animal on

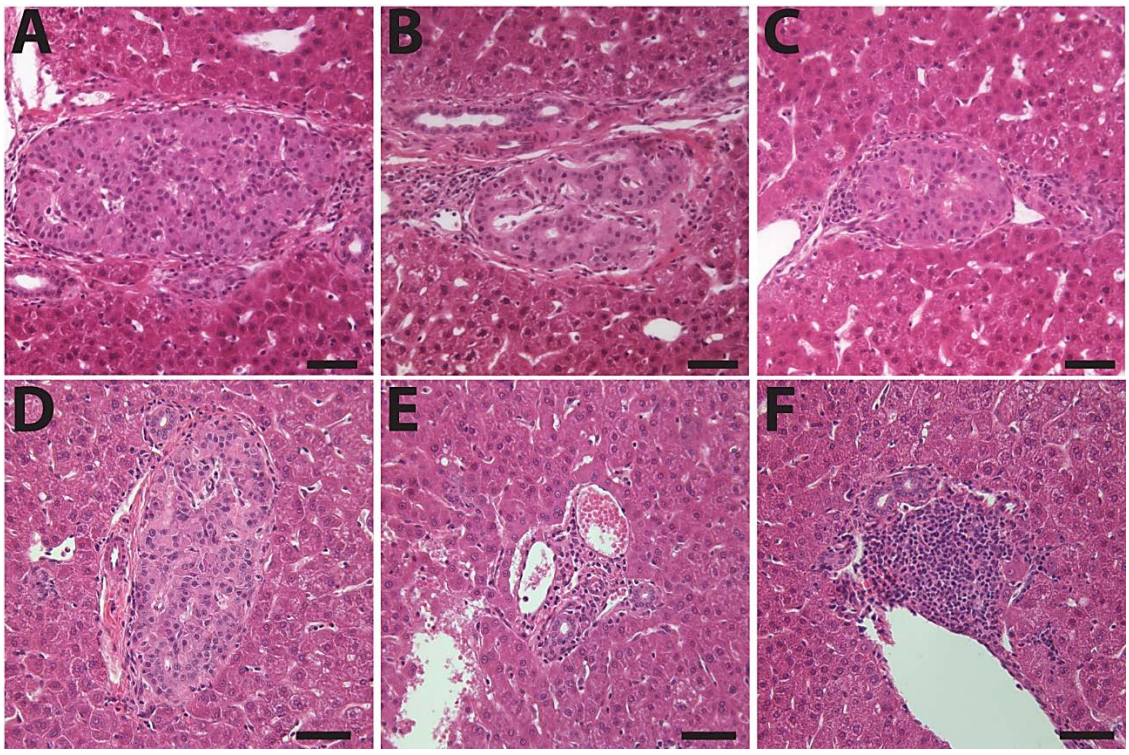

Figure 27. Histological evaluation of PEGylated NHP islets on POD 207 (A-C) and 272 (D-E) via H/E. Representative images of islets explanted 207 d post-transplant (A-C) and 272 d post-transplant (D-E) illustrating islets within the liver microvasculature. Note accumulation of mononuclear cells within F. Scale bar = 50 μm.

POD 272, less robust islets and active mononuclear infiltration were observed (**Figure 27, D-F**). These results appear to support the hypothesis that the PEGylation procedure assists in dampening inflammatory responses and immunological recognition; however, this impact is transient, as recognition and immunological attack of the graft initiates over time. These observations are consistent with those obtained from the mouse transplants. Immunofluorescent staining can provide further insight as to the type of immunological responses to the graft for both time points. Extensive optimization was made to permit IHC for NHP grafts; however, staining of the actual grafts remains to be performed. These should be completed in the upcoming weeks.

6.3.2.2 ONGOING STUDIES

Due to these promising pilot results, a recent NIH award provided an opportunity to perform a more robust study. In this study, recipient animals were closely matched for weight and thus exogenous insulin requirement, which permits comparison of graft function. Further, MHC class II alleles of recipients were matched (both H3 and H4). For donor islets, 3 pancreata were used for islet isolation and the resulting islets were pooled. The MHC class II alleles for the donor islets were a complete mismatch from the recipients. Following pooling of the islets, the islets were split into two groups: control and PEGylated. Islets were subsequently transplanted into the matched recipients within several hours of each other, with the control recipient receiving 8,305 IEQ/kg and the PEGylated recipient receiving 8,705 IEQ/kg.

Assessment of islet viability and function revealed no difference between control and PEGylated islets as expected (section 6.3.1). For this study, blood plasma coagulation assessments were conducted pre- and post-transplantation to track activation of

inflammatory pathways (**Figure 28**). Data from these experiments show that, relative to the pre-transplant period, PPT increased by approximately 20 seconds in blood samples collected from the control animal 15 minutes and 1 hr after the transplantation procedure. This change was not observed in the animal receiving PEGylated islets, which displayed a more stable response before and after transplantation (**Figure 28B**). This suggest there is a coagulation factor deficiency in the samples collected from the control animal indicative of increased *in vivo* coagulation activity. As coagulation takes place due to contact of blood with the islet surface *in vivo*, the amount coagulation factors in the blood is reduced resulting in an increase of the PTT of the blood samples collected. However, additional studies are needed to validate this observation. Similarly, TAT levels (**Figure 28C**) appear equivalent during the pre-transplant period and spike up in both animals; however, the intensity of the spike appears larger in the control animal than in the animal receiving PEGylated islets. Over time, starting at about 3 hours post-transplant, samples from both subjects reveal a drop to equivalent levels of TAT. This coincides with a sharp spike in D-dimer (**Figure 26D**), a product of fibrin breakdown and thus clot degradation, observed in the control animal and not in the experimental one, albeit the reading for this peptide are not very stable to begin with. Taken together, these data suggest clotting was occurring and was being regulated by the antithrombin negative feedback loop; however, as mentioned earlier, this is just one animal for each group. Further studies need to be performed to confirm and validate these observations. The measurement of fibrinogen is a good example of why these data must be validated and confirmed, as the levels detected in the PEGylation group, where one would expect it to remain relatively steady if there was no response taking place, rise over time whereas the control group remains steady for

during the early time point sampled, contradicting the data discussed previously (**Figure 28E)**. This reflects reduced *in vivo* coagulation activity, since there is more fibrinogen available to form a clot if necessary. Taken altogether, coagulation and blood analysis data

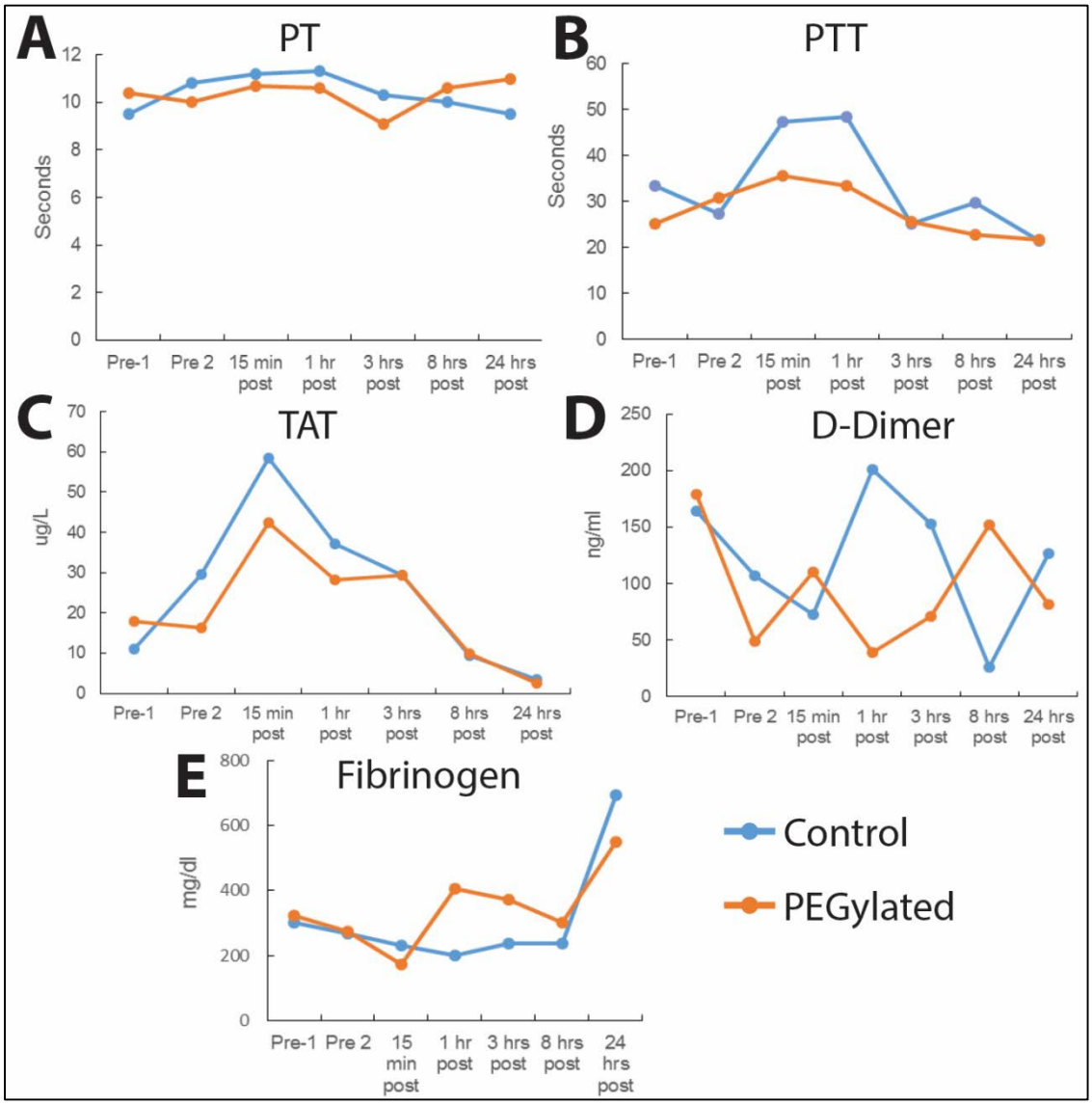

Figure 28. Blood plasma coagulation assessments conducted pre- and post-transplantation for the animal receiving control (unmodified) islets and the animal receiving PEGylated islets. Assessments of prothrombin (PT; A), partial thromboplastin time (PTT; B), Thrombin-Antithrombin Complex (TAT; C), D-Dimer (D), and fibrinogen (E) were measured at the time points specified.

indicate that PEGylation of the islet surface could result in reduced coagulation activity in the recipient, mitigation of IBMIR, and thus the acute inflammatory response.

Evaluation of graft function for the recipients of either control or PEGylated islets was conducted via tracking of metabolic parameters, as outlined in the pilot study. A summary of these metabolic assessments is shown in **Figure 29**. Presently, although the control animal achieved insulin independence for a period of approximately 7 days, fasting and post-prandial blood glucose rapidly destabilized following this period around POD 25 indicating islet graft rejection. In contrast, albeit not having experienced insulin independence, the animal that received PEGylated islets still maintains stable fasting and post-prandial blood glucose levels. The insulin requirement for this animal has been reduced by approximately 50% to that prior to the transplant, indicating the graft is functional. To compare to the first PEG transplant, the subject did not reach insulin independence until POD 47. Evaluation of c-peptide levels indicate, at this point, sustained c-peptide release (indicating insulin release from the transplanted islets) for the PEGylated transplant at POD 47, while the c-peptide levels were less than 0.2 mg/dL, considered a negative reading, for the animal receiving the control islets on POD 39. Of note, it is too early into the duration of these transplants to make any solid conclusions, thus only further time will indicate if the trends observed for the initial transplants will hold for these paired experiments.

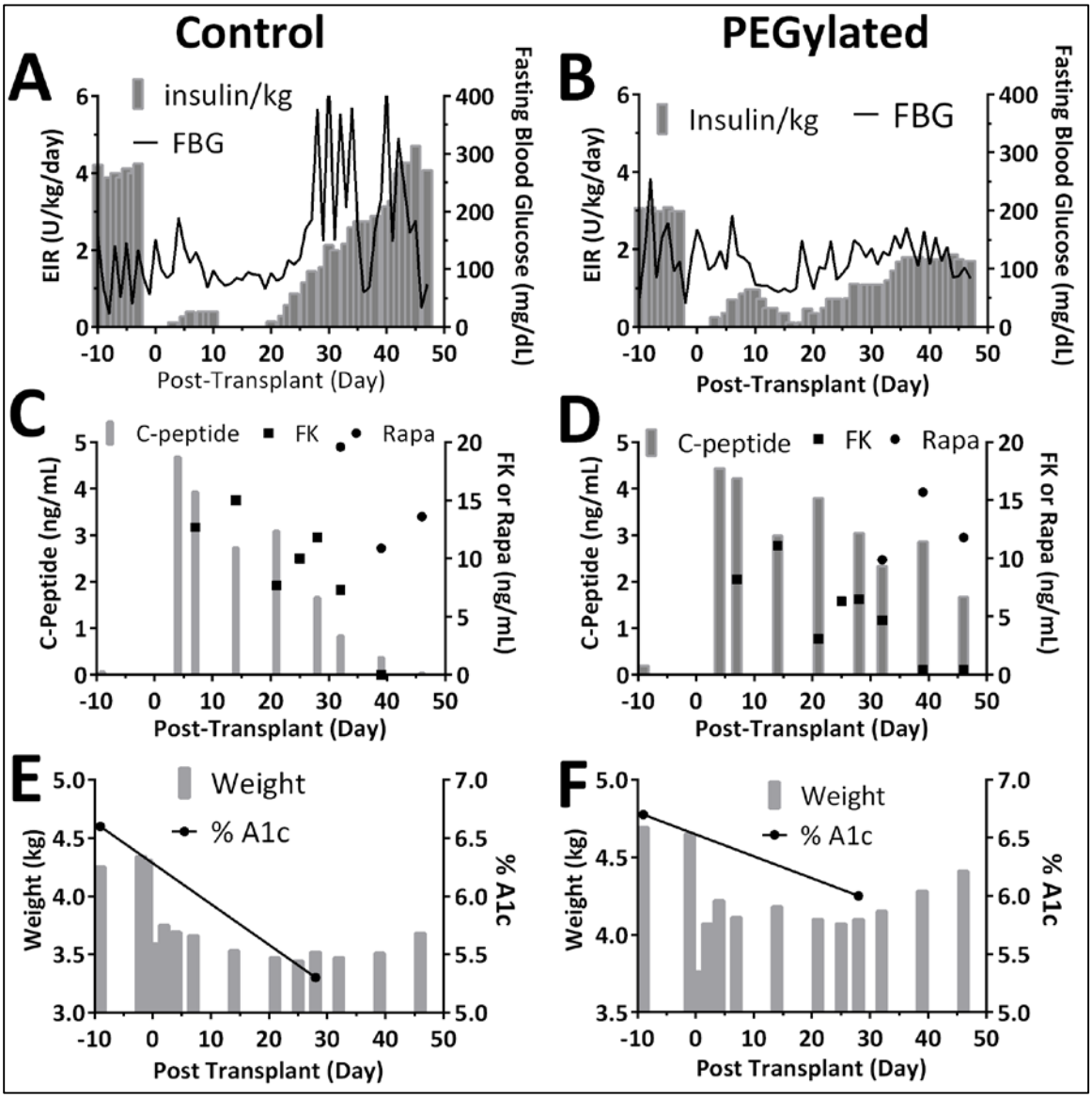

Figure 29. Transplantation of Paired Transplantation of Control (A, C, and E) or PEGylated (B, D, F) islets complemented by mild immunotherapy in a Cynomolgus monkey model of transplantation. A-B) Fasting blood glucose and exogenous insulin requirements; C-D) C-peptide (grey bars) and systemic immunosuppression levels; and E-F) weight (grey bars) and % A1C of the recipient at this more recent time point for this experiment – *transplant on-going*.

6.4 DISCUSSION AND CONCLUSIONS

As with the murine islets, grafting of the polymer onto the NHP islet surface was successful and *in vitro* characterization confirmed that PEGylation had no adverse effects on NHP islet viability or function, as determined by the cell membrane permeabilization imaging and perifusion assays. In addition, plasma recalcification assays demonstrated that modification of the islets with PEG mitigated the reactivity of the cell surface to platelet poor plasma. These benchtop studies support the hypothesis that PEGylation provides a steric barrier that is capable of masking proteins that serve to activate inflammatory pathways. As mentioned previously, one of the main challenges in islet transplantation is IBMIR, the initiation of the blood coagulation cascade which takes place when blood comes into direct contact with the islet surface and thus Tissue Factor[17, 18]. This event is the first in a long chain reaction that ultimately results in the activation of inflammatory pathways and recruitment of innate and adaptive immune cells to eliminate the foreign body in question. If this initial event could be circumvented, one might be able to significantly dampen the intensity of the acute immune response and greatly improve the chances of successful engraftment.

Moreover, we explored the impact of PEGylation, in combination with a modest immunosuppressive regimen, on the overall graft persistence and function in an NHP preclinical transplant model. When compared to animals that received untreated control islets, the animal that received PEGylated islets demonstrated a significant enhancement of glycemic stabilization, reduced insulin requirement, and an extended duration of function. Surprisingly, while only observed in a sample size of one, the islet dose requirement to achieve insulin independence was reduced by 50%. As the experiment

progressed, blood glucose measurements pointed to a disruption of glucose regulation, which led to the reinstitution of exogenous insulin therapy. A biopsy performed more than 60 days prior to termination revealed robust islets with minimal, if any, amount of immune infiltrate. Upon euthanization of the animal, histological evaluation of the liver confirmed an increase in the infiltrate present since the biopsy was taken. Additional immunohistochemical analysis is needed to further characterize the host response.

Data collected in on-going experiments provide further support to the promising of PEGylation as a complementary tool for improving islet engraftment. Preliminary measurements of factors involved in coagulation in blood samples taken immediately prior to and following transplantation appear to indicate elevated clot formation in the control animals, corroborating *in vitro* data obtained from the plasma recalcification assay. Increased PTT shows a deficiency of coagulation factors in the sample, while increased levels of TAT and D-dimer suggest negative regulation of a clotting reaction is taking place. However, these are only preliminary measurements of a sample size of 1, having negligible statistical power. Further studies must be carried out to confirm and validate these observations. They do, however, fit nicely with the results discussed in previous Chapters with the murine mechanistic studies and the *in vitro* plasma recalcification assays. While highly preliminary, data collected to date indicate PEGylation of the islet surface results in reduced coagulation activity in the recipient, mitigation of IBMIR, and thus the acute inflammatory response. While the long term results from this experiment regarding insulin independence and c-peptide levels remain to be seen, it is highly encouraging when taking into consideration other studies published that support this hypothesis. In particular, the work done by Dr. Kenyon's team, where Tissue Factor was targeted by a monoclonal

antibody in order to prevent IBMIR and enhance engraftment in a cynomolgus monkey model of transplantation.[157] Berman et. al show that mitigating IBMIR and acute inflammation with this strategy resulted in elevated c-peptide levels, decreased coagulation activation, and prolonged graft function. Given that these observations, to date, appear to follow this same trend, the PEGylation approach may serve to provide this benefit without the need to administer agents that have the potential to impart systemic inhibition of inflammatory pathways.

With these studies, we move the concept of islet surface modification with polymers along the path of preclinical research towards clinical research and hopefully one day treatment of human patients. Scale-up of the process to the NHP level was not a significant challenge, although modification to permit scale-up to the industrial scale or clinical use will likely be more complex. Manipulation of a large number of cells, and thus large volumes of polymer solutions, will be necessary if this is to be translated for treatment of humans as was the case in these experiments. This is compounded when one takes into account the fact that once the polymer has been dissolved, the time to resuspend the cells and transfer them to the incubator is very limited since the NHS ester reactive group is very volatile in aqueous conditions and is hydrolyzed very quickly. As a result, one must time the procedure properly so that the cells are ready for modification as soon as the polymer is dissolved. Our approach to circumvent this issue simply involved aliquoting the majority of the polymer solution into the culture vessels where the PEGylation reaction was to take place ahead of time, followed by resuspending the islets in a small volume of polymer solution for distribution into said vessels. This drastically reduced the volume of cell suspension being manipulated and the time it took to distribute the cell suspension and

transfer the cells to the incubator, which is critical, as it allows gentler manipulation of the cells to ensure maximal viability. Both of these variables must be considered collectively, since manipulation of the cells must be carried out gently so as not to cause cell death but quickly to maximize polymer grafting and batch size. Increasing the density of the cells in the polymer solution to evade this issue should be avoided since this will reduce the amount or density of polymer grafted onto the surface of the islets.

Moreover, as the procedure is carried out in serum free conditions, adherence of the islets to different surfaces such as pipet walls and surfaces of culture dishes is common; resulting in the loss of a significant portion of the islets undergoing modification. In order to prevent this, it was necessary to use pipets precoated with full culture media and washed thoroughly. Adsorption of serum proteins from the culture media onto the pipet surface prevents the attachment of islets; however, because the NHS can react with these proteins, the islets must be transferred to the incubation culture vessel quickly. Looking ahead as one imagines this type of therapy being implemented as standard procedure, one must consider whether it would be best to perform the PEGylation at a large/industrial scale in a central location for distribution to transplant centers or if one could commercialize some sort of single-use/procedure PEGylation kits for transplant centers around the world to perform the PEGylation themselves. This of course would involve some sort of training and certificate program where only trained qualified professionals perform the modification. If this were to be the case, one can also imagine some sort of bioreactor that includes several pumps for different solutions, which can perform the process under sterile conditions such as the fully automated cell separation instruments now commercially available. This would minimize human error and carry out the procedure in a reproducible

manner. Again, this would be for batches of limited size which could be carried out on site at the transplant center.

Chapter 7. Engineering Surfaces for Modulation of Immune cell Function.

7.1 INTRODUCTORY REMARKS

Thus far, this dissertation has explored the benefits of PEGylating islet surfaces to enhance graft survival. The data presented indicate that the mechanism by which PEGylation achieves this improvement is through interference of the pathways that lead to IBMIR and the subsequent inflammatory response, as indicated by plasma coagulation experiments and the change in macrophage subpopulations seen at the graft site during the early engraftment period. Moreover, this change in the inflammatory response must translate to a change in the adaptive immune response observed, as the two are intimately linked, as discussed in Chapter 2, section 2.2.1. PEGylation alone, however, cannot provide complete protection from the immune response, thus requiring supplementation with complementary immunotherapy.

Alternative strategies to reduce the need for systemic immunosuppression have also been discussed in Chapter 2, section 2.3. There, different approaches were presented in which encapsulation materials, such as PEG, are modified with bioactive motifs to modulate immune cell function. One pathway involved in the regulation of the adaptive immune system is the PD-1:PD-L1 pathway. To reiterate the discussion in Chapter 2, this pathway has been shown to regulate T cell proliferation and differentiation, T cell survival, and cytokine production.[38, 117-123] Additionally, this pathway has been identified as a major mechanism in regulation of peripheral tolerance through induction of regulatory T cells (Tregs) and T cell exhaustion.[38, 117-124] Harnessing this pathway to supplement PEGylation by tethering PD-L1 onto the surface of islets destined for transplant could

prove highly beneficial, as one could exploit its inhibitory functions and further promote allograft survival by directing immune cell function towards a more tolerogenic nature.

The method by which these molecules are tethered to the islet surface must be carefully considered. The chemical ligation scheme must be compatible so as not to induce cell death. One such method is already in use for the stabilization of alginate gels for encapsulation[158] and for layer-by-layer assembly of polymer coatings on cell surfaces[105, 106]: the Staudinger ligation. This is a chemoselective reaction whereby azide (N_3) and 1-methyl-2-diphenylphosphino-terephthalate (MDT; Phoshine; Pph) groups spontaneously form covalent bonds (**Figure 30**). Due to its specificity and pH requirements, this is a highly biocompatible reaction that can take place in full media and in the presence of multiple types of compounds; an important quality when considering the end goal is to employ this strategy onto live cells. By using a heterobifunctional polymer with a terminal NHS group to react with primary amines on proteins and an MDT reactive group on the opposite end, one can functionalize the protein of interest for tethering onto surfaces presenting the complementary azide groups.

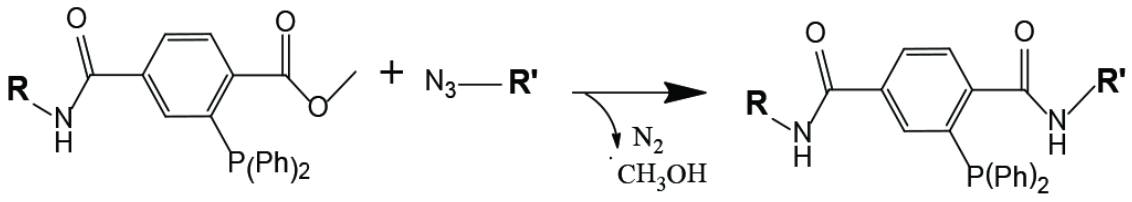

Figure 30. Staudinger ligation scheme, whereby phosphine spontaneously reacts with azide to form a stable covalent bond.

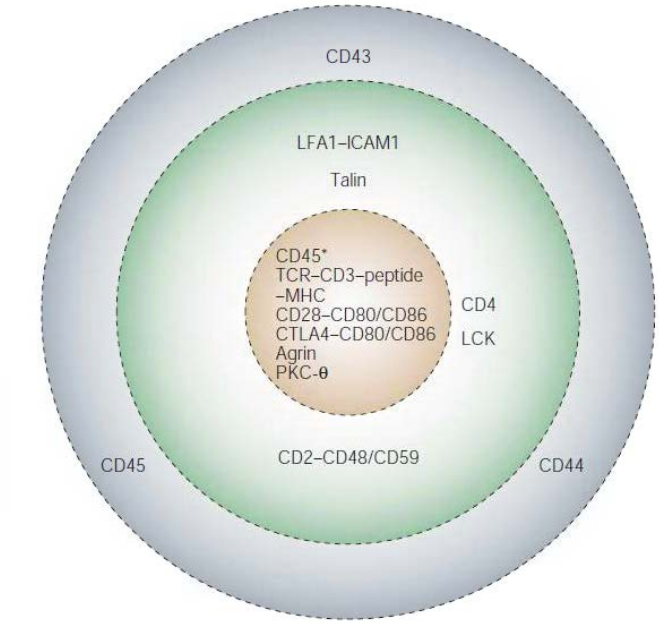

Figure 31. Spatial distribution of different receptors in the immune synapse. Face view of the immune synapse showing the arrangement of different receptors on the cell surface. Of particular interest is the central supra-molecular activation complex (cSMAC).[159]

Furthermore, the manner in which these signals are presented on the islet surface is of utmost importance. As previously described, the immune synapse is a highly complex and dynamic interaction between APCs and T cells in which spatial and temporal components are critical factors in communication between these cells (**Figure 31**).[159] Recent studies indicate that micropatterning of these signaling molecules in different configurations indeed results in diverse responses from T cells.[160-162] Herein, we explore the functionalization of immune signaling proteins for tethering and controlled presentation of PD-L1 by using a heterobifunctional polymers with the goal of inhibiting T cell activation and function. It is important to point out that due to time constraints, the data presented in this chapter are from preliminary screening experiments, which must be confirmed by additional studies.

7.2 MATERIALS AND METHODS

7.2.1 NHS-PEG-MDT POLYMER SYNTHESIS

NHS-PEG-MDT was fabricated by the following two step process. First 200 mg of H2N-PEG-COOH (Laysan Bio, NH2-PEG-CM-3400) and 31 mg MDT-OPfp (2-(Diphenylphosphino)terephthalic acid 1-methyl 4-pentafluorophenyl diester; Sigma-Aldrich, Cat. No. 679011), were dissolved in 800 µL anhydrous DMF by vortexing in a 15mL falcon tube under Argon gas. 32 µL of TEA (triethylamine; Sigma-Aldrich, Cat. No. 471283) were then added and the mixture was vortexed under Argon gas for an additional 3 hours. A Kaiser's test was performed to confirm all amine groups had been modified (negative Kaiser's test result). The polymer was then purified by precipitation using 10 mL of cold diethyl ether, resuspending in 10mL of ethanol (200 proof; Sigma-Aldrich, Cat. No. 459844), vortexed, and warmed until it had dissolved. Subsequently, the polymer was precipitated by cooling in an ice-water bath while undergoing periodic vortexing. The precipitate was then dissolved in 10 mL of diethyl ether, and precipitated once more by cooling in an ice-water bath. The diethyl ether was the decanted and the precipitate dried under reduced pressure overnight to yield a white-yellow, solid powder.

For the second step of the fabrication process 180 mg of product from Step I and 16 mg NHS were dissolved in 700 µL DMF in a 15ml Falcon tube by vortexing under Argon gas. 22 µL fresh DIC (5.N,N'-Diisopropylcarbodiimide, Sigma-Aldrich, Cat. No. D125407) were then added and the solution was vortexed under Argon for an additional 3 hours. The polymer was purified as described in step 1 with the successive precipitation and dissolution in diethyl ether, ethanol, and diethyl ether. The final precipitate was then

dried under vacuum to yield a white-yellow solid powder. The process was evaluated by analysis of ATR-FT-IR to ensure polymer modification.

7.2.2 PEG-PROTEIN CONJUGATES

7.2.2.1 CONJUGATE SYNTHESIS AND PURIFICATION

Due to the oxidation of the MDT reactive group in aqueous solution over time, modification of proteins was carried out immediately prior to each experiment or bead modification. This reaction was carried out in PBS after adjusting the pH to 8.5 and using a freshly prepared 2.5 mM concentrated stock solution of NHS-PEG-MDT polymer synthesized as described in section 7.2.1. For each experiment, a 250 μL aliquot of anti-CD3 stock solution (BioXCell, Cat. No. BE0001-1) was taken and the pH adjusted to ~8.0-8.5 using 1M NaOH stock solution (4 μL NaOH/250 μL anti-CD3) and pH paper. The concentration of the anti-CD3 solution was then adjusted to 2 mg/mL using PBS (pH 8.5). Following pH adjustment, the polymer was dissolved and the appropriate amount of polymer stock solution was added to achieve the desired molar ratios of polymer to protein. The tubes were gently vortexed and incubated at room temperature for 2 hours. BSA was modified following a similar procedure where BSA powder was dissolved in PBS (pH 8.5) at 2 mg/mL, polymer stock solution was added, and the mixture incubated for 2 hours at room temperature. For modification of PD-L1 (R&D Systems, Cat. No. 1019-B7-100)), a fresh vial was reconstituted in PBS (pH 8.5) at a concentration of 400 μg/mL, and the desired amount to be modified was aliquoted into an eppendorf tube, to which fresh polymer solution was added to achieve the desired polymer to protein ratio.

After incubation, buffer exchange into PBS (pH 7.4) was carried out using 100K and 30K molecular weight cut-off Amicon centrifugal filter devices (Millipore; 100K for

anti-CD3, 30K for BSA and PD-L1) following the manufacturer's instructions to purify the protein and remove any unreacted PEG. The concentration of the recovered PEG-protein conjugates were then measured on a NanoDrop spectrophotometer using the Protein A280 module. The "sample type" setting used for anti-CD3 and BSA were the IgG and BSA setting, respectively. To ensure accuracy in concentration measurements of PD-L1, the "other protein" sample type setting was used, where the values for the molar exctinction coefficient, 66070, and molecular weight, 51.4 KDa, were entered manually. These values were obtained by analyzing the protein's amino acid sequence, listed on the manufacturer's product insert, on the ProtParam tool of the ExPASy Swiss Institute of Bioinformatics' website (http://web.expasy.org/protparam/). Samples were kept on ice after buffer exchange until they were used.

7.2.2.2 CONJUGATE CHARACTERIZATION

Anti-CD3 modification was confirmed by fluoraldehyde assay, which was carried out for initial anti-CD3 experiments following the manufacturer's instructions. Briefly, a sample:reagent ratio of 1:10 was used, where 4 μg/20 μL sample was reacted with 200 μL reagent. The reaction was carried out in a 96-well clear-bottom assay plate on a shaker for 1.5min and the emission at 460 nm was measured (ex 355). The assay was carried out in replicates of 5 for unmodified anti-CD3 as a baseline control, each experimental group, and PBS alone as a blank. Subsequently, and for other proteins modified, PEGylation was confirmed by a shift in the observed molecular weight after automated electrophoresis carried out using the Pro260 Analysis Kit (BioRad, Cat. No. 700-7101) following the manufacturer's instructions.

Activity of the proteins was then tested by T cell proliferation and activation assays as determined by Cell Trace Violet dye dilution and CD25 expression, respectively. Anti-CD3-PEG conjugates were tested by soluble addition to T cell/APC cell cultures (0.5 μg/mL) and measuring of T cell proliferation and activation levels comparing to unmodified protein controls. Similarly, PD-L1-PEG conjugates were tested by T cell proliferation assay. In this case, plate wells were coated overnight at 4°C with native anti-CD3 alone (10 μg/mL), or with PD-L1-PEG conjugates (30 μg/mL) prior to incubation with the cells. Again, native PD-L1 was used as a control. In this case, the activity of the protein was determined by measuring inhibition of proliferation and activation as well as by comparing the number of dead and viable cells. Cells were cultured for 72 h prior to analysis by multicolor flow cytometry. For anti-CD3 samples the entire sample was analyzed. For PD-L1 samples either 10^5 events were collected. Please refer to sections 7.2.5 and 7.2.6 for further details on cell culture and flow cytometry, respectively.

7.2.3 MODIFICATION OF GLASS BEADS

7.2.3.1 AZIDE MODIFICATION OF GLASS BEADS

Large batches (~1 g) of 150 – 212 μm diameter glass beads (Sigma-Aldrich, Cat. No. G1145-10G) were washed in acetone, followed by an incubation in 0.1M NaOH for 3 min at 80°C. Beads were then rinsed thrice in water, twice in 0.1M HCl, thrice in water, followed by ethanol and finally dried. Beads were then resuspended in a 3 μL/mL solution of 11-bromoundecyltrichlorosilane (Gelest, Cat. No. SIB1908.0) in anhydrous Toulene (Sigma) and incubated at 80°C for 20 min mixing frequently. Afterwards, beads were washed thrice in Toulene, thrice in 5% H_2O in dimethylformamide (DMF), thrice in ethanol, and drie. Beads were then cured at 110°C for 10 min and allowed to cool to room

temperature. Following cooling, beads were reacted in a 5 mg/mL solution of sodium azide (NaN_3) in DMF for 1 h at 80 °C mixing frequently. After the incubation, beads were rinsed thrice in DMF, six times in water, thrice in 50% H2O/ethanol solution, thrice in ethanol and dried. All steps were carried out under an inert atmosphere using Argon gas. Beads were then stored under Argon at 4 °C until use.

7.2.3.2 BIOACTIVE MODIFICATION OF AZIDE BEADS

Depending on the experimental design, the appropriate amount of azide beads was weighed into Eppendorf tubes for each group, or set of triplicates, for modification. Beads were resuspended in PBS with the desired amounts of proteins and incubated overnight for 24 h at 37 °C. After incubation, the beads were washed thrice in filtered 1% BSA/PBS solution and stored at 4 °C until use.

Initial experiments determined the optimal amount of protein to be used during modification by varying the amount of protein relative to the amount of beads being modified, thus giving a measure of the density of protein bound to the surface (protein/surface area). Protocols for modifying commercially available M-450 Epoxy Dynabeads (Invitrogen, Cat. No. 14011) were used as a reference point to determine how much protein to use during modification. The dynabead protocol instructs to use 5 μg of protein per 10^7 beads. To determine how this translates to the glass beads first we determine the protein surface density by dividing the amount of protein used during modification by the total surface area as follows:

$$S.A._{sphere} = 4\pi r \quad (1)$$

Substituting 2.5 μm for the radius (dynabead diameter = 5 μm) we obtain:

$$S.A._{Dynabead} = 4\pi(2.5)^2 = 25\pi\ um^2 \quad (2)$$

To calculate the protein surface density we simply divide the amount of protein by the surface area:

$$S.D._{protein} = \frac{mass}{S.A.} = \frac{5\ ug}{25\pi\ um^2 \times 10^7 beads} = \frac{1\ ug}{1.57x10^8\ um^2} \quad (3)$$

Next we translate this onto the larger glass beads to obtain amount of beads required to achieve the equivalent protein surface density. According to the manufacturer the glass beads have a diameter of 150-212 μm. Using an average diameter of 181 μm and equation 1 we get an approximate average diameter of 90 μm and a surface area of 32400π μm^2. Dividing the area of 10^7 Dynabeads calculated above by this value, we obtain the number of glass beads that will give us the equivalent area:

$$\frac{1.57x10^8 um^2}{32400\pi\ um^2} = 1542\ glass\ beads \quad (4)$$

Subsequently, we count the beads to determine the number of beads per milligram. This was determined to be 1000 beads per 6 mg, therefore 9.25 mg gives us 1542 beads. As such

$$\frac{1\ ug\ protein}{1.57x10^8 um^2} = \frac{1ug\ protein}{1542\ beads} = \frac{1\ ug\ protein}{9.25\ mg\ beads} = \frac{0.108\ ug\ protein}{1\ mg\ beads} \quad (5)$$

Thus we determine that to perform the modification at the same density as the dynabead protocol, we must use 0.108 μg of protein per milligram of glass beads.

Optimization of the protocol for bioactive modification of azide beads was carried out using antiCD3-(5)PEG-MDT conjugate by testing the cellular response to beads modified with protein at a surface density equal to (1x), ten times greater than (10x), or one tenth (0.1x) of that used in the Dynabead modification protocol. As controls, beads were modified with equal amounts of BSA. Beads used in subsequent experiments testing T cell inhibition by tethered PD-L1-(4)PEG-MDT conjugates were modified using the same density (1x) as that used for Dynabead modification protocols, as this proved to be

the optimal protein surface density. To ensure any response observed was specific to tethered PD-L1, beads were modified with BSA in its stead as controls.

7.2.4 T CELL AND APC ENRICHMENT

Mice were euthanized via IACUC approved methods. An incision was made on their left dorsal flank and the spleen was removed and placed in ice-cold HBSS solution. The spleen was then minced into small pieces which were placed in a 40 μm cell strainer (Corning, Cat.No. 352340) sitting in a well of a 6-well plate. A 5 mL syringe plunger was used to gently mash the pieces of spleen against the strainer mesh using a circular motion to extract the cells from the tissue. The strainer was then placed in a 50 mL falcon tube and the cell suspension filtered through once again. The cells were then spun down (1500RPM x 5 min), resuspended in ACK lysing buffer (Gibco, Cat.No.A10492-01), and incubated at 37°C for 2 min to lyse the red blood cells. The cells are then washed in HBSS and counted using Trypan Blue and a hemocytometer; A spleen regularly generates 10^8 cells.

Enrichment for CD4+ T cells was done using the EasySep Negative Selection Enrichment Kit (StemCell Technologies, Cat. No. 19752). After enrichment, a sample of cells was collected for purity assessment, which was normally >90%. The remaining CD4+ cells were washed in PBS and labeled using the CellTrace Violet Cell Proliferation Kit (Invitrogen, Cat. No. 34557) by dissolving CellTrace Violet dye stock in PBS (2 μl/10mL) and resuspending cells at a concentration of 10^6 cells/mL Cells were incubated for 10 min at 37°C, then washed thrice in complete culture medium, resuspended in complete culture medium and kept on ice until plating. APC enrichment was carried out as previously described.[163, 164] Briefly, splenic cells incubated with HO2.2 (anti-CD8) and RL-172 (anti-CD4) supernatant, and rabbit complement for 45 min at 37°C followed by an identical

incubation with Mitomycin C. Purity was assessed at >80%. Purity assessments were carried out by flow cytometry (Sect 7.2.6).

7.2.5 MODIFIED BEAD, T CELL, AND APC CO-CULTURE

Co-culture experiments were carried out by plating a total of 200,000 cells/well using a CD4+ to APC ratio of 1:1 (i.e. 100,000 each). First, beads were aliquoted into their corresponding wells as evenly as possible; amount of beads added varied according to the experimental design. Due to their size, these beads tend to settle, making accurate aliquoting a challenge. Therefore visual inspection of the bead distribution among replicate wells was necessary. After appropriate distribution of beads was confirmed, the 1% BSA/PBS solution was removed and cells were added to their respective wells. For cells activated with soluble anti-CD3, media supplemented with indicated amounts of antibody was added to each well; otherwise complete culture media was added. Cells were cultured in a total volume of 200 μL of complete RPMI media which consisted of (cRPMI: 10%FBS, 1xGlutaMax, 1xPen/Strep, 25 mM Hepes, 55 μM β-Mercaptoethanol). The cells were cultured with the beads for 72 h at 37°C in a 5% CO_2 atmosphere and processed for analysis by flow cytometry.

7.2.6 FLOW CYTOMETRY

Purity assessments were carried out by multicolor flow cytometry staining for CD4 (eFluor710), CD8 (PacBlue), B220 (APC), and LiveDead Yellow (Invitrogen) as a viability stain. For cell proliferation, activation, and viability assessments samples were collected from each well and passed through a cell strainer snap cap into FACS tubes for processing. The panel used for analysis is as follows: LiveDead Yellow, CellTrace Violet (proliferation, Invitrogen), CD4-eFluor710, CD62L-APC/Cy7, CD25-PE/Cy7, B220-

APC, and CD80-FITC. Samples were stained and fixed following standard procedures and stored at 4°C until analyzed on an LSRII Flow Cytometer (BD).

7.3 RESULTS AND DISCUSSION

The first phase of this study consisted of functionalizing the proteins to permit tethering to surfaces via Staudinger ligation. As the PEGylation of proteins has the potential to affect their activity,[165] optimization of the degree of PEGylation/functionalization was carried out for both anti-CD3 and PD-L1, with the goal of maximizing the degree of functionalization to increase the chances of the protein binding to the bead surface, while retaining protein activity. To find this optimal balance the PEGylation procedure of the proteins was performed using different molar ratios of NHS-PEG-MDT to protein and the activity of the resulting PEGylated proteins was tested *in vitro* by incubation with responder cells. Subsequently, the protocol for modifying glass beads was optimized to determine the optimal protein surface density to achieve the desired cell response. Finally, the inhibitory activity of tethered PD-L1 was tested on naïve cells and cells stimulated by soluble anti-CD3. A summary of these experiments is depicted in **Figure 32.**

7.3.1 OPTIMIZATION OF PROTEIN FUNCTIONALIZATION

7.3.1.1 ANTI-CD3 FUNCTIONALIZATION AND RESULTING ACTIVITY

Automated gel electrophoresis and OPA fluoraldehyde assay confirmed functionalization of antiCD3, as indicated by the increase in molecular weight seen in the virtual gel and a decrease in available free amines measured (**Figure 33**). As the ratio of PEG to protein increases, larger changes in the molecular weight of the resulting conjugate were observed. To evaluate the activity of the resulting functionalized anti-CD3 protein,

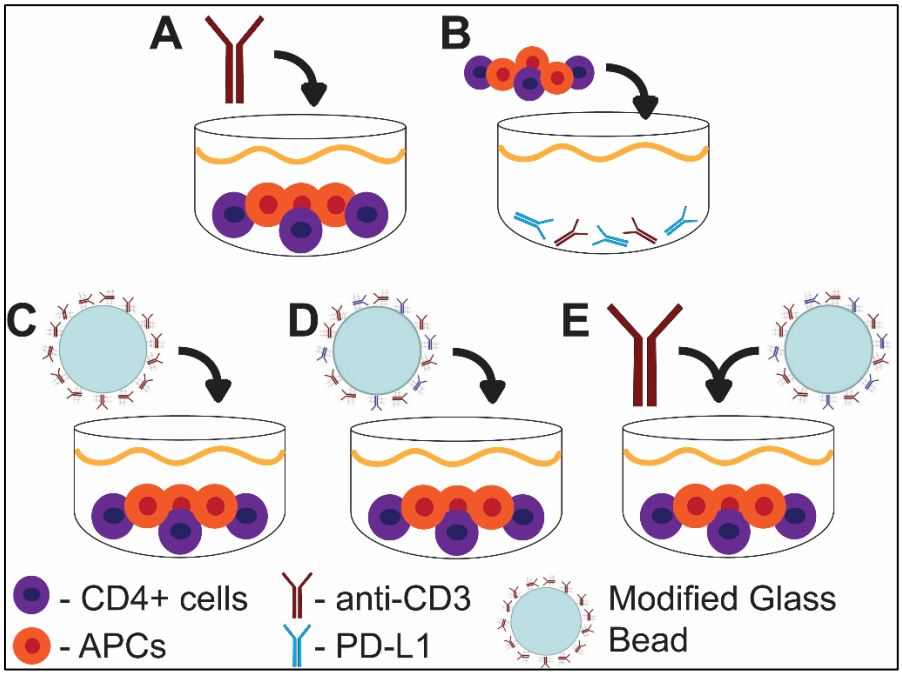

Figure 32. Summary of experimental setup for testing of protein-linker conjugate and modified bead activity. Schematics depicting culture conditions for different experiments performed. All experiments were performed using enriched CD4+ cells labeled with CellTrace Violet and T cell depleted splenocytes at a ratio of 1 to 1. A: Testing of functionalized anti-CD3 antibody was performed by addition of soluble antibody to cell cultures. B: Testing of functionalized PD-L1 was carried out by pre-coating plate wells with native anti-CD3 and different versions of PD-L1. C-D: Bead modification optimization and tethered PD-L1 mediated inhibition was done by co-culture of cells and glass beads. E: Signal co-delivery requirements were evaluated by stimulating cells with soluble anti-CD3 and inhibiting with modified glass beads.

the conjugates were added to responder T cell/APC cultures and subsequent proliferation and activation was tracked. Interestingly, the percentage of viable CD25+ and proliferating cells, as measured by CellTrace dye dilution, remained relatively constant across all groups, with a slight reduction in the percentage of proliferating cells observed for the group cultured with anti-CD3-(20)PEG. However, when examining the number of events, it is clear there is an inverse relationship between the degree of anti-CD3 functionalization and the number of proliferating and activated cells (**Figure 34**), with these numbers being

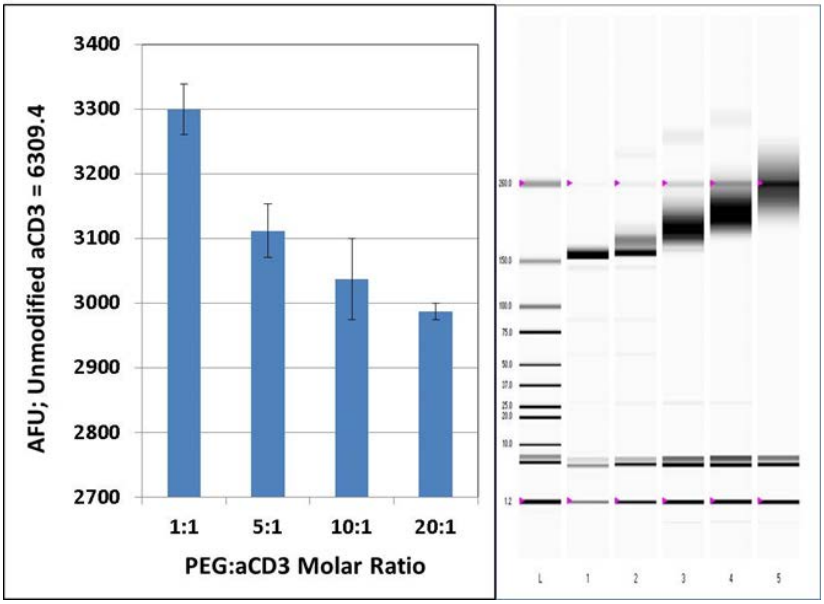

Figure 33. OPA-Fluoraldehyde assay and automated gel electrophoresis confirms anti-CD3 functionalization. Gel lanes: (L) Ladder, (1) anti-CD3, (2-5) functionalized anti-CD3 with 1, 5, 10, and 20 PEG linkers per anti-CD3, respectively.

reduced approximately by half ($P \leq 0.05$). In addition, the ratio between dead and viable CD4+ cells shows a direct relationship between the death CD4+ cells and the degree of PEGylation (**Figure 34**), with the index doubling in the cells incubated with anti-CD3 functionalized with 20 linkers per protein ($P \leq 0.05$). This is indicative of lack of stimulation, and thus loss of anti-CD3 activity, which results in T cell death *in vitro*. Taken together these data show the threshold for anti-CD3 functionalization to elude a reduction in activity is 5 PEG molecules per anti-CD3 molecule.

7.3.1.2 PD-L1 FUNCTIONALIZATION AND RESULTING ACTIVITY

Taking the data from the anti-CD3 experiments into consideration and the fact that PD-L1 has a much lower molecular weight, PD-L1 proteins were modified under the same reaction conditions using 2 and 4 PEG molecules per PD-L1 molecule for testing. PEGylation was confirmed by automated gel electrophoresis (not shown) and the activity

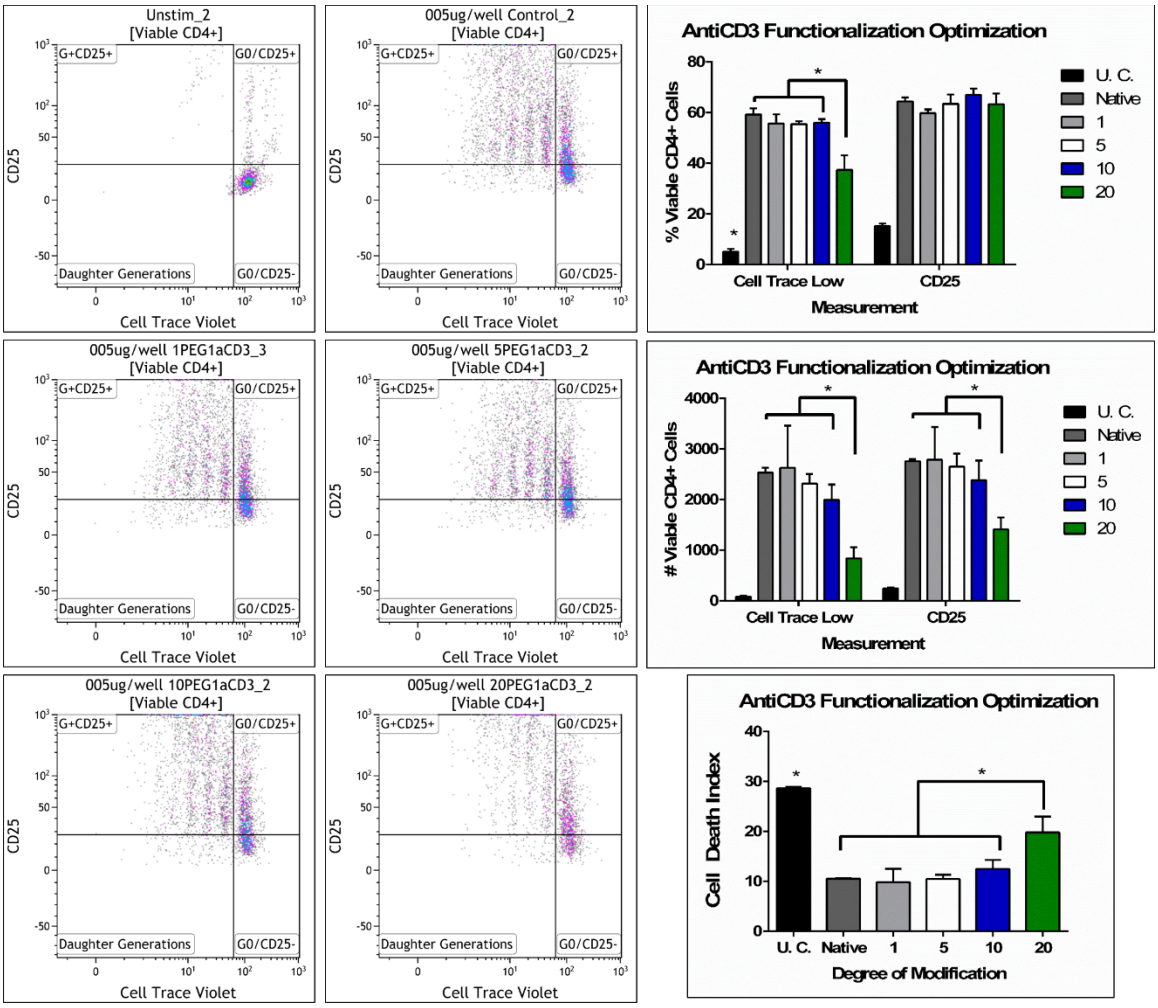

Figure 34. Higher degree of functionalization results in reduced anti-CD3 activity. Left and center columns: Representative dot plots showing differences in proliferation and CD25 expression of CD4+ cells cultured with anti-CD3 functionalized to varying degrees (X axis: Cell Trace; Y axis: CD25). Top row: unstimulated control (left) and cells stimulated with native anti-CD3 (center). Middle and bottom rows: experimental groups. Cells were stimulated with anti-CD3 modified with 1, 5 (middle left and right, respectively), 10, and 20 (bottom left and right, respectively) PEG linkers per protein molecule. Right column: Bar graphs (average ± S.D) showing statistical analysis of the percentage (top) and number (middle) of proliferating and CD25+ CD4 cells after incubation with anti-CD3. The bottom bar graph shows the cell death index for each treatment group. The entire sample was analyzed for all groups. * $P \leq 0.05$, One way ANOVA, Tukey multiple comparison post-test.

of the protein was tested by cell culture experiments. In this case the culture wells were pre-coated overnight with anti-CD3 (10ug/mL) and PD-L1 (30ug/mL), where necessary, prior to cell culture. Similar to the data from anti-CD3 experiments, the results show the percentage of CD25+ and proliferating viable cells remains relatively stable, with a slight statistically significant reduction in PD-L1 treated samples ($P \leq 0.05$). However, when comparing number of viable proliferating or CD25+ cells, the effect of PD-L1 was more pronounced, with approximately half the number of cells gated as proliferating or CD25+ when compared to anti-CD3 alone controls (**Figure 35;** $P \leq 0.05$). In addition, there was no difference observed between the inhibition exerted by native PD-L1 or either of the functionalized versions of the protein. There was slightly reduced inhibition observed with PD-L1 functionalized with 2 linkers per protein; however, since this effect was not seen in the sample with 4 linkers per protein it is safe to assume this is due to experimental variability. As mentioned before, these data are from preliminary experiments that should be validated by additional studies. Moreover, although not statistically significant, addition of any of the versions of PD-L1 results in a two fold increase in the ratio of dead to live cells when compared to stimulation with anti-CD3 alone **(Figure 35).** As a result, to enhance the chances of protein tethering, the optimal degree of functionalization was determined to be 4 PEG molecules per PD-L1 molecule.

7.3.2 OPTIMIZATION OF BEAD MODIFICATION PROTOCOL

Following the evaluation of protein activity after PEGylation, the next phase of the study sought to tether these proteins, now presenting PEG-MDT, to a material surface. To examine this, glass beads were modified to exhibit azide and incubated with the functionalized protein. The MDT linked protein should covalently bind to the azide bead

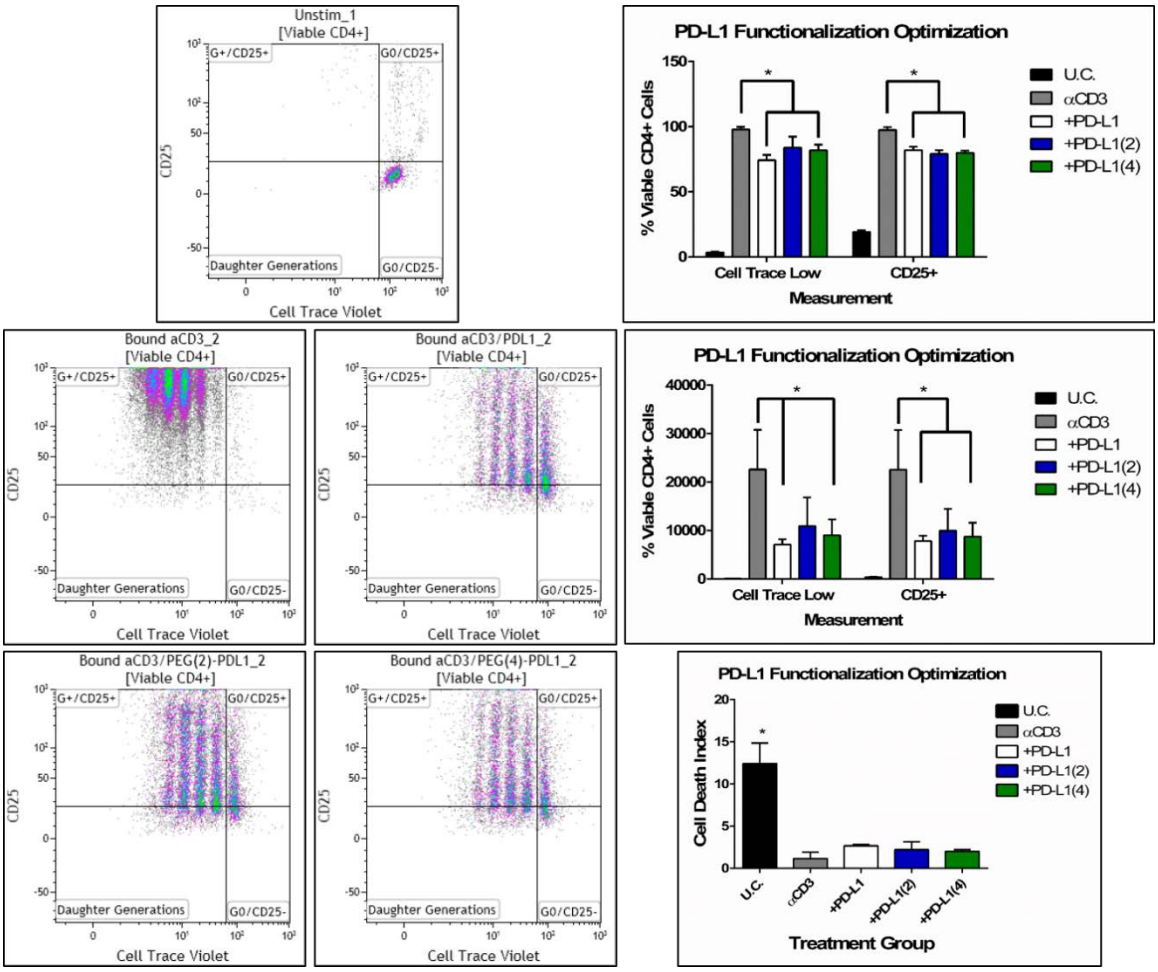

Figure 35. Functionalization of PD-L1 with 2 or 4 PEG molecules does not affect protein activity. Left and center columns: Representative dot plots showing differences in proliferation and CD25 expression of CD4+ cells cultured in wells pre-coated with anti-CD3 and native or functionalized PD-L1 (X axis: Cell Trace; Y axis: CD25). Top left: Unstimulated cell control used to define gates. Middle row: Cells cultured in wells pre-coated with anti-CD3 alone (left) or in combination with native PD-L1 (right). Bottom row: Cells cultured in wells pre-coated with anti-CD3 and PD-L1 functionalized with 2 (left) and 4 (right) PEG linkers. Right column: Bar graphs (average ± S.D) showing statistical analysis of the percentage (top) and number (middle) of proliferating and CD25+ CD4 cells after incubation with anti-CD3. The bottom bar graph shows the cell death index for each treatment group. The entire sample was analyzed for all groups up to 10^5 events. * $P \leq 0.05$, One way ANOVA, Tukey multiple comparison post-test.

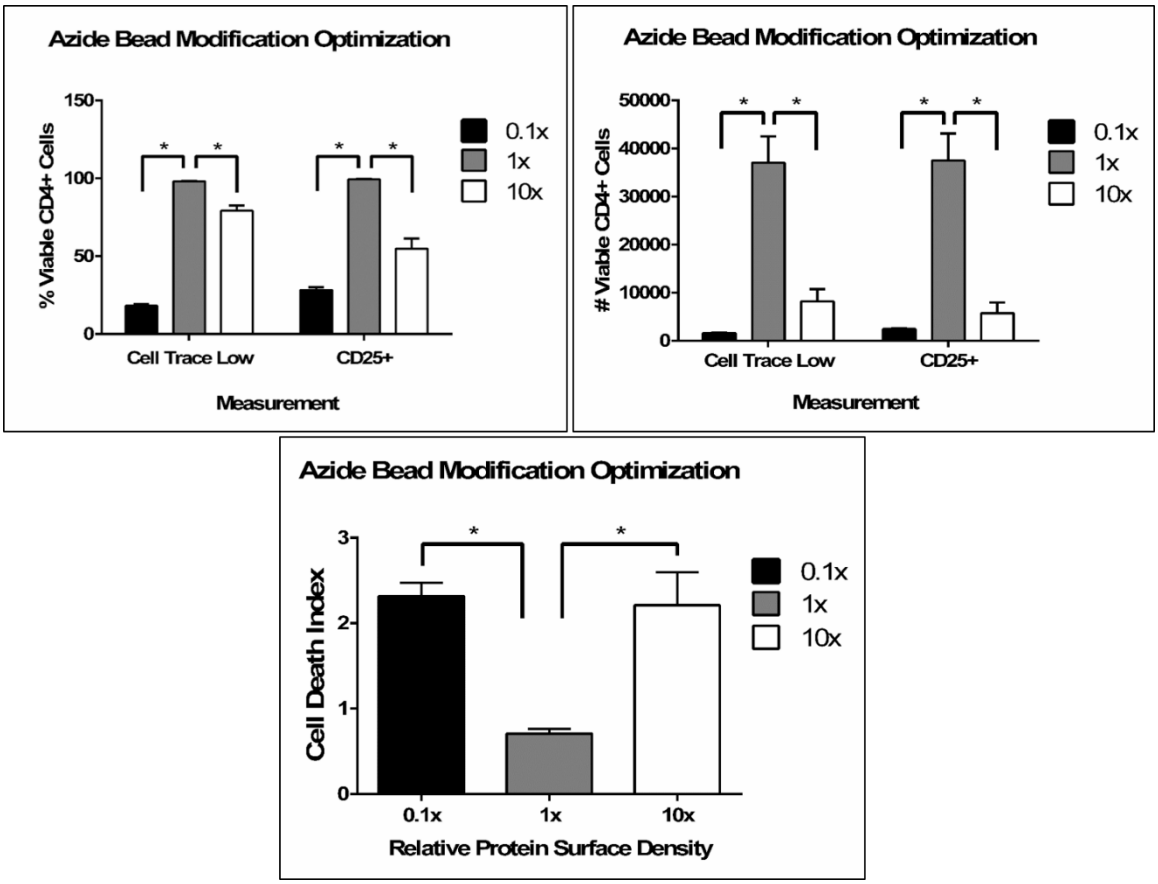

Figure 36. Modification of azide beads with 0.108 ug / mg beads resulted in the optimal cell response. Varying the density of anti-CD3 tethered onto the bead surface revealed maximal levels of activation, as measured by the number of proliferating and CD25 expressing cells (top right) and minimal cell death (bottom) achieved by replicating the protein surface density resulting from Dynabead modification procedures. * $P \leq 0.05$, One way ANOVA, Tukey multiple comparison post-test.

via Staudinger ligation. However, the amount of protein to be tethered to the beads was a variable that required optimization. To confirm the capacity to conjugate these functionalized proteins to surfaces and evaluate their subsequent activity, beads were modified with varying amounts of anti-CD3 conjugate and incubated with responder T cell/APC cultures. Analysis of CD4+ cell proliferation and activation after co-culture with beads presenting anti-CD3 confirmed an optimal response when cells were exposed to surfaces modified with proteins at a density equivalent to that achieved using modification

protocols for commercially available Dynabeads. As shown in **Figure 36**, beads modified at this density exhibited the highest level of activation and proliferation, while concomitantly resulting in the lowest amount of cell death. The percentage of proliferating cells dropped from approximately 98 ± 0.27% to 80 ± 3.35% (Avg. ± S.D.; $P \leq 0.05$), whereas the percentage of CD25 expressing cells dropped from 99 ± 0.31% to 55 ± 6.56% (Avg. ± S.D.; $P \leq 0.05$) when comparing beads modified with a protein surface density equivalent to the Dynabead protocol with beads modified with 10 times that amount. Moreover, the number of proliferating or CD25 expressing cells was 4-fold higher in this group compared to cells co-cultured with beads modified with 10 times the amount of protein ($P \leq 0.05$). Controls of unmodified azide beads and beads modified with BSA had negligible amounts of Cell Trace low or CD25+ cells (not shown). Consequently, beads modification for subsequent experiments was performed using the same protein surface density as that used for modification of Dynabeads (0.108 μg protein / mg beads).

7.3.3 INHIBITION OF T CELL ACTIVATION BY TETHERED PD-L1

7.3.3.1 TETHERED PD-L1 INHIBITS ACTIVATION OF CD4+ T CELLS

Once the optimal method for bioactive bead modification was established, efforts were directed at determining whether or not tethering of PD-L1 to these beads could inhibit T cell activation. Incubation of cells and beads modified with anti-CD3 and PD-L1 at a ratio of 1 to 4, respectively, showed a significant reduction in proliferation and CD25 expression when compared to control beads modified with equivalent amounts of anti-CD3 and BSA (**Figure 37**). As the amount of beads, and thus the level of stimulation, increased from 2 to 4, 6 and 8 mg per well, the percentage of proliferating cells dropped from 69.22 ± 0.81%, 79.50 ± 1.87%, 91.62 ± 0.18 %, and 92.22 ± 0.57% for cells co-cultured with

anti-CD3/BSA beads to 53.59 ± 2.43%, 50.28 ± 6.85%, 44.63 ± 4.90%, and 67.17 ± 3.86%respectively, for cells co-cultured with anti-CD3/PD-L1 beads (Avg. ± S.D.; $P \leq 0.05$). Similarly, the percentage of CD25 expressing cells dropped from 79.76 ± 0.79%, 94.06 ± 1.34%, 98.37 ± 0.20%, and 98.43 ± 0.08% for cells co-cultured with anti-CD3/BSA beads to 65.87 ± 0.22%, 62.56 ± 2.83%, 59.38 ± 3.12%, and 77.46 ± 2.53%, respectively, for cells co-cultured with anti-CD3/PD-L1 beads (Avg. ± S.D.; $P \leq 0.05$). Furthermore, PD-L1 signaling also resulted in significantly elevated levels of cell death, with the ratio of dead to live cells increasing from 4.77 ± 0.57, 4.92 ± 0.45, 2.56 ± 0.57 for cells co-cultured with anti-CD3/BSA beads to 8 ± 1.8, 7.68 ± 1.93, and 6.83 ± 1.07 for cells co-cultured with anti-CD3/PD-L1 beads (2mg, 4mg, and 6mg;Avg. ± S.D.; $P \leq 0.05$).For this measure there was no statistically significant difference in the groups co-cultured with 8mg beads per well. It is clear that the degree of inhibition increased with each additional amount of beads added to the well; however, this increase seemed to reach a limit and started to fall upon addition of 8 mg of beads per well. This is in accordance with what has been reported in the literature, which states that inhibition of PD-L1 can be overcome by strong primary signaling or high levels of IL-2, which activated cells produce.[35-38, 117-123]

7.3.3.2 CHALLENGES IN INHIBITING PRE-ACTIVATED T CELLS

To determine whether surfaces modified with PD-L1 alone are capable of inhibiting preactivated cells, experiments were performed where cells were stimulated with soluble anti-CD3 at a high (0.25 μg/mL) and low (0.1 μg/mL) concentration, as routinely performed in regulatory T cell suppressor assays to test regulatory T cell (Treg) function[166], and co-cultured with modified beads. Beads modified with PD-L1 alone

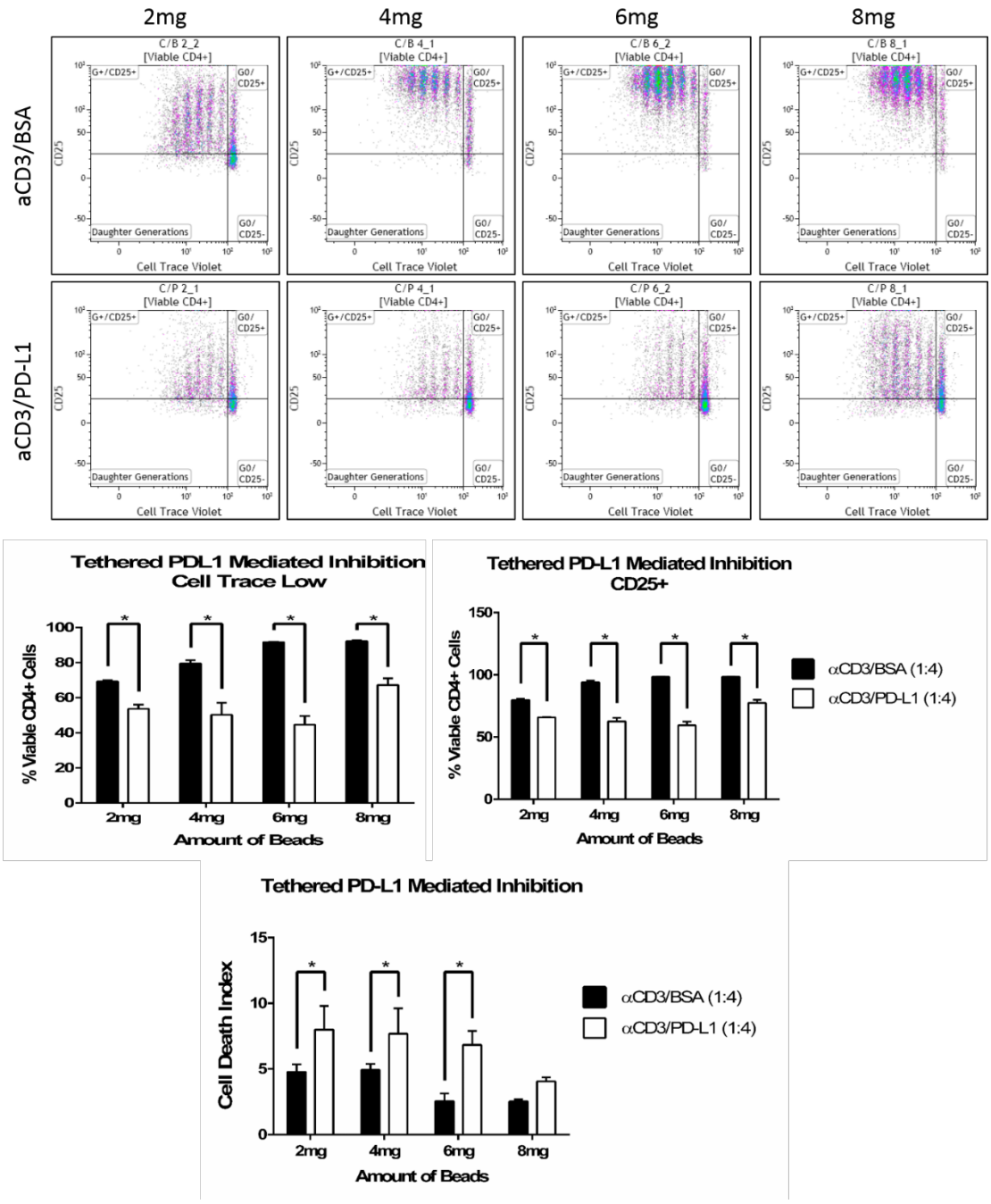

Figure 37. Tethered PD-L1 inhibits T cell activation and induces cell death. Top: Representative dot plots showing cell proliferation and CD25 expression of cells cultured for 72hrs with varying amounts of anti-CD3/BSA (top row) or anti-CD3/PDL1 beads (bottom row) per well (X axis: Cell Trace; Y axis: CD25). Bottom: Bar graphs showing statistical differences in these variables, as well as the cell death. Beads were modified with 0.108ug protein/mg beads at a ratio of 1:4 aCD3:BSA or PD-L1. * $P \leq 0.05$, Two way ANOVA, Sidak's multiple comparison post-test. 10^5 events collected per sample.

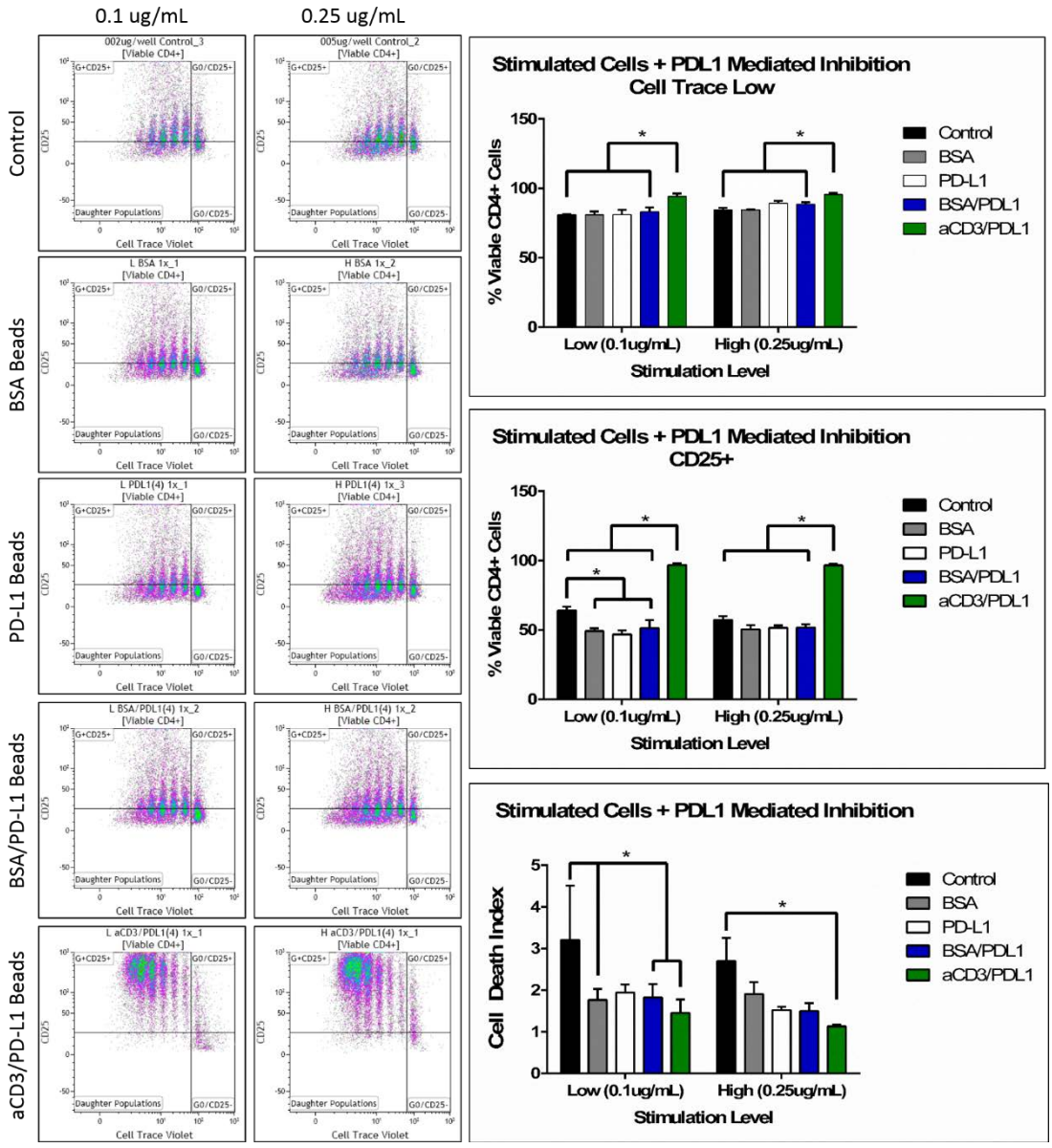

Figure 38. PD-L1 must be delivered with primary anti-CD3 signal which can result in enhanced activation of prestimulated cells. Left columns: Representative dot plots showing proliferation and CD25 expression of **c**ells cultured in the presence of low (left: 0.1 ug/mL) and high (right: 0.25 ug/mL) amounts of soluble anti-CD3 for stimulation and modified beads (modification indicated on left margin) to test bead mediated inhibition (X axis: Cell Trace; Y axis: CD25). Right column: Bar graphs showing statistical differences in these variables, as well as the cell death. Beads were modified with 0.108ug protein/mg beads as indicated. Combination beads were modified at a ratio of 1:4 BSA or aCD3 : PD-L1. * $P \leq 0.05$, Two way ANOVA, Sidak's multiple comparison post-test. 10^5 events collected per sample.

did not have an effect on cell proliferation or activation at either level of stimulation, consistent with published data that indicates the PD-L1 co-stimulatory signal must be co-delivered with anti-CD3 primary signal in order to exert its inhibitory functions (**Figure 38**). This means that, although the cells are being exposed to both signals, in order for the PD-L1 signal to exert its inhibitory activity it must be co-delivered with the primary signal on the same surface. What was particularly interesting was the fact that co-delivery of both signals at a ratio of 1 to 4 (aCD3:PD-L1) resulted in enhanced CD25 expression at both high and low levels of stimulation, indicative of augmented stimulation (**Figure 38**). This is an important observation, as it has critical implications in the choice of signals tethered to surfaces for inhibition of immune effector cells, as it could result in a heightened reaction and defeats the purpose of such strategies. Although titration of the anti-CD3 signal could mitigate this issue, it is an avoidable complication that results in an increased risk. Thus, careful consideration must be taken when choosing candidates for tethering.

7.4 CONCLUSIONS

The preliminary studies presented in this chapter have demonstrated that it is indeed possible to directly modulate immune cell function *in situ* by tethering of signaling molecules through the use of chemoselective PEG linkers. Several factors must be considered when modifying surfaces for such purposes. Functionalization of proteins destined for tethering must be carefully optimized in order to maximize the likelihood of crosslinking while preserving protein activity. In these studies, random functionalization was employed. Future efforts could attempt site specific functionalization of proteins to carefully predict changes in protein activity and yield highly defined conjugates. Furthermore, the manner in which these signals are presented is of critical importance.

Protein surface density must be carefully controlled in order to achieve the desired response. Additionally, delivery of co-stimulatory signals must be taken into account when selecting a candidate for tethering, as these requirements will result in an additional and sometimes avoidable complications for the development of these kind of systems. In the case of PD-L1, the requirement of co-delivery of primary anti-CD3 signal poses a risk, since it could result in an augmented reaction if not carefully optimized.

Chapter 8. Conclusions and Recommendations for Future Work

8.1 SUMMARY AND CONCLUDING REMARKS

Clinical islet transplantation has shown great promise as a potential cure for Type I Diabetes; however, several obstacles remain which must be addressed before it can become the standard of care. IBMIR and the acute inflammatory reaction play a major role in the early loss of the transplant mass and greatly contributes to the recurring immune response experienced by patients, which ultimately leads to graft rejection. As such, strategies capable of curtailing, if not completely eliminating, these early reactions would represent a major development in the advancement of CIT.

The central hypothesis of this dissertation was that modification of the islet surface with (poly)ethylene-glycol polymer would serve to mask factors directly responsible for the initiation of the coagulation cascade (tissue factor), and thus IBMIR, and camouflage the graft from recognition by cells of the immune system through the generation of a steric barrier. In addition, it sought to explore the use of these same polymers for tethering signaling molecules to directly modulate immune cell function *in situ*. We tested this hypothesis through the pursuit of several aims.

We first sought to optimize the islet modification procedure to ensure maximal islet cell viability and function while maximizing polymer grafting to the islet surface. The reaction conditions for the grafting procedure required optimization, pH in particular, since drastic changes in these variables will surely adversely affect the islets which are highly sensitive to their environment. Moreover, the source of the polymer became a major factor to take into consideration since the manufacturing process of these materials employ toxic organic solvents that, if not properly removed, will surely result in cell death, as

demonstrated in Chapter 3. Once these matters were addressed, testing was carried out to ensure grafting of polymer to the islet surface was taking place using fluorescently labeled polymer. The results confirmed polymer was grafted onto the islet surface, albeit in a non-uniform fashion with noticeable variability between islets of the same preparation and between different isolations. We suspect this is due to the variability in the ECM peri-islet capsule, which the polymer binds to, remaining after the isolation procedure. In addition, the viability and function of the modified islets was examined to confirm the procedure did not adversely affect the islets. The data clearly demonstrates that although there is a slight reduction in the amount of insulin secreted, the islets remain responsive to glucose stimulation and secrete insulin in amounts comparable to control islets. Finally, once all these questions were answered, the immunoprotective effect of islet PEGylation was evaluated *in vivo* by transplantation in a fully-MHC mismatch rodent model. These experiments revealed that in the long term (>100 days) islet PEGylation enhances the rate of graft survival in these models from 10%, observed in animals receiving control islets, to 60% ($P = 0.01$). Subsequently, we sought to determine if supplementing PEGylation with a mild short-course immunotherapy would enhance the improvement in graft survival observed by PEGylation alone. Transplants were performed in the same rodent model with the addition of LFA-1 blockade. Remarkably, these experiments demonstrated that PEGylation alone results in an enhancement of graft survival rates comparable to that of short-course LFA-1 blockade (50%; $P = 0.80$). Moreover, when the two strategies were combined, a synergistic effect was observed which resulted in a graft survival rate of 78% after 100 d ($P = 0.003$).

After witnessing these encouraging results, we sought to elucidate the mechanism by which PEGylation, alone or in combination with LFA-1 blockade, resulted in improved graft outcomes. Analysis of the graft site after long term engraftment by histological evaluation revealed low amounts of immune infiltrates restricted to the periphery of the islet graft. Immunofluorescent staining revealed strong insulin expression in these islets indicative of their robustness and health. Additional immunohistochemical evaluation of T cells showed minimal presence of T cells for most grafts with sporadic cells related to the periphery of the islet graft. For some PEG and αLFA-1/PEG combination grafts, however, areas of $CD3^{+}FoxP3^{+}$ cells were observed. Pockets of mononuclear cell infiltration were also noted adjacent to intact islets, most likely as a result of the incomplete coating mentioned above.

Real time RT-PCR experiments performed for evaluation of the graft site during the early engraftment period (<15 d) showed signs of a delayed immunological response, as is expected with the administration of LFA-1 blockade, as well as a reduction in gene expression of inflammatory cytokines with concomitant elevated expression of anti-inflammatory cytokines, indicative of a dampened inflammatory response. Immunofluorescent staining of samples acquired during this time frame showed reduced amounts of CD68+ macrophages at the site for animals receiving PEGylated islets or LFA-1 blockade, with these cells being relegated to the periphery of the islets, in contrast to macrophages observed infiltrating islets in the control samples. It is important to note that this contradicts the RT-PCR data of the samples from mice receiving PEGylated islets. More importantly, this staining showed an increased amount of infiltrating macrophages for mice receiving the combination of PEGylated islets and LFA-1 blockade. Of particular

interest is the fact that a large number of these cells exhibited an alternatively activated (M2) CD206+ phenotype. To reiterate, this is an important finding since macrophages are critical regulators of inflammation and the wound healing response. These results suggest that the mechanism by which grafting of PEG on the islet surface enhances graft survival during early time points is mediated by macrophages, particularly the higher incidence of alternatively activated macrophages (M2) in the αLFA-1/PEG group, which ultimately demonstrated the highest rate of graft survival.

Challenges encountered while performing these experiments include the variability introduced due to the variability in the grafting of the polymer to the islet surface. In addition, the vast number of animals, and thus amount of time, required to gain statistical power proved to be problematic. In our experiments, the sample size was limited to four mice per group per time point, which is relatively low. However, this amounted to a total of 48 kidneys to be processed. Furthermore, due to the time frame in which these samples were collected, grafts were not screened for "success", meaning we were unaware of which grafts would survive and which one would be rejected. Pooling these samples together for each treatment groups hinders the ability to accurately characterize the response to different successful treatments and increases variation in the measurements made.

Following testing in these small animal models, the project advanced along the development pipeline and the procedure was tested on non-human primate islets. At this point additional *in vitro* experiments consisting of plasma recalcification assays were performed to test the effects of PEGylation on the thrombotic activity of the islets. As with murine islets, modification with fluorescently labeled polymers confirmed PEG grafting onto the islet surface, albeit in a non-uniform manner. Viability staining and perifusion

assays demonstrated that the procedure had no adverse effects on islet cell viability or secretory function, with cells responding to glucose challenge no differently than control islets. Moreover, plasma recalcification assays clearly showed a significant reduction in the thrombotic activity of PEGylated islets when compared to control islets.

Once *in vitro* testing was completed, the protective effects of the modification were tested in an NHP model of transplantation employing donors and recipients fully or partially mismatched for MHC class II alleles. These studies allowed testing of the procedure on animals with a complex immune system that more closely resembles that of humans as well as testing the feasibility of scaling up the procedure. Remarkably, mirroring the results obtained from the mouse experiments, when compared to animals that received untreated control islets, the animal that received PEGylated islets demonstrated a significant enhancement of glycemic stabilization, reduced insulin requirement, and an extended duration of function. Additionally, while only observed in a sample size of one, the islet dose requirement to achieve insulin independence was reduced by 50%. A biopsy performed 207 days after transplant and more than 60 days prior to termination revealed robust islets with minimal, if any, amount of immune infiltrate. Upon euthanization of the animal, histological evaluation of the liver confirmed an increase in the infiltrate present since the biopsy was taken. These results appear to support the hypothesis that the PEGylation procedure assists in dampening initial inflammatory responses and immunological recognition; however, this impact is transient, as recognition and immunological attack of the graft initiates over time.

Data collected from on-going paired transplantation experiments provide further support of the promise of PEGylation as a complementary tool for improving islet

engraftment. Coagulation assays performed on blood samples collected from control animals immediately prior to and following transplantation demonstrated increased PTT, showing a deficiency of coagulation factors in the sample, along with increased levels of TAT and D-dimer, which suggest negative regulation of a clotting reaction is taking place and indicative of increased coagulation activity in the animal. These observations were either not reflected in samples collected from animals receiving PEGylated islets, or seen to a lesser degree. However, these are only preliminary measurements of a sample size of 1, having negligible statistical power. Further studies must be carried out to confirm and validate these observations. While highly preliminary, these data indicate PEGylation of the islet surface results in reduced coagulation activity in the recipient, mitigation of IBMIR, and thus the acute inflammatory response. While the long term results from this experiment regarding insulin independence and c-peptide levels remain to be seen, initial data collected shows that although the control animal achieved insulin independence for a period of approximately 7 days, fasting and post-prandial blood glucose rapidly destabilized following this period around POD 25 indicating islet graft rejection. In contrast, albeit not having experienced insulin independence, the animal that received PEGylated islets presently maintains stable fasting and post-prandial blood glucose levels. Furthermore, the insulin requirement for this animal has been reduced by approximately 50% to that prior to the transplant, indicating the graft is functional. Taking into account the fact that similar results were obtained in previous studies by systemic blockade of Tissue Factor, these data are highly encouraging since PEGylation appears to have an equivalent effect and protect the islet graft from inflammatory pathways without systemic interference.

Scale-up of the procedure was also discussed, with time constraints due to NHS ester reactive group volatility and manipulation of large volumes of cell suspensions being critical factors that need to be addressed. While scale-up of the process to the NHP level in an experimental setting was not a significant challenge, modification of the procedure to permit scale-up to the industrial scale or clinical use will likely be more complex. Manipulation of a large number of cells, and thus large volumes of polymer solutions, will be necessary if this is to be translated for treatment of humans as was the case in these experiments. Further, because the procedure is carried out in serum/protein free conditions, coating and washing of consumables where islet suspensions will be handled is critical to prevent islet loss. However, these surfaces will be susceptible to react with the polymer. Consequently, carefully planning to conceive a method in which timing is optimized and manipulation is minimized will be critical both to maximize polymer grafting onto the islet surface and minimize islet death.

Finally, the possibility of using PEG as a platform for bioactive modification of islet surfaces through Staudinger ligation to supplement PEGylation with modulation of the adaptive immune response was also explored. These studies focused on optimizing the tethering of PD-L1, a main regulator of T cell function, idealized surfaces and evaluating its effects when exposed to cell cultures *in vitro*. Preliminary experiments showed that the degree of protein functionalization with polymer linkers is a critical factor that must be considered since these modification can drastically reduce protein activity if not properly optimized. In addition, optimization of the protein tethering procedure onto the surface must be carried out, since the manner in which these signals are presented to T cells are critical for successful modulation of immune cell function, with protein surface density

being the main factor presented herein. Inhibition of immune cell activation was achieved when co-culturing beads with naïve cells; however, this was more challenging when cells were stimulated by exogenous anti-CD3 protein. Incubation of modified beads with these cells resulted in augmented activation, which forces us to consider a more pragmatic selection of signaling pathways to target since the requirement for co-delivery of the primary CD3 signal for PD-L1 signal transduction on the same surface posed an unnecessary and avoidable complication in our system that could pose serious risks for the patient.

8.2 RECOMMENDATIONS FOR FUTURE WORK

A clear first step in improving this procedure which has been evident from the beginning of this project is the development of a method to generate a uniform peri-islet ECM capsule. This would enhance the efficacy of the procedure in two ways. First, it would provide a uniform foundation for the grafting of polymer to completely cover the islet surface, masking all antigens that would otherwise be exposed to the surrounding environment and result in either blood coagulation and IBMIR or direct antigen recognition by the adaptive immune system. In addition, re-establishing the ECM-islet interactions will enhance islet viability and function, as previously described.[107-109] This will have the downstream effect of reducing shed antigen, thus reducing the chances of activation of the adaptive immune system via the indirect pathway. Possible means of accomplishing this include incubating islets in concentrated protein solutions composed of the same proteins that make up the native islet capsule ECM to promote protein adsorption and binding. Additionally, islets could be cultured in the presence of growth factors that

stimulate ECM regeneration prior to PEGylation or co-culture these islets with fibroblasts or MSCs that could promote ECM regeneration.

Another area that could be explored is the connection between the changes in the macrophage population infiltrating the graft site during the first few weeks following transplantation described in Chapter 5 and the ensuing adaptive immune response. The fact that M2 macrophages where observed shortly after transplant only in the group receiving the combination therapy of PEGylated islets and LFA-1 blockade and that this same group exhibited some sporadic FoxP3+ T regs after long term engraftment seem to indicate a downstream effect. It is known that the innate immune system serves as a bridge to the adaptive immune system by presenting antigens. It could be that by modulating early inflammatory events and macrophage behavior, we could indirectly affect the ensuing adaptive immune response they promote. Further staining could shed some light in this regard.

Further, PEGylation serves as the foundation for layer-by-layer assembly of polymeric coatings. By alternating polymers with complementary reactive groups one can build ultrathin layers and generate more stable and robust coatings. In addition, as seen with the tethering of bioactive motifs, one can functionalize these coatings at different layers with different agents to modulate inflammation, the adaptive immune response, or to sequester effector molecules as previously described. Testing of more pragmatic signaling molecules such as those that do not require co-delivery of another signal should also be explored. Moreover, molecules involved in the regulation of inflammation and the innate immune system should also be considered, such as CD47.[167-169] As we have seen, the data indicates PEGylation enhances islet graft survival by mitigating acute

inflammatory events and it is possible, and seems highly likely, that these effects carry on to downstream reactions such as the adaptive immune response.

Finally, work should continue on testing PEGylation in the non-human primates. Preliminary results are very promising and further studies are needed to gain enough statistical power to arrive at more definitive conclusions. As progress is made in the areas mentioned above, they should be incorporated and tested in these models. Moreover this is an important step as the procedure advances towards clinical trials.

References

[1] Mathis D, Vence L, Benoist C. beta-Cell death during progression to diabetes. Nature. 2001;414:792-8.

[2] JDRF. Type 1 Diabetes Facts. http://jdrf.org/about-jdrf/fact-sheets/type-1-diabetes-facts/. Accessed 07/28/2014

[3] Silva AI, de Matos AN, Brons IG, Mateus M. An overview on the development of a bio-artificial pancreas as a treatment of insulin-dependent diabetes mellitus. Medicinal research reviews. 2006;26:181-222.

[4] Shapiro AM, Lakey JR. Future trends in islet cell transplantation. Diabetes technology & therapeutics. 2000;2:449-52.

[5] Shapiro AM, Ricordi C, Hering BJ, Auchincloss H, Lindblad R, Robertson RP, et al. International trial of the Edmonton protocol for islet transplantation. The New England journal of medicine. 2006;355:1318-30.

[6] Pileggi A, Ricordi C, Kenyon NS, Froud T, Baidal DA, Kahn A, et al. Twenty years of clinical islet transplantation at the Diabetes Research Institute--University of Miami. Clinical transplants. 2004:177-204.

[7] Faradji RN, Tharavanij T, Messinger S, Froud T, Pileggi A, Monroy K, et al. Long-term insulin independence and improvement in insulin secretion after supplemental islet infusion under exenatide and etanercept. Transplantation. 2008;86:1658-65.

[8] Froud T, Faradji RN, Pileggi A, Messinger S, Baidal DA, Ponte GM, et al. The use of exenatide in islet transplant recipients with chronic allograft dysfunction: safety, efficacy, and metabolic effects. Transplantation. 2008;86:36-45.

[9] Faradji RN, Froud T, Messinger S, Monroy K, Pileggi A, Mineo D, et al. Long-term metabolic and hormonal effects of exenatide on islet transplant recipients with allograft dysfunction. Cell transplantation. 2009;18:1247-59.

[10] Tharavanij T, Betancourt A, Messinger S, Cure P, Leitao CB, Baidal DA, et al. Improved long-term health-related quality of life after islet transplantation. Transplantation. 2008;86:1161-7.

[11] Cure P, Pileggi A, Froud T, Messinger S, Faradji RN, Baidal DA, et al. Improved metabolic control and quality of life in seven patients with type 1 diabetes following islet after kidney transplantation. Transplantation. 2008;85:801-12.

[12] Biarnes M, Montolio M, Nacher V, Raurell M, Soler J, Montanya E. Beta-cell death and mass in syngeneically transplanted islets exposed to short- and long-term hyperglycemia. Diabetes. 2002;51:66-72.

[13] Davalli AM, Scaglia L, Zangen DH, Hollister J, Bonner-Weir S, Weir GC. Vulnerability of islets in the immediate posttransplantation period. Dynamic changes in structure and function. Diabetes. 1996;45:1161-7.

[14] Mattsson G, Jansson L, Nordin A, Andersson A, Carlsson PO. Evidence of functional impairment of syngeneically transplanted mouse pancreatic islets retrieved from the liver. Diabetes. 2004;53:948-54.

[15] Yin D, Ding JW, Shen J, Ma L, Hara M, Chong AS. Liver ischemia contributes to early islet failure following intraportal transplantation: benefits of liver ischemic-preconditioning. American journal of transplantation : official journal of the American Society of Transplantation and the American Society of Transplant Surgeons. 2006;6:60-8.

[16] Ozmen L, Ekdahl KN, Elgue G, Larsson R, Korsgren O, Nilsson B. Inhibition of thrombin abrogates the instant blood-mediated inflammatory reaction triggered by isolated human islets: possible application of the thrombin inhibitor melagatran in clinical islet transplantation. Diabetes. 2002;51:1779-84.

[17] Moberg L, Johansson H, Lukinius A, Berne C, Foss A, Kallen R, et al. Production of tissue factor by pancreatic islet cells as a trigger of detrimental thrombotic reactions in clinical islet transplantation. Lancet (London, England). 2002;360:2039-45.

[18] Johansson H, Lukinius A, Moberg L, Lundgren T, Berne C, Foss A, et al. Tissue Factor Produced by the Endocrine Cells of the Islets of Langerhans Is Associated With a Negative Outcome of Clinical Islet Transplantation. Diabetes. 2005;54:1755-62.

[19] Witkowski P, Sondermeijer H, Hardy MA, Woodland DC, Lee K, Bhagat G, et al. Islet grafting and imaging in a bioengineered intramuscular space. Transplantation. 2009;88:1065-74.

[20] Cardani R, Pileggi A, Ricordi C, Gomez C, Baidal DA, Ponte GG, et al. Allosensitization of islet allograft recipients. Transplantation. 2007;84:1413-27.

[21] Huurman VA, Velthuis JH, Hilbrands R, Tree TI, Gillard P, van der Meer-Prins PM, et al. Allograft-specific cytokine profiles associate with clinical outcome after islet cell transplantation. American journal of transplantation : official journal of the American Society of Transplantation and the American Society of Transplant Surgeons. 2009;9:382-8.

[22] Huurman VA, Hilbrands R, Pinkse GG, Gillard P, Duinkerken G, van de Linde P, et al. Cellular islet autoimmunity associates with clinical outcome of islet cell transplantation. PloS one. 2008;3:e2435.

[23] Lunsford KE, Jayanshankar K, Eiring AM, Horne PH, Koester MA, Gao D, et al. Alloreactive (CD4-Independent) CD8+ T cells jeopardize long-term survival of intrahepatic islet allografts. American journal of transplantation : official journal of the American Society of Transplantation and the American Society of Transplant Surgeons. 2008;8:1113-28.

[24] Rickels MR, Kamoun M, Kearns J, Markmann JF, Naji A. Evidence for allograft rejection in an islet transplant recipient and effect on beta-cell secretory capacity. The Journal of clinical endocrinology and metabolism. 2007;92:2410-4.

[25] Coronel MM, Stabler CL. Engineering a local microenvironment for pancreatic islet replacement. Current opinion in biotechnology. 2013;24:900-8.

[26] Widmaier EP, Raff H, Strang KT, Vander AJ. Vander, Sherman, & Luciano's human physiology : the mechanisms of body function. 9th ed. Boston: McGraw-Hill Higher Education; 2004.

[27] Ratner BD. Biomaterials science : an introduction to materials in medicine. 2nd ed. Amsterdam ; Boston: Elsevier Academic Press; 2004.

[28] Nilsson B, Ekdahl KN, Korsgren O. Control of instant blood-mediated inflammatory reaction to improve islets of Langerhans engraftment. Current opinion in organ transplantation. 2011;16:620-6.

[29] Shizuru JA, Gregory AK, Chao CT, Fathman CG. Islet allograft survival after a single course of treatment of recipient with antibody to L3T4. Science. 1987;237:278-80.
[30] Hao L, Wang Y, Gill RG, Lafferty KJ. Role of the L3T4+ T cell in allograft rejection. Journal of immunology (Baltimore, Md : 1950). 1987;139:4022-6.

[31] Wolf LA, Coulombe M, Gill RG. Donor antigen-presenting cell-independent rejection of islet xenografts. Transplantation. 1995;60:1164-70.

[32] Coulombe M, Yang H, Wolf LA, Gill RG. Tolerance to antigen-presenting cell-depleted islet allografts is CD4 T cell dependent. Journal of immunology (Baltimore, Md : 1950). 1999;162:2503-10.

[33] Sleater M, Diamond AS, Gill RG. Islet allograft rejection by contact-dependent CD8+ T cells: perforin and FasL play alternate but obligatory roles. American journal of transplantation : official journal of the American Society of Transplantation and the American Society of Transplant Surgeons. 2007;7:1927-33.

[34] Waldmann H. Transplantation tolerance-where do we stand? Nature medicine. 1999;5:1245-8.

[35] Sharpe AH, Freeman GJ. The B7-CD28 superfamily. Nature reviews Immunology. 2002;2:116-26.

[36] Chen L. Co-inhibitory molecules of the B7-CD28 family in the control of T-cell immunity. Nature reviews Immunology. 2004;4:336-47.

[37] Sharpe AH. Mechanisms of costimulation. Immunological reviews. 2009;229:5-11.

[38] Nurieva RI, Liu X, Dong C. Yin-Yang of costimulation: crucial controls of immune tolerance and function. Immunological reviews. 2009;229:88-100.

[39] Thomson AW, Bonham CA, Zeevi A. Mode of action of tacrolimus (FK506): molecular and cellular mechanisms. Therapeutic drug monitoring. 1995;17:584-91.

[40] McAlister VC, Mahalati K, Peltekian KM, Fraser A, MacDonald AS. A clinical pharmacokinetic study of tacrolimus and sirolimus combination immunosuppression comparing simultaneous to separated administration. Therapeutic drug monitoring. 2002;24:346-50.

[41] Samaniego M, Becker BN, Djamali A. Drug insight: maintenance immunosuppression in kidney transplant recipients. Nature clinical practice Nephrology. 2006;2:688-99.

[42] Vincenti F, Kirkman R, Light S, Bumgardner G, Pescovitz M, Halloran P, et al. Interleukin-2-receptor blockade with daclizumab to prevent acute rejection in renal transplantation. Daclizumab Triple Therapy Study Group. The New England journal of medicine. 1998;338:161-5.

[43] Yun Lee D, Hee Nam J, Byun Y. Functional and histological evaluation of transplanted pancreatic islets immunoprotected by PEGylation and cyclosporine for 1 year. Biomaterials. 2007;28:1957-66.

[44] Mueller TF. Mechanisms of action of thymoglobulin. Transplantation. 2007;84:S5-S10.

[45] Deeks ED, Keating GM. Rabbit antithymocyte globulin (thymoglobulin): a review of its use in the prevention and treatment of acute renal allograft rejection. Drugs. 2009;69:1483-512.

[46] Korsgren O, Nilsson B. Improving islet transplantation: a road map for a widespread application for the cure of persons with type I diabetes. Current opinion in organ transplantation. 2009;14:683-7.

[47] Reach G, Jaffrin MY. Kinetic modelling as a tool for the design of a vascular bioartificial pancreas: feedback between modelling and experimental validation. Computer methods and programs in biomedicine. 1990;32:277-85.

[48] Silva AI, Mateus M. Development of a polysulfone hollow fiber vascular bio-artificial pancreas device for in vitro studies. Journal of biotechnology. 2009;139:236-49.

[49] Maki T, Ubhi CS, Sanchez-Farpon H, Sullivan SJ, Borland K, Muller TE, et al. Successful treatment of diabetes with the biohybrid artificial pancreas in dogs. Transplantation. 1991;51:43-51.

[50] Petruzzo P, Pibiri L, De Giudici MA, Basta G, Calafiore R, Falorni A, et al. Xenotransplantation of microencapsulated pancreatic islets contained in a vascular prosthesis: preliminary results. Transplant international : official journal of the European Society for Organ Transplantation. 1991;4:200-4.

[51] Maki T, Ubhi CS, Sanchez-Farpon H, Sullivan SJ, Borland K, Muller TE, et al. The biohybrid artificial pancreas for treatment of diabetes in totally pancreatectomized dogs. Transplantation proceedings. 1991;23:754-5.

[52] Altman JJ, Penfornis A, Boillot J, Maletti M. Bioartificial pancreas in autoimmune nonobese diabetic mice. ASAIO transactions / American Society for Artificial Internal Organs. 1988;34:247-9.

[53] Delaunay C, Darquy S, Honiger J, Capron F, Rouault C, Reach G. Glucose-insulin kinetics of a bioartificial pancreas made of an AN69 hydrogel hollow fiber containing porcine islets and implanted in diabetic mice. Artificial organs. 1998;22:291-9.

[54] Suzuki K, Bonner-Weir S, Trivedi N, Yoon KH, Hollister-Lock J, Colton CK, et al. Function and survival of macroencapsulated syngeneic islets transplanted into streptozocin-diabetic mice. Transplantation. 1998;66:21-8.

[55] Desai TA, Chu WH, Rasi G, Sinibaldi-Vallebona P, Guarino E, Ferrari M. Microfabricated biocapsules provide short-term immunoisolation of insulinoma xenografts. Biomedical microdevices. 1999;1:131-8.

[56] Olivares E, Piranda S, Malaisse WJ. Long-term correction of hyperglycaemia in streptozotocin-induced diabetic rats transplanted with islets placed in an implantation device. Hormone and metabolic research = Hormon- und Stoffwechselforschung = Hormones et metabolisme. 2001;33:687-8.

[57] Young TH, Chuang WY, Hsieh MY, Chen LW, Hsu JP. Assessment and modeling of poly(vinyl alcohol) bioartificial pancreas in vivo. Biomaterials. 2002;23:3495-501.

[58] Qi M, Gu Y, Sakata N, Kim D, Shirouzu Y, Yamamoto C, et al. PVA hydrogel sheet macroencapsulation for the bioartificial pancreas. Biomaterials. 2004;25:5885-92.

[59] Yang KC, Wu CC, Sumi S, Tseng CL, Wu YH, Kuo TF, et al. Calcium phosphate cement chamber as an immunoisolative device for bioartificial pancreas: in vitro and preliminary in vivo study. Pancreas. 2010;39:444-51.

[60] Storrs R, Dorian R, King SR, Lakey J, Rilo H. Preclinical development of the Islet Sheet. Annals of the New York Academy of Sciences. 2001;944:252-66.

[61] Edamura K, Itakura S, Nasu K, Iwami Y, Ogawa H, Sasaki N, et al. Xenotransplantation of porcine pancreatic endocrine cells to total pancreatectomized dogs. The Journal of veterinary medical science / the Japanese Society of Veterinary Science. 2003;65:549-56.

[62] Grundfest-Broniatowski SF, Tellioglu G, Rosenthal KS, Kang J, Erdodi G, Yalcin B, et al. A new bioartificial pancreas utilizing amphiphilic membranes for the immunoisolation of porcine islets: a pilot study in the canine. ASAIO journal (American Society for Artificial Internal Organs : 1992). 2009;55:400-5.

[63] Dulong JL, Legallais C. Contributions of a finite element model for the geometric optimization of an implantable bioartificial pancreas. Artificial organs. 2002;26:583-9.

[64] Dulong JL, Legallais C, Darquy S, Reach G. A novel model of solute transport in a hollow-fiber bioartificial pancreas based on a finite element method. Biotechnology and bioengineering. 2002;78:576-82.

[65] Dulong JL, Legallais C. What are the relevant parameters for the geometrical optimization of an implantable bioartificial pancreas? Journal of biomechanical engineering. 2005;127:1054-61.

[66] Dulong JL, Legallais C. A theoretical study of oxygen transfer including cell necrosis for the design of a bioartificial pancreas. Biotechnology and bioengineering. 2007;96:990-8.

[67] Lim F, Moss RD. Microencapsulation of living cells and tissues. Journal of pharmaceutical sciences. 1981;70:351-4.

[68] van Schilfgaarde R, de Vos P. Factors influencing the properties and performance of microcapsules for immunoprotection of pancreatic islets. Journal of molecular medicine (Berlin, Germany). 1999;77:199-205.

[69] Safley SA, Cui H, Cauffiel S, Tucker-Burden C, Weber CJ. Biocompatibility and immune acceptance of adult porcine islets transplanted intraperitoneally in diabetic NOD mice in calcium alginate poly-L-lysine microcapsules versus barium alginate microcapsules without poly-L-lysine. Journal of diabetes science and technology. 2008;2:760-7.

[70] Iwata H, Takagi T, Amemiya H, Shimizu H, Yamashita K, Kobayashi K, et al. Agarose for a bioartificial pancreas. Journal of biomedical materials research. 1992;26:967-77.

[71] Gin H, Dupuy B, Baquey C, Ducassou D, Aubertin J. Agarose encapsulation of islets of Langerhans: reduced toxicity in vitro. Journal of microencapsulation. 1987;4:239-42.

[72] De Vos P, De Haan B, Pater J, Van Schilfgaarde R. Association between capsule diameter, adequacy of encapsulation, and survival of microencapsulated rat islet allografts. Transplantation. 1996;62:893-9.

[73] Dionne KE, Colton CK, Yarmush ML. Effect of hypoxia on insulin secretion by isolated rat and canine islets of Langerhans. Diabetes. 1993;42:12-21.

[74] Trivedi N, Keegan M, Steil GM, Hollister-Lock J, Hasenkamp WM, Colton CK, et al. Islets in alginate macrobeads reverse diabetes despite minimal acute insulin secretory responses. Transplantation. 2001;71:203-11.

[75] de Haan BJ, Faas MM, de Vos P. Factors influencing insulin secretion from encapsulated islets. Cell transplantation. 2003;12:617-25.

[76] Strand BL, Ryan TL, In't Veld P, Kulseng B, Rokstad AM, Skjak-Brek G, et al. Poly-L-Lysine induces fibrosis on alginate microcapsules via the induction of cytokines. Cell transplantation. 2001;10:263-75.

[77] Koo SK, Kim SC, Wee YM, Kim YH, Jung EJ, Choi MY, et al. Experimental microencapsulation of porcine and rat pancreatic islet cells with air-driven droplet generator and alginate. Transplantation proceedings. 2008;40:2578-80.

[78] Wolters GH, Fritschy WM, Gerrits D, van Schilfgaarde R. A versatile alginate droplet generator applicable for microencapsulation of pancreatic islets. Journal of applied biomaterials : an official journal of the Society for Biomaterials. 1991;3:281-6.

[79] Klokk TI, Melvik JE. Controlling the size of alginate gel beads by use of a high electrostatic potential. Journal of microencapsulation. 2002;19:415-24.

[80] Lewinska D, Rosinski S, Werynski A. Influence of process conditions during impulsed electrostatic droplet formation on size distribution of hydrogel beads. Artificial cells, blood substitutes, and immobilization biotechnology. 2004;32:41-53.

[81] Halle JP, Leblond FA, Pariseau JF, Jutras P, Brabant MJ, Lepage Y. Studies on small (< 300 microns) microcapsules: II--Parameters governing the production of alginate beads by high voltage electrostatic pulses. Cell transplantation. 1994;3:365-72.

[82] Zekorn T, Siebers U, Horcher A, Schnettler R, Zimmermann U, Bretzel RG, et al. Alginate coating of islets of Langerhans: in vitro studies on a new method for microencapsulation for immuno-isolated transplantation. Acta diabetologica. 1992;29:41-5.

[83] May MH, Sefton MV. Conformal coating of small particles and cell aggregates at a liquid-liquid interface. Annals of the New York Academy of Sciences. 1999;875:126-34.

[84] Wyman JL, Kizilel S, Skarbek R, Zhao X, Connors M, Dillmore WS, et al. Immunoisolating pancreatic islets by encapsulation with selective withdrawal. Small (Weinheim an der Bergstrasse, Germany). 2007;3:683-90.

[85] Leung A, Ramaswamy Y, Munro P, Lawrie G, Nielsen L, Trau M. Emulsion strategies in the microencapsulation of cells: pathways to thin coherent membranes. Biotechnology and bioengineering. 2005;92:45-53.

[86] Cruise GM, Hegre OD, Scharp DS, Hubbell JA. A sensitivity study of the key parameters in the interfacial photopolymerization of poly(ethylene glycol) diacrylate upon porcine islets. Biotechnology and bioengineering. 1998;57:655-65.

[87] Sawhney AS, Pathak CP, Hubbell JA. Modification of islet of langerhans surfaces with immunoprotective poly(ethylene glycol) coatings via interfacial photopolymerization. Biotechnology and bioengineering. 1994;44:383-6.

[88] Headen DM, Aubry G, Lu H, Garcia AJ. Microfluidic-based generation of size-controlled, biofunctionalized synthetic polymer microgels for cell encapsulation. Advanced materials (Deerfield Beach, Fla). 2014;26:3003-8.

[89] Tomei AA, Manzoli V, Fraker CA, Giraldo J, Velluto D, Najjar M, et al. Device design and materials optimization of conformal coating for islets of Langerhans. Proceedings of the National Academy of Sciences of the United States of America. 2014.

[90] Abuchowski A, McCoy JR, Palczuk NC, van Es T, Davis FF. Effect of covalent attachment of polyethylene glycol on immunogenicity and circulating life of bovine liver catalase. The Journal of biological chemistry. 1977;252:3582-6.

[91] Abuchowski A, van Es T, Palczuk NC, Davis FF. Alteration of immunological properties of bovine serum albumin by covalent attachment of polyethylene glycol. The Journal of biological chemistry. 1977;252:3578-81.

[92] Scott MD, Murad KL, Koumpouras F, Talbot M, Eaton JW. Chemical camouflage of antigenic determinants: stealth erythrocytes. Proceedings of the National Academy of Sciences of the United States of America. 1997;94:7566-71.

[93] Panza JL, Wagner WR, Rilo HL, Rao RH, Beckman EJ, Russell AJ. Treatment of rat pancreatic islets with reactive PEG. Biomaterials. 2000;21:1155-64.

[94] Lee DY, Yang K, Lee S, Chae SY, Kim KW, Lee MK, et al. Optimization of monomethoxy-polyethylene glycol grafting on the pancreatic islet capsules. Journal of biomedical materials research. 2002;62:372-7.

[95] Lee DY, Nam JH, Byun Y. Effect of polyethylene glycol grafted onto islet capsules on prevention of splenocyte and cytokine attacks. Journal of biomaterials science Polymer edition. 2004;15:753-66.

[96] Jang JY, Lee DY, Park SJ, Byun Y. Immune reactions of lymphocytes and macrophages against PEG-grafted pancreatic islets. Biomaterials. 2004;25:3663-9.

[97] Teramura Y, Iwata H. Surface modification of islets with PEG-lipid for improvement of graft survival in intraportal transplantation. Transplantation. 2009;88:624-30.

[98] Teramura Y, Iwata H. Islets surface modification prevents blood-mediated inflammatory responses. Bioconjugate chemistry. 2008;19:1389-95.

[99] Lee DY, Park SJ, Lee S, Nam JH, Byun Y. Highly poly(ethylene) glycolylated islets improve long-term islet allograft survival without immunosuppressive medication. Tissue engineering. 2007;13:2133-41.

[100] Wilson JT, Krishnamurthy VR, Cui W, Qu Z, Chaikof EL. Noncovalent cell surface engineering with cationic graft copolymers. Journal of the American Chemical Society. 2009;131:18228-9.

[101] Wilson JT, Cui W, Chaikof EL. Layer-by-layer assembly of a conformal nanothin PEG coating for intraportal islet transplantation. Nano letters. 2008;8:1940-8.

[102] Wilson JT, Haller CA, Qu Z, Cui W, Urlam MK, Chaikof EL. Biomolecular surface engineering of pancreatic islets with thrombomodulin. Acta biomaterialia. 2010;6:1895-903.

[103] Stabler CL, Sun XL, Cui W, Wilson JT, Haller CA, Chaikof EL. Surface re-engineering of pancreatic islets with recombinant azido-thrombomodulin. Bioconjugate chemistry. 2007;18:1713-5.

[104] Miura S, Teramura Y, Iwata H. Encapsulation of islets with ultra-thin polyion complex membrane through poly(ethylene glycol)-phospholipids anchored to cell membrane. Biomaterials. 2006;27:5828-35.

[105] Rengifo HR, Giraldo JA, Labrada I, Stabler CL. Long-Term Survival of Allograft Murine Islets Coated via Covalently Stabilized Polymers. Advanced healthcare materials. 2014.

[106] Gattas-Asfura KM, Stabler CL. Bioorthogonal layer-by-layer encapsulation of pancreatic islets via hyperbranched polymers. ACS applied materials & interfaces. 2013;5:9964-74.

[107] Wang RN, Rosenberg L. Maintenance of beta-cell function and survival following islet isolation requires re-establishment of the islet-matrix relationship. The Journal of endocrinology. 1999;163:181-90.

[108] Weber LM, Cheung CY, Anseth KS. Multifunctional pancreatic islet encapsulation barriers achieved via multilayer PEG hydrogels. Cell transplantation. 2008;16:1049-57.

[109] Lin CC, Anseth KS. Glucagon-like peptide-1 functionalized PEG hydrogels promote survival and function of encapsulated pancreatic beta-cells. Biomacromolecules. 2009;10:2460-7.

[110] Su J, Hu BH, Lowe WL, Jr., Kaufman DB, Messersmith PB. Anti-inflammatory peptide-functionalized hydrogels for insulin-secreting cell encapsulation. Biomaterials. 2010;31:308-14.

[111] Lin CW, Chen LJ, Lee PL, Lee CI, Lin JC, Chiu JJ. The inhibition of TNF-alpha-induced E-selectin expression in endothelial cells via the JNK/NF-kappaB pathways by highly N-acetylated chitooligosaccharides. Biomaterials. 2007;28:1355-66.

[112] Hume PS, He J, Haskins K, Anseth KS. Strategies to reduce dendritic cell activation through functional biomaterial design. Biomaterials. 2012;33:3615-25.

[113] Cabric S, Sanchez J, Lundgren T, Foss A, Felldin M, Kallen R, et al. Islet surface heparinization prevents the instant blood-mediated inflammatory reaction in islet transplantation. Diabetes. 2007;56:2008-15.

[114] Dong H, Fahmy TM, Metcalfe SM, Morton SL, Dong X, Inverardi L, et al. Immuno-isolation of pancreatic islet allografts using pegylated nanotherapy leads to long-term normoglycemia in full MHC mismatch recipient mice. PloS one. 2012;7:e50265.

[115] Hall BM. Cells mediating allograft rejection. Transplantation. 1991;51:1141-51.

[116] Diamond AS, Gill RG. An essential contribution by IFN-gamma to CD8+ T cell-mediated rejection of pancreatic islet allografts. Journal of immunology (Baltimore, Md : 1950). 2000;165:247-55.

[117] Francisco LM, Sage PT, Sharpe AH. The PD-1 pathway in tolerance and autoimmunity. Immunological reviews. 2010;236:219-42.

[118] Fife BT, Bluestone JA. Control of peripheral T-cell tolerance and autoimmunity via the CTLA-4 and PD-1 pathways. Immunological reviews. 2008;224:166-82.

[119] Riley JL. PD-1 signaling in primary T cells. Immunological reviews. 2009;229:114-25.

[120] Sharpe AH, Wherry EJ, Ahmed R, Freeman GJ. The function of programmed cell death 1 and its ligands in regulating autoimmunity and infection. Nature immunology. 2007;8:239-45.

[121] Fife BT, Pauken KE. The role of the PD-1 pathway in autoimmunity and peripheral tolerance. Annals of the New York Academy of Sciences. 2011;1217:45-59.

[122] Riella LV, Paterson AM, Sharpe AH, Chandraker A. Role of the PD-1 pathway in the immune response. American journal of transplantation : official journal of the American Society of Transplantation and the American Society of Transplant Surgeons. 2012;12:2575-87.

[123] Francisco LM, Salinas VH, Brown KE, Vanguri VK, Freeman GJ, Kuchroo VK, et al. PD-L1 regulates the development, maintenance, and function of induced regulatory T cells. The Journal of experimental medicine. 2009;206:3015-29.

[124] Barber DL, Wherry EJ, Masopust D, Zhu B, Allison JP, Sharpe AH, et al. Restoring function in exhausted CD8 T cells during chronic viral infection. Nature. 2006;439:682-7.

[125] Pileggi A, Molano RD, Berney T, Cattan P, Vizzardelli C, Oliver R, et al. Heme oxygenase-1 induction in islet cells results in protection from apoptosis and improved in vivo function after transplantation. Diabetes. 2001;50:1983-91.

[126] Berney T, Pileggi A, Molano RD, Poggioli R, Zahr E, Ricordi C, et al. The effect of simultaneous CD154 and LFA-1 blockade on the survival of allogeneic islet grafts in nonobese diabetic mice. Transplantation. 2003;76:1669-74.

[127] Murad KL, Gosselin EJ, Eaton JW, Scott MD. Stealth cells: prevention of major histocompatibility complex class II-mediated T-cell activation by cell surface modification. Blood. 1999;94:2135-41.

[128] Badell IR, Russell MC, Thompson PW, Turner AP, Weaver TA, Robertson JM, et al. LFA-1-specific therapy prolongs allograft survival in rhesus macaques. The Journal of clinical investigation. 2010;120:4520-31.

[129] Tedesco D, Haragsim L. Cyclosporine: a review. Journal of transplantation. 2012;2012:230386.

[130] Kitchens WH, Haridas D, Wagener ME, Song M, Ford ML. Combined costimulatory and leukocyte functional antigen-1 blockade prevents transplant rejection mediated by heterologous immune memory alloresponses. Transplantation. 2012;93:997-1005.

[131] Ford ML, Larsen CP. Translating costimulation blockade to the clinic: lessons learned from three pathways. Immunological reviews. 2009;229:294-306.

[132] Kozlovskaya V, Zavgorodnya O, Chen Y, Ellis K, Tse HM, Cui W, et al. Ultrathin polymeric coatings based on hydrogen-bonded polyphenol for protection of pancreatic islet cells. Advanced functional materials. 2012;22:3389-98.

[133] Lee DY, Lee S, Nam JH, Byun Y. Minimization of immunosuppressive therapy after islet transplantation: combined action of heme oxygenase-1 and PEGylation to islet. American journal of transplantation : official journal of the American Society of Transplantation and the American Society of Transplant Surgeons. 2006;6:1820-8.

[134] Lee DY, Park SJ, Nam JH, Byun Y. A combination therapy of PEGylation and immunosuppressive agent for successful islet transplantation. Journal of controlled release : official journal of the Controlled Release Society. 2006;110:290-5.

[135] Arai K, Sunamura M, Wada Y, Takahashi M, Kobari M, Kato K, et al. Preventing effect of anti-ICAM-1 and anti-LFA-1 monoclonal antibodies on murine islet allograft rejection. International journal of pancreatology : official journal of the International Association of Pancreatology. 1999;26:23-31.

[136] Fotino C, Pileggi A. Blockade of leukocyte function antigen-1 (LFA-1) in clinical islet transplantation. Current diabetes reports. 2011;11:337-44.

[137] Schmittgen TD, Livak KJ. Analyzing real-time PCR data by the comparative C(T) method. Nature protocols. 2008;3:1101-8.

[138] Rainsford KD. Frans P. Nijkamp, Michael J. Parnham (eds): Principles of immunopharmacology, 3rd revised and extended edition. Inflammopharmacol. 2013;21:199-200.

[139] Gordon S. Alternative activation of macrophages. Nature reviews Immunology. 2003;3:23-35.

[140] Edwards JP, Zhang X, Frauwirth KA, Mosser DM. Biochemical and functional characterization of three activated macrophage populations. Journal of leukocyte biology. 2006;80:1298-307.

[141] Mosser DM, Edwards JP. Exploring the full spectrum of macrophage activation. Nature reviews Immunology. 2008;8:958-69.

[142] Lawrence T, Natoli G. Transcriptional regulation of macrophage polarization: enabling diversity with identity. Nature reviews Immunology. 2011;11:750-61.

[143] Liles WC, Van Voorhis WC. Review: nomenclature and biologic significance of cytokines involved in inflammation and the host immune response. The Journal of infectious diseases. 1995;172:1573-80.

[144] Berman DM, Willman MA, Han D, Kleiner G, Kenyon NM, Cabrera O, et al. Mesenchymal stem cells enhance allogeneic islet engraftment in nonhuman primates. Diabetes. 2010;59:2558-68.

[145] Nehlsen-Cannarella SL, Bohn ML. A direct approach to determine the ABH phenotype of baboons. Immunological investigations. 1987;16:57-62.

[146] O'Connor SL, Blasky AJ, Pendley CJ, Becker EA, Wiseman RW, Karl JA, et al. Comprehensive characterization of MHC class II haplotypes in Mauritian cynomolgus macaques. Immunogenetics. 2007;59:449-62.

[147] Kenyon NS, Fernandez LA, Lehmann R, Masetti M, Ranuncoli A, Chatzipetrou M, et al. Long-term survival and function of intrahepatic islet allografts in baboons treated with humanized anti-CD154. Diabetes. 1999;48:1473-81.

[148] Kenyon NS, Chatzipetrou M, Masetti M, Ranuncoli A, Oliveira M, Wagner JL, et al. Long-term survival and function of intrahepatic islet allografts in rhesus monkeys treated with humanized anti-CD154. Proceedings of the National Academy of Sciences of the United States of America. 1999;96:8132-7.

[149] Ricordi C, Lacy PE, Finke EH, Olack BJ, Scharp DW. Automated method for isolation of human pancreatic islets. Diabetes. 1988;37:413-20.

[150] Selvaggi G, Fernandez L, Bottino R, Lehmann R, Kenyon NS, Inverardi L, et al. Improved baboon pancreatic islet cell isolation. Transplantation proceedings. 1997;29:1967-8.

[151] Ricordi C, Gray DW, Hering BJ, Kaufman DB, Warnock GL, Kneteman NM, et al. Islet isolation assessment in man and large animals. Acta diabetologica latina. 1990;27:185-95.

[152] Latif ZA, Noel J, Alejandro R. A simple method of staining fresh and cultured islets. Transplantation. 1988;45:827-30.

[153] Johnson JE. Methods for studying cell death and viability in primary neuronal cultures. Methods in cell biology. 1995;46:243-76.

[154] Idahl LA. A micro perifusion device for pancreatic islets allowing concomitant recordings of intermediate metabolites and insulin release. Analytical biochemistry. 1972;50:386-98.

[155] Fachado A, Molina J, Rodriguez-Diaz R, Jacques-Silva MC, Cabrera O, Abdulreda MH, et al. Measuring dynamic hormone release from pancreatic islets using perifusion assay. 2011.

[156] Wijkstrom M, Kirchhof N, Graham M, Ingulli E, Colvin RB, Christians U, et al. Cyclosporine toxicity in immunosuppressed streptozotocin-diabetic nonhuman primates. Toxicology. 2005;207:117-27.

[157] Berman DM, Cabrera O, Kenyon NM, Miller J, Tam SH, Khandekar VS, et al. Interference with tissue factor prolongs intrahepatic islet allograft survival in a nonhuman primate marginal mass model. Transplantation. 2007;84:308-15.

[158] Gattas-Asfura KM, Stabler CL. Chemoselective cross-linking and functionalization of alginate via Staudinger ligation. Biomacromolecules. 2009;10:3122-9.

[159] Huppa JB, Davis MM. T-cell-antigen recognition and the immunological synapse. Nature reviews Immunology. 2003;3:973-83.

[160] Shen K, Thomas VK, Dustin ML, Kam LC. Micropatterning of costimulatory ligands enhances CD4+ T cell function. Proceedings of the National Academy of Sciences of the United States of America. 2008;105:7791-6.

[161] Bashour KT, Tsai J, Shen K, Lee JH, Sun E, Milone MC, et al. Cross talk between CD3 and CD28 is spatially modulated by protein lateral mobility. Molecular and cellular biology. 2014;34:955-64.

[162] Bashour KT, Gondarenko A, Chen H, Shen K, Liu X, Huse M, et al. CD28 and CD3 have complementary roles in T-cell traction forces. Proceedings of the National Academy of Sciences of the United States of America. 2014;111:2241-6.

[163] Adeegbe D, Bayer AL, Levy RB, Malek TR. Cutting edge: allogeneic CD4+CD25+Foxp3+ T regulatory cells suppress autoimmunity while establishing transplantation tolerance. Journal of immunology (Baltimore, Md : 1950). 2006;176:7149-53.

[164] Ashbaugh JJ, Brambilla R, Karmally SA, Cabello C, Malek TR, Bethea JR. IL7Ralpha contributes to experimental autoimmune encephalomyelitis through altered T cell responses and nonhematopoietic cell lineages. Journal of immunology (Baltimore, Md : 1950). 2013;190:4525-34.

[165] Chapman AP. PEGylated antibodies and antibody fragments for improved therapy: a review. Advanced drug delivery reviews. 2002;54:531-45.

[166] Bayer AL, Yu A, Malek TR. Function of the IL-2R for thymic and peripheral CD4+CD25+ Foxp3+ T regulatory cells. Journal of immunology (Baltimore, Md : 1950). 2007;178:4062-71.

[167] Brown EJ, Frazier WA. Integrin-associated protein (CD47) and its ligands. Trends in cell biology. 2001;11:130-5.

[168] Jiang P, Lagenaur CF, Narayanan V. Integrin-associated protein is a ligand for the P84 neural adhesion molecule. The Journal of biological chemistry. 1999;274:559-62.

[169] Willingham SB, Volkmer JP, Gentles AJ, Sahoo D, Dalerba P, Mitra SS, et al. The CD47-signal regulatory protein alpha (SIRPa) interaction is a therapeutic target for human solid tumors. Proceedings of the National Academy of Sciences of the United States of America. 2012;109:6662-7.